GEOLOGIAN TUTKIMUSKESKUS
GEOLOGICAL SURVEY OF FINLAND

TUTKIMUSRAPORTTI 73
REPORT OF INVESTIGATION 73

Editors

L. Eskola and A. Fokin

Electrical prospecting for ore deposits in the Baltic Shield

Part 1: Galvanic methods

1886 *1986*

Espoo 1986

GEOLOGIAN TUTKIMUSKESKUS
Tutkimusraportti 73

GEOLOGICAL SURVEY OF FINLAND
Report of Investigation 73

Editors

L. Eskola and A. Fokin

ELECTRICAL PROSPECTING FOR ORE DEPOSITS IN THE BALTIC SHIELD

Part 1: Galvanic methods

Espoo 1986

ISBN 951-690-215-4
ISSN 0781-4240

Helsinki 1986. Valtion painatuskeskus

ELECTRICAL PROSPECTING FOR ORE DEPOSITS IN THE BALTIC SHIELD

Part 1: Galvanic methods
Editors L. Eskola and A. Fokin

ПРИМЕНИЕ ЭЛЕКТРОРАЗВЕДКИ НА РУДЫХ МЕСТОРОЖДЕНИЯХ БАЛТИСКОГО ЩИТА

Вып. И. ЭЛЕКТРОРАЗВЕДКА ПОСТОЯННЫМ ТОКОМ

Редактор с финской стороны __ Л. Эскола
Редактор с советской стороны __ А. Фокин

Теоретические вопросы и моделирование

Методика и техника электроразведки постоянных током

Интерпретация данных электроразведи постоянным током

PREFACE

Cooperation in the use of geophysical methods within the framework of the agreement on Scientific and Technical Cooperation in Geology between Finland and the Soviet Union began ten years ago, in 1975. The exchange visits paid by Finnish and Soviet scientists in the first couple of years provided an overall view of the geophysical exploration methods in use in the Baltic Shield areas of each country. In 1977—80 the cooperation was focused on magnetic bore hole measurements; the results were published in Finland in 1981 as a collection of articles in English entitled "Interpretation of bore hole magnetic data and some special problems of magnetometry" in a series of reports from the University of Oulu.

As a result of the growing popularity and increasing scope of electrical methods in prospecting the theme selected for 1981—85 was "Electrical prospecting methods on the Baltic Shield". The work was divided into two phases: 1981—82 — galvanic methods, and 1983—84 — inductive methods; only ground and drill hole methods were included. Each phase consisted of introductory reports, field and laboratory visits, quantitative interpretation with various methods of theoretical and practical survey data, examination of case histories, and comparison of results. The cooperation has made it possible to follow recent developments in equipment and methods of interpretation in exploration geophysics in both countries. In the Soviet Union the project was undertaken by the Production Geological Amalgamation "Sevzap-geologia" (SZPGO), and in Finland by the Geological Survey of Finland, the Department of Geophysics of the University of Oulu, Outokumpu Oy and Rautaruukki Oy.

The results of the cooperation have been published as two reports in a series of Report of Investigation from the Geological Survey of Finland. Report 73 deals with galvanic methods. The undersigned express their gratitude to the Geological Survey of Finland, which made it possible to publish the results of the cooperation, and to the Finnish-Soviet Commission for Scientific and Technical cooperation for their financial support.

M. Ketola *N. Khrustalev*

Key words: geophysical methods, electrical methods, metal ores, ore bodies, models, Baltic Shield, Precambrian, Finland, USSR

Theory and modelling

CONSTRUCTION OF GEOELECTRICAL MODELS FOR COPPER-NICKEL DEPOSITS OF THE KOLA-KARELIAN REGION

by

G. Vargin, N. Borovko & A. Savin

Vargin G., Borovko N. & Savin A., 1986. Construction of Geoelectrical models for Copper-Nickel deposits of the Kola-Karelian region. *Geologian tutkimuskeskus, Tutkimusraportti 73.* 8—19, 8 figs, one table.

Presented briefly are the principles of constructing generalized geoelectrical models for various types of ore deposits. Described are also generalized geoelectrical models applied to a geological setting of Cu-Ni deposits in the Kola-Karelian region, viz., the Pechenga, Allarechka and Monchegorsk ore fields, on the one hand, and the Lovnozero deposit and the deposits of the Windy Belt synclinorium zone on the other.

Key words: electrical methods, models, copper ores, nickel ores, electrical properties, magnetic properties, Precambrian, USSR, Kola Peninsula, Karelia,

Варгин Г.П., Боровко Н.Н., & Савин А.П. 1986. Построение геоэлекрических моделей медно-никелевых месторождений карело-кольского Региона. Геологический центр финляндии, Рапорт исследования, 73. 8__19, Идд. 8.

Кратко излагается принцип построения обобщенных геоэлектрических моделей для пазличных типов рудных месторождений. Приведены обобщенные геоэлектрические модели для геологических условий медно-никелевых месторождений Карело-Кольского региона: Печенского, Аллареченского, Мончегорского, рудных полей, Ловнозерского месторождения и месторождения синклинорой зоны Ветреный пояс.

When prospecting for Cu-Ni deposits, we make wide use of electrical prospecting methods to find sulphide ore deposits that possess anomalous current conduction or chargeability, as well as to solve problems in geological mapping. It is the type of deposit based upon wich we choose the problems to be solved and select the most effective combination of electrical methods. The generalized geoelectrical models of targets are based on the available data concerning the three-dimensional (3D) geological structure and electrical properties of the rocks and ores of known occurrences assigned to one and the same type according to Borovko's (1979) principles. The geoelectrical models thus generalized are used when (a) calculating (theoretical modelling) or reproducing (physical and analog modelling) the anticipated anomalous effect while choosing the particular combination of methods and justifying the procedure parameters (operating frequency, array dimensions, current in the generator circuit, etc.), and (b) interpreting the data obtained and selecting an appropriate model of the geoelectrical section that suits best the observed electrical anomaly.

When devising generalized geoelectrical models, we think it is reasonable to consider nothing but those most common elements of the geoelectrical section that can influence the electrical prospecting results. One should disregard in the model those specific peculiarities (in the morphology or physical properties of rocks and ores) that are characteristic only of particular ore occurrences, as well as such as do not essentially affect the properties of the electrical or EM field. In other words, when making a model, we need to present schematically the morphology of geoelectrical targets and substitute them with simple bodies. Again, the solution of a normal geophysical problem may become much simpler if an ideal form is given to target bodies. Calculating anomaly intensity is a relatively easier problem, which can be successfully solved using extremely schematized and fairly simple models. On the other hand, to obtain a typical plot along the profile considered is a noticeably more complex task, involving a selection of suitable models with the subsequent modelling of the field to be used in making the interpretation and representing the geological idea as to the results of field measurements.

When establishing the generalized geoelectrical models, account is taken of those properties of rocks and ores that affect the distribution of the field applied in electrical prospecting methods — in particular, resistivity-, induction- and IP methods. Such properties include resistivity ϱ, chargeability η and relative magnetic permeability μ. Used are the geometrical means of ϱ, η and μ obtained from the ground and borehole data (logging data included), and also the results of laboratory measurements yielding reliable ϱ values of conductive ores and η and μ values of rocks and ores.

The dip and strike angles, geometry and dimensions of the section elements were chosen as representing averages, or most probable ones, for noteworthy orebodies and for the complexes of their country rocks. In contrast with actual ore deposits or occurrences, which are usually represented by erosionally stripped orebodies, provision in typical geoelectrical models is made for so-called ''blind'' objects, their depth being considered as a variable value. The initial form of stripped bodies is reconstructed by extrapolation to the upper half-space.

The principles stated for constructing the types of geoelectrical models are demonstrated on the most commonly known Cu-Ni deposits of the Kola-Karelian region. Again, these types of geoelectrical models are to a large extent characteristic of the Eastern Baltic Shield (Ketola, 1982).

Presented in Table 1 are the electrical properties and magnetic permeability values possessed by the elements of the generalized geoelectrical models. Basically, these are the results of statistical processing, which enable us to establish the most probable

Table 1. Electrical and magnetic properties of geoelectric model elements

Ore region (deposit)	No. of Fig. characterizing type of model	Model element No.	Rocks or ores	ϱ [Ωm]		η [%]	μ
				Limits	Mean values		
1	2	3	4	5	6	7	8
Pechenga ore field	2	1	Quaternary deposits	2000—15000	5400	2	1.0
		2	Diabases, gabbro-diabases	4000—100000	20000	0.4	1.0
		3	Phyllites	1—400	20	3.5	1.0
		4	Serpentinites	2000—20000	9000	10	1.15
		5	Impregnated ores in serpentinites	10—1000	350	16	1.1
		6	Massive and breccia-like sulphide ores	200	1		1.1
Allarechka ore field	4	1	Quaternary deposits	1000—6000	3500	2	1.0
		2	Granitic gneisses, amphibolites	3900—22000	10000	3.5	1.0
		3	Ultrabasic rocks (poorly mineralized)	28—30000	920	17	1.1
		4	Impregnated sulphide ores	3.2—46	12	42	1.15
		5	Breccia-like sulphide ores	0.14—5.7	0.9	35	1.2
			Massive sulphide ores	0.013—0.17	0.04	35	1.2
		6	Fault zone	2100—19000	6400	3.5	1.0
Monchegorsk ore field	6	1	Quaternary deposits	700—30000	5000	2	1.0
		2	Pyroxenites, peridotites, amphibolites, granites, pegmatites, gneisses	10000—100000	30000	2	1.0
		3	Norites	200—20000	2000	2	1.0
		4	Impregnated, streaky-impregnated and schlieren accumulations of sulphide ores	1—1000		30	1.0
		5	Streaky-impregnated sulphide ores	5—80	20	50	1.0
		6	Sulphide veins		<0.1		1.2
Lovnozero deposit	8a	1	Hypersthene plagiogneisses, granulites, ore-barren norites, Q-deposits	1000—20000	6000	2.5	1.0
		2	Impregnated and cluster-impregnated sulphide ores	(10—1000)n (n = 1—5)		40	1.0
Deposits of Windy Belt synclinorium zone	8b	1	Quaternary deposits	65—1200	270	2	1.0
		2	Tuffaceous-sedimentary rocks	1200—7500	3000	2	1.0
		3	Apoperidotites and antigorite serpentinites	330—6800	1500	2	1.1
		4	Apoolivinite serpentinites	45—880	200	27	1.1
		5	Massive, streaky-impregnated breccialike sulphide ores		~0.3		1.1
		6	Impregnated sulphide ores		1500	30	1.0-1.1

values (geometric means) of these properties and the limits of their variations (only for ϱ values).

The Pechenga ore field has been studied most thoroughly, its deposits being confined to the ultrabasic and basic intrusives that break through a sequence of tuffaceous-sedimentary rocks occurring amidst volcanic (chiefly diabasic) sheets. There are also to be found minor so-called "detached" orebodies that lie entirely in tuffaceous-sedimentary and volcanic rocks.

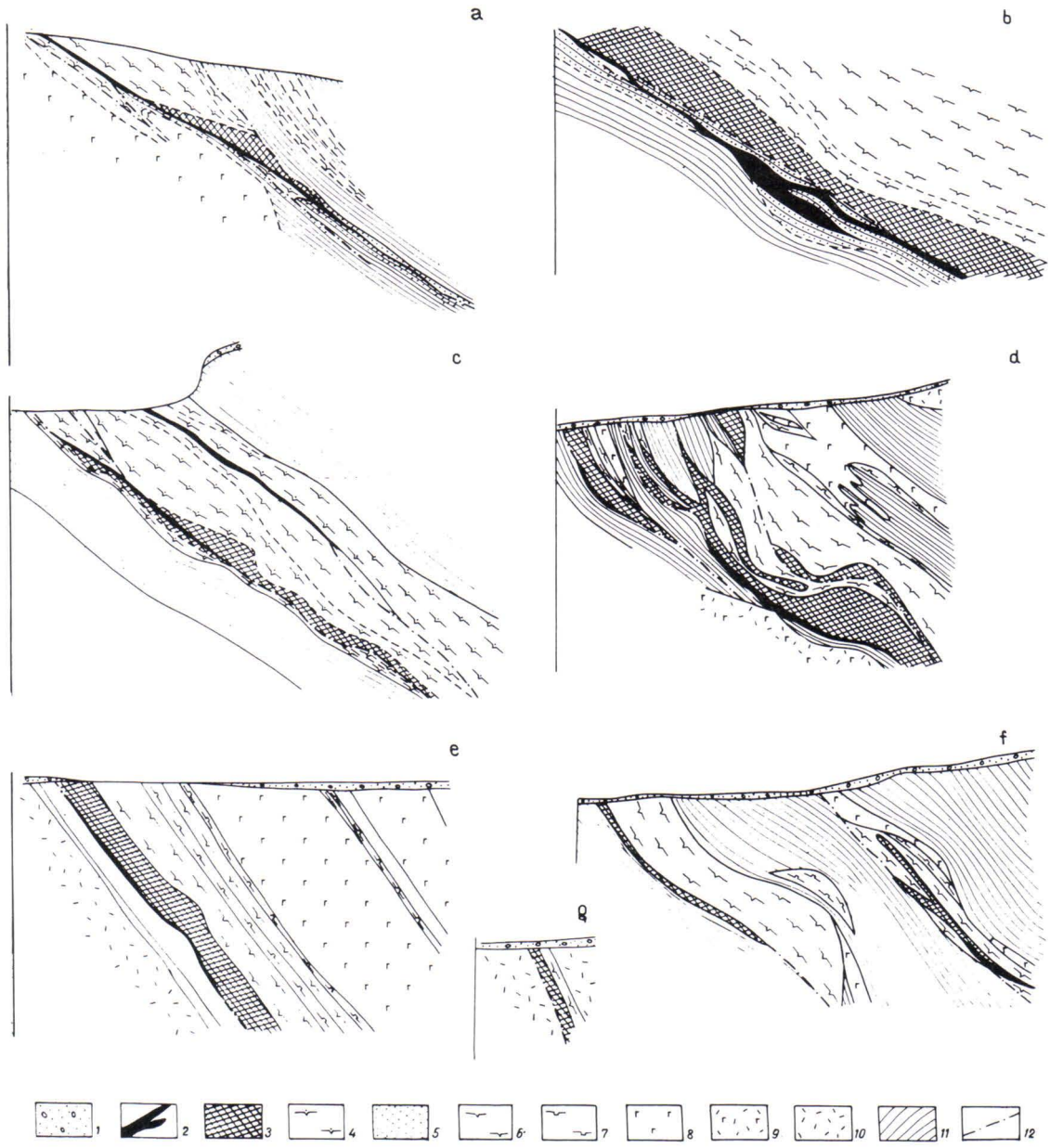

Fig. 1. Geological sections of orebodies known in the Pechenga nickel-bearing district Gorbunov (ed.), 1978: a) Kaula deposit b) Flangovoe deposit c) main orebody of Semiletka deposit d) western and southwestern orebodies of Vostochnoe ore zone e) central orebody of Vostochnoe ore zone f) Onki deposit g) Pakhtajarvi deposit. 1: Quaternary deposits 2: massive and breccia-like sulphide ores 3: rich impregnated ores in serpentinites (a, b, c), inpregnated ores (d, e, f, g) 4: run-of-mine impregnated ores in serpentinites 5: mineralized phyllites 6: serpentinites 7: pyroxenites 8: gabbro 9: gabbro-diabases 10: effusive diabases 11: phyllites and other tuffaceous-sedimentary rocks 12: faults.

In spite of the complexity and variety of the sections examined, there are common features that we make use of when drawing the generalized sections. Apart from the above-mentioned main structural peculiarities of the deposits, their common features can also include: (a) a sheet form of ore objects (b) impregnated mineralization margins of the breccia-like and massive ores (c) phyllites that prevail in the sequence and represent a variety of so-called black schists.

Fig. 1 shows some of the most typical sections of the deposits and large orebodies. The generalized geoelectrical models of the Pechenga ore field deposits are shown on the plots of Fig. 2a,b,c.

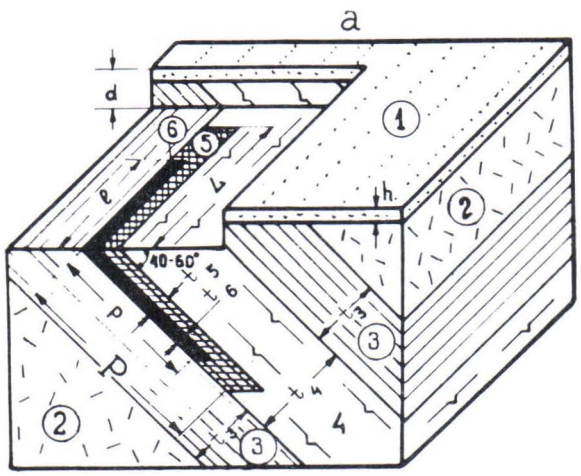

Linear dimensions,m

ℓ	600	t_4	200
L	800	t_5	40
p	400	t_6	10
P	500	h	5
t_3	150	d	variable

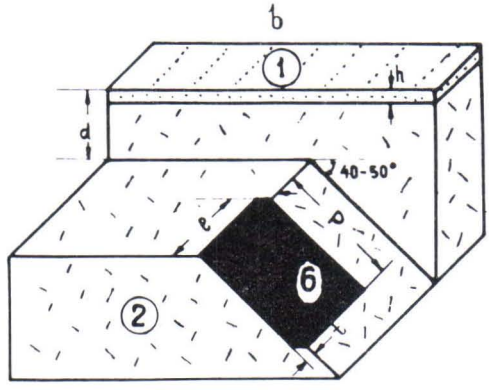

ℓ	600
p	800
t	30
h	5
d	variable

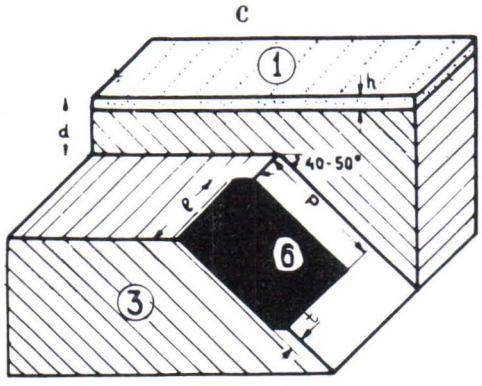

Fig. 2. Generalized geoelectrical models of the Pechenga nickelbearing district: a) deposits b) detached orebodies in diabases c) detached orebodies in phyllites.

As seen from Table 1, the resistivity of each lithological-petrographic complex discriminated in a model of Fig. 2a, as well as in the other models represented here, varies greatly because the rocks are inhomogenous in their mineral composition and structure. Such spatial heterogeneity of the electrical properties is one of the reasons why the normal field displays a complex nature, which is particularly obvious in electrical logging. In the Pechenga ore field, for instance, fluctuations in the resistivity values of phyllites (400 times) cause the appearance of false anomalies compatible with ore-object anomalies measured by various electrical prospecting methods. No regularities have been

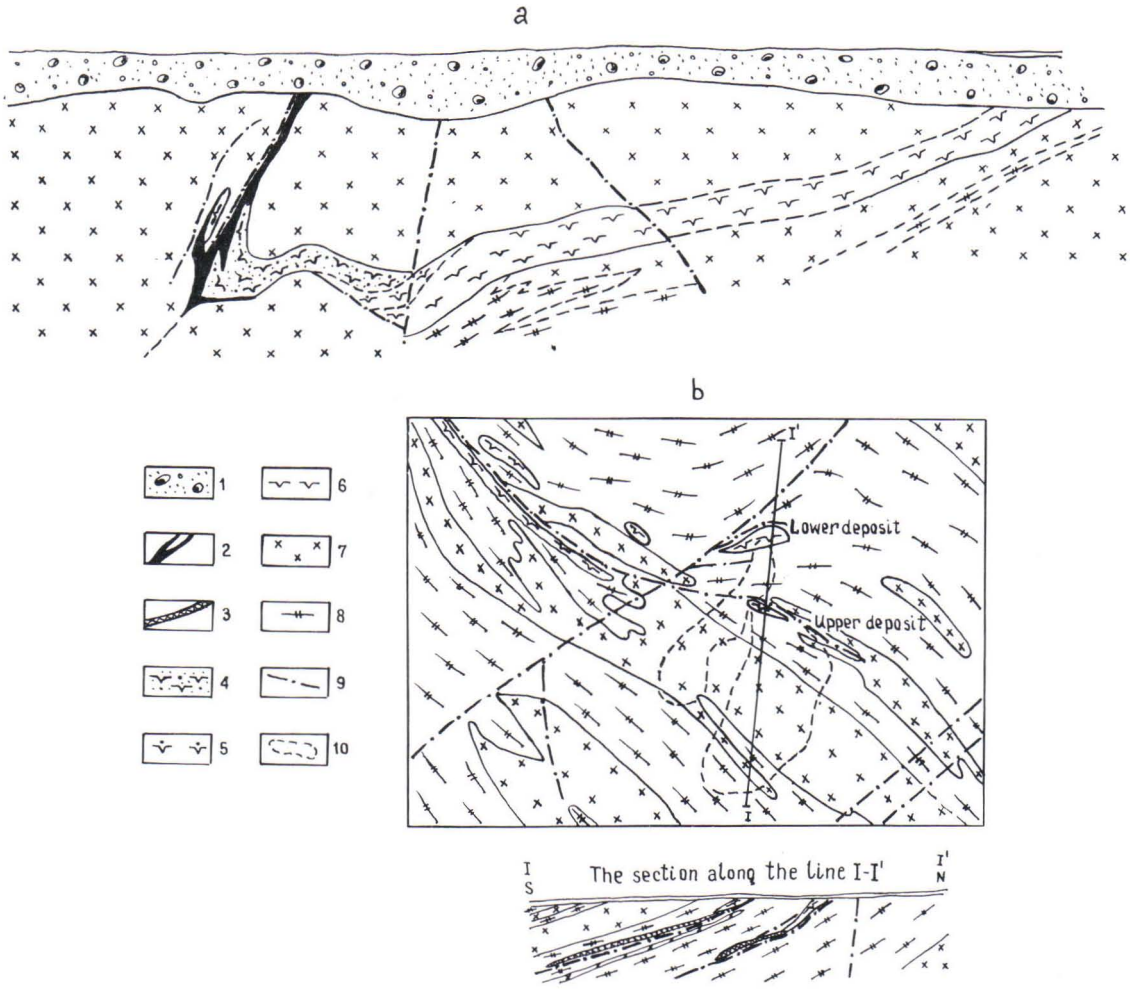

Fig. 3. Schematic geological sections and maps of Allarechka ore field deposit Gorbunov (ed.), 1978: a) section across Allarechka deposit b) map and section across Vostok deposit. 1: Quaternary sediments 2: massive ores 3: breccia-like ores 4: rich impregnated ores 5: run-of-mine impregnated ores 6: ultramafites 7: plagiomicrocline and plagioclase granite-gneisses, biotite and biotite amphibole gneisses 8: amphibolites 9: faults 10: projections of orebody outlines.

established in the distribution of anomalously conducting phyllites in the ore-bearing rock sequence, and thus the fluctuations can hardly be taken into account while constructing generalized geoelectrical models.

The Allarechka deposit is confined to the ultrabasic massif stretching over distance of some 1.5—2 km along the periphery of one of the dome structures of the Allarechka ore field. The structure of the deposit is quite complicated, as can be demonstrated by the geological section transversal to the intrusive (see Fig. 3a).

It turned out to be impossible to reduce the generalized geoelectrical model, corresponding to the Allarechka deposit, to a geometrically simplified construction because of the complex geological, hence geoelectrical, structure. The remarkable strike length of the deposit enabled a 2D-model to be constructed, the latter being characterized by its cross section only. Simplifying the pattern of geological boundaries and making the strucutre somewhat schematic, we thus simplified the geoelectrical section, as shown in Fig. 4a.

Located within the Allarechka ore field, the Vostok deposit comprises two occurrences (Upper and Lower), which are associated with ultrabasic massifs forming two elongated zones in granitegneisses and amphibolites (Fig. 3b). The generalized

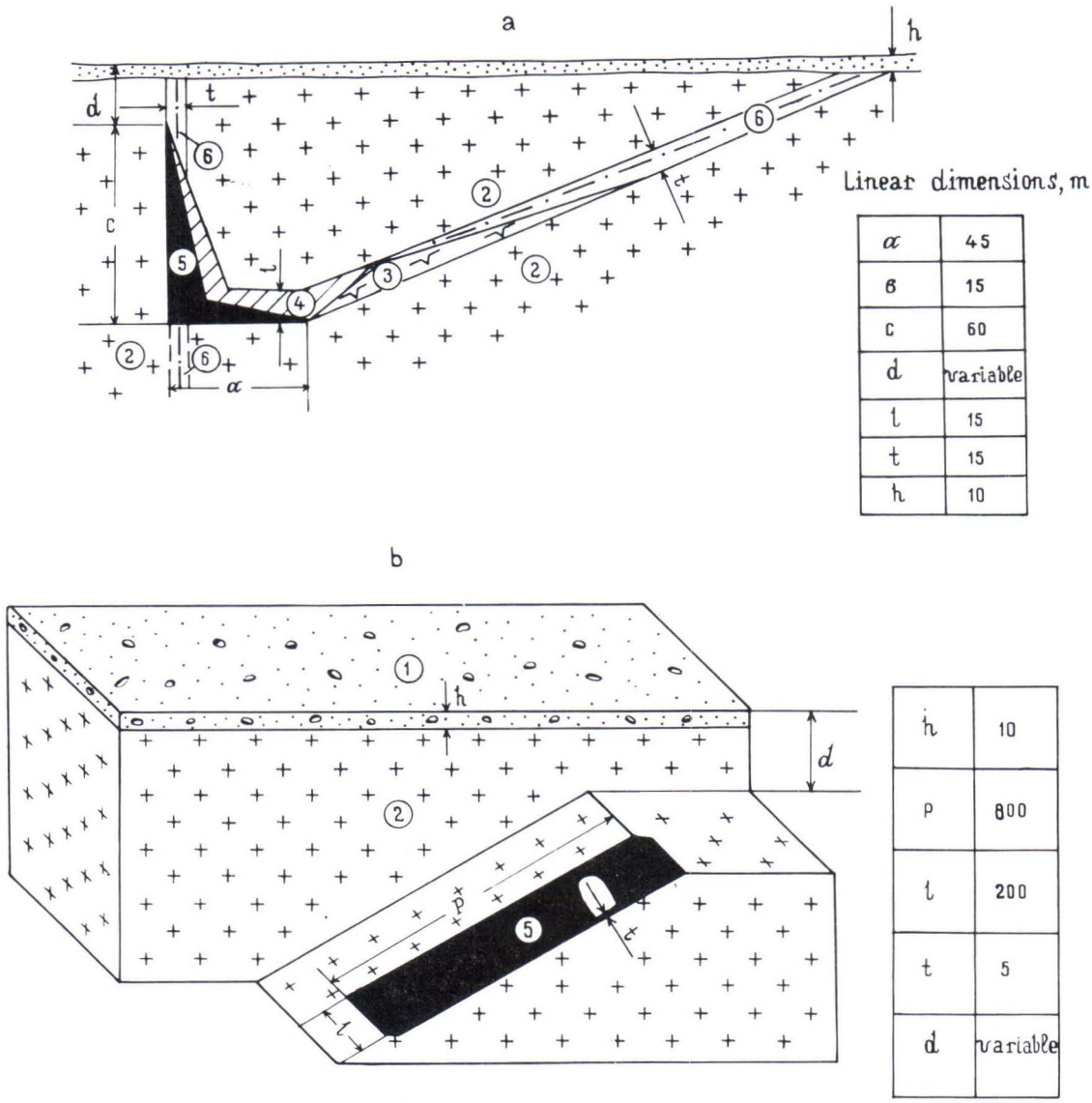

Fig. 4. Generalized geoelectrical models of a) Allarechka and b) Vostok deposits.

geoelectrical model of one of the Vostok deposit occurrences is reduced to a simple model of a thin conductive sheet in a high-resistivity medium overlain by a horizontal conductive layer (Fig. 4b).

The copper-nickel ore deposits of the Monchegorsk ore field are confined to the differentiated massif composed of basic and ultrabasic rocks (a so-called Monche pluton occurring between the greenstone volcanic-sedimentary rocks and underlying gneisses). Within the Nittis—Kumuzhia—Travyanaya and Sopcha massifs constituting the Monche pluton vein deposits (under the same names) are known to occur as elongated swarms of veins oriented subvertically. An example of a geological section of one of these deposits is shown in Fig. 5 a. A generalized geoelectrical model corresponding to this type of deposit is represented as a group of thin sheets oriented vertically and parallel to each other (Fig. 6a).

The Nud — II deposit is situated in the southwestern part of the Nud—Poaz massif which is a part of the Monchegorsk pluton. It is composed of rocks of a so-called "critical" horizon, comprising norite and olivinite rocks and containing impregnated and streaky-impregnated sulphide ores, as well as massive sulphide schlieren and discrete

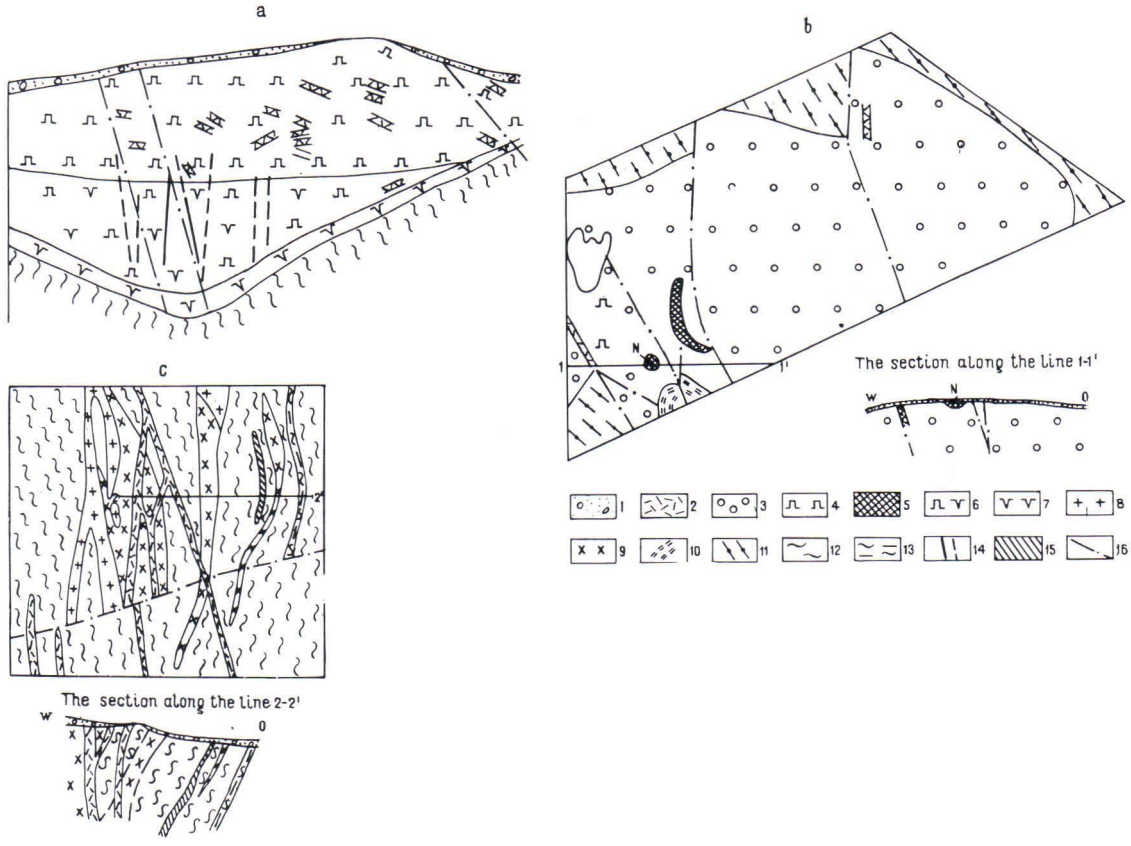

Fig. 5. Schematic geological maps and sections of deposits of the Monchegorsk ore field; a) section across Sopcha massif Kozlov et al., 1967 b) map and section of Nud-II Gorbunov (ed.), 1978 c) map and section of Priozernoye Gorbunov (ed.), 1978. 1: Quaternary deposits 2: dykes of diabase and lemprophyre composition 3: norites 4: pyroxenites 5: areas of rocks composing a so-called "critical" horizon 6: alternating pyroxenites and peridotites 7: peridotites 8: granites and plagiomicrocline pegmatites 9: leucocratic granite-gneisses 10: metaporphyrites 11: mylonitized diorite-gneisses 12: garnet-biotite and amphibole-biotite gneisses 13: migmatites after garnet-biotite and amphibole-biotite gneisses 13: migmatites after garnet-biotite gneisses 14: sulphide veins 15: mineralized amphibolites 16: faults. N — the Nud-II deposit.

veinlets. Morphologically, the deposit is an irregular stock (Fig. 5 b). On the whole, the orebody appears to be an isometric object in approximately the form of a sphere (Fig. 6b).

The Priozernoye deposit, located in the area adjacent to the Monche pluton, is represented by a sheet-like, steeply dipping body confined to the tectonic zone at the contact between an amphibolite sheet and the garnet-biotite gneisses (Fig. 5c). A generalized geoelectrical model of the Priozernoye deposit is shown in Fig. 6c.

The ore objects of the Lovnozero deposit are defined as impregnated mineralized norite and gabbro-norite intrusives occurring among gneisses and granulites. The main orebody of the Lovnozero deposit in its vertical section across its centre has a curved wedge form (Fig. 7a), while at the flanks its wedged shape changes to the lenticular. In its erosion section, the orebody displays an irregular lens-like form. Reconstruction of the orebody by its arbitrary extension to the upper half-space gives us reason to suggest that originally it had the shape of a lens, which in this case approximates on ellipsoid (Fig. 8a).

As for the Windy belt synclinorium zone (Eastern Karelia), the idea as to the structure of the Cu-Ni deposits and ore occurrences can be formed on the basis of a generalized schematic geological section (Fig. 7b) that reproduces major features of the

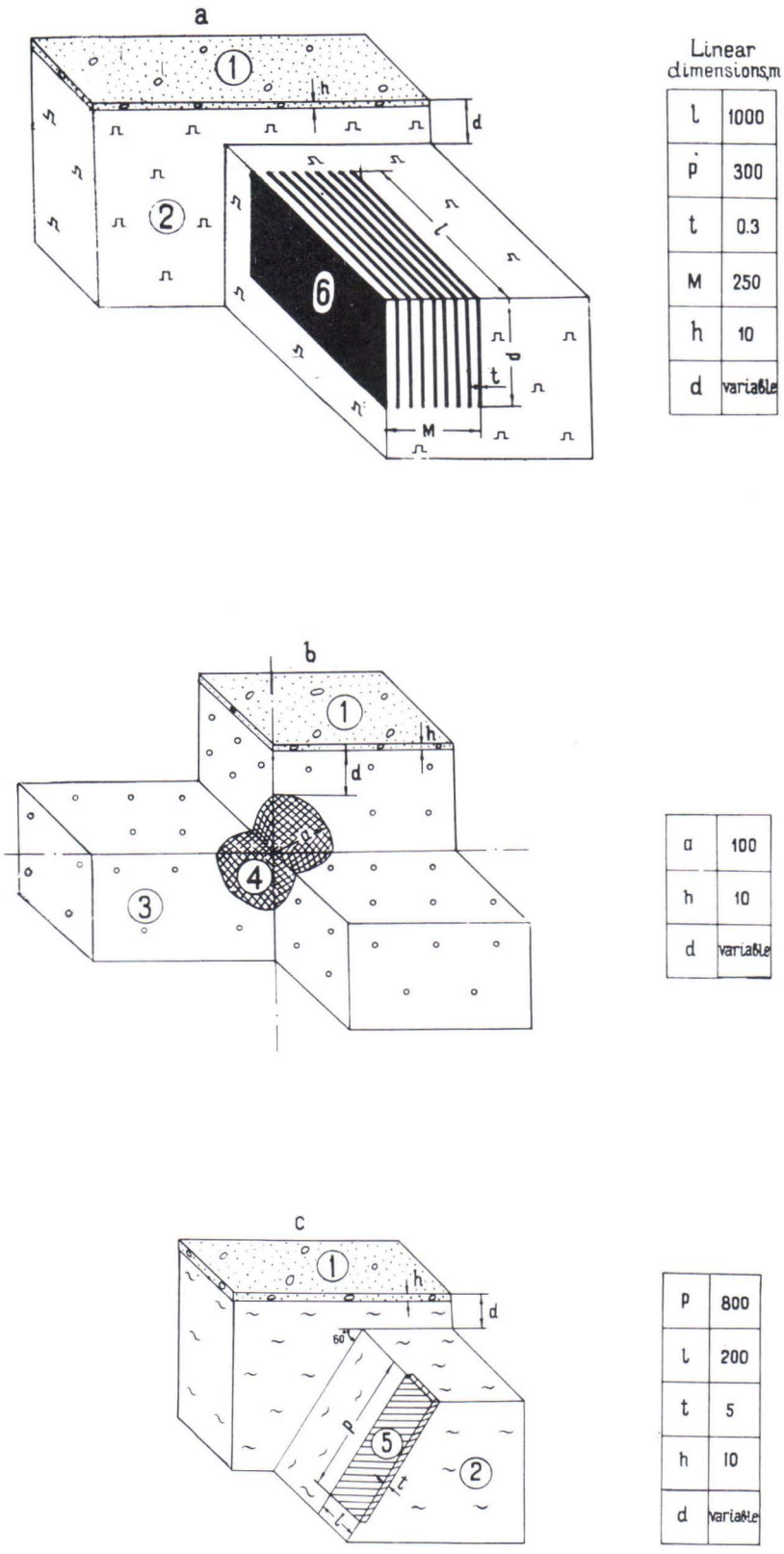

Fig. 6. Generalized geoelectrical models of the Monchegorsk ore field: a) a type of vein ore deposit b) a type of Nud-II deposit c) a type of Priozernoye deposit.

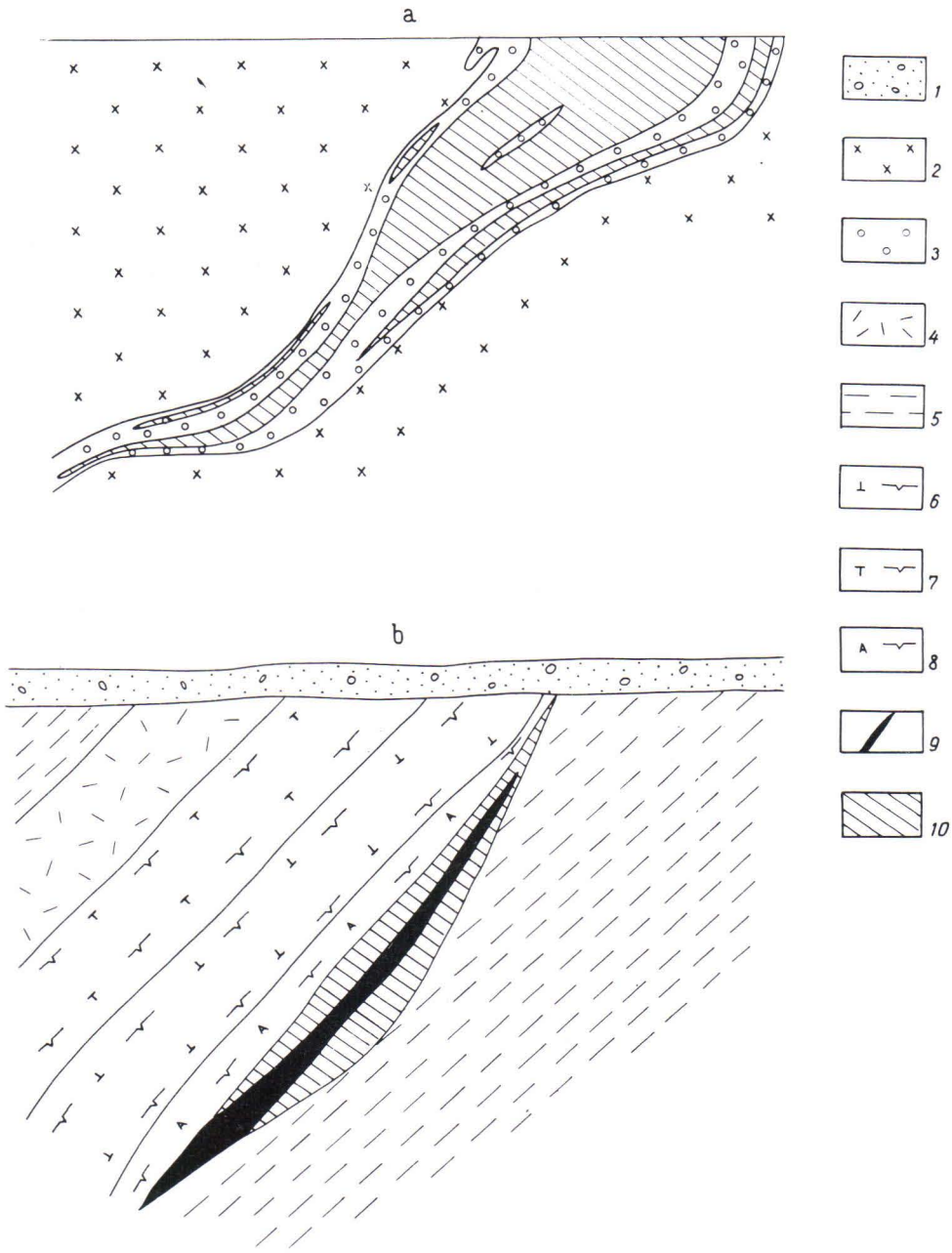

Fig. 7. a) Cross section showing the central part of the Lovnozero deposit orebody Gorbunov (ed.), 1978 b) generalized geological schematic section of deposits in the Windy Belt zone. 1: Quaternary deposits 2: hypersthene plagiogneisses, granulites 3: norites with poor mineralization 4: metadiabases, metamandelstones, basic tuffs 5: tuffaceous-sedimentary rocks 6: apoolivinite serpentinites 7: apoperioditite serpentinites 8: antigorite serpentinites 9: massive streaky-impregnated sulphide ores 10: impregnated sulphide ores.

geological pattern of ore objects and country rocks. Taking into consideration the data on the dimensions of the orebodies along the strike, a fairly sophisticated generalized geoelectrical model (shown in Fig. 8b) proves to correspond to the already known section.

From what has been said, it follows that the types of geoelectrical models considered show the objects to be most often simulated by a sheet-like form (Fig. 2,4b,6a,c,8), which is also characteristic of the majority of the ore object models in

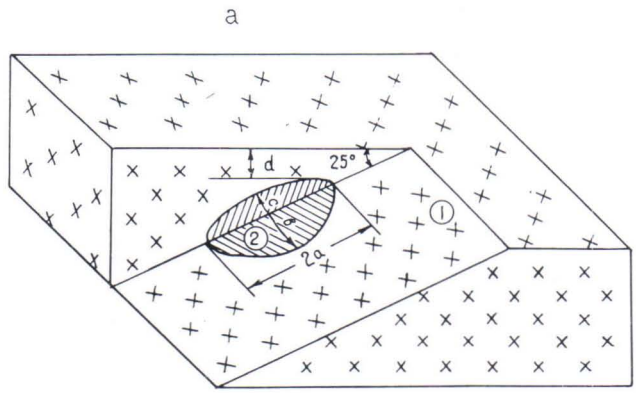

Linear dimensions, m

2a	1000
2b	700
2c	150
d	variable

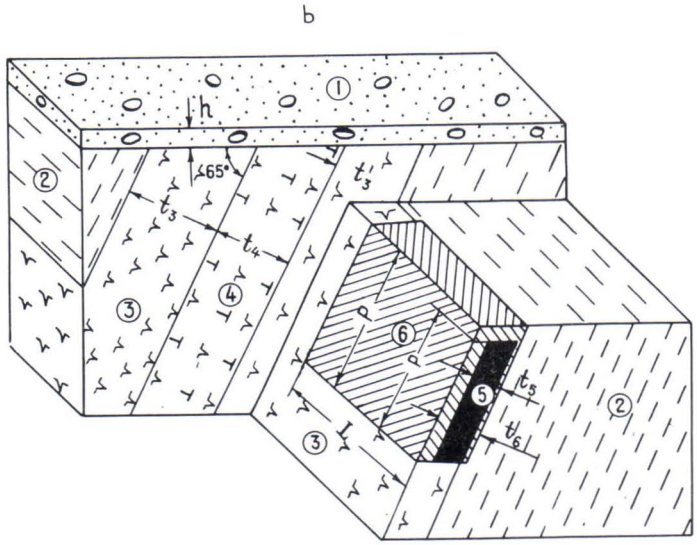

L	350
P	350
P	250
t_6	50
t_5	20
t_4	150
t_3	200
t_3'	100
h	20
d	variable

Fig. 8. Generalized geoelectrical models of the a) Lovnozero and b) Windy Belt zone deposits.

Finland (Eloranta, 1981). When solving normal and inverse geophysical problems, the anomalous effect is, therefore, most often calculated for a local object in the form of a plate possessing increased conduction and/or chargeability. There are also examples of approximating the ore objects to a spherical form (Fig. 6b) and an ellipsoid (Fig. 8a). We failed, however, to find a geometrically simple form for one object and this is shown in Fig. 4a.

The generalized geoelectrical models can be based upon modelling (mathematically or physically) the electrical fields and obtaining adequate anomalies that match a certain electrical prospecting method. These models may be brought to perfection, provided there are more comprehensive data on the geometry, dimensions and physical properties of geological objects. Factors producing an effect on the heterogeneity and sophisticated character of a normal field (presence of fault zones, irregular thickness of Quaternary deposits, heterogeneity of electrical properties, etc.) are not reproduced in the models. To estimate the efficiency of electrical prospecting methods, however, one should consider in carrying out field measurements such behaviour of the normal field as is related to the foregoing heterogeneities.

References

Borovko N., 1979. Optimization of geophysical measurement in ore prospecting. Leningrad, Nedra, 230 p. (Оптимизация геофизических исследований при поисках рудных месторождений)

Eloranta E. 1981. Piirteitä suomen malmiesiintymien malmioiden morfologiasta. Geologi, 33 (8), 121—123.

Gorbunov, G. 1978. Structures of copper-nickel ore fields and deposits of the Kola peninsula. Leningrad, Nedra, 160 p. (Стпуктуры медно-никелевых рудных полей и месторождений Кольского полуострова. Ред. Горбунов Г.).

Ketola M. 1982. On the application of geophysics and geology to exploration for nickel-copper ore deposits in Finland. Geol. tutk. lait., Tutk. rap. 53, 103 p.

Kozlov Ye., Yudin B., & Dokuchaeva V. 1967. Basic and ultrabasic complexes of Monche-Volche-Losevaya tundras. Leningrad, Nauka, 166 p. (Основной и ультраосновной комплексы Монче-Волчье-Лосевых тундр)

NUMERICAL CALCULATION OF MISE-À-LA-MASSE MODEL ANOMALIES BY USING THE INTEGRAL EQUATION TECHNIQUE

by

L. Eskola and E. Eloranta

Eskola L. & Eloranta E., 1986. Numerical calculation of mise-à-la-masse model anomalies by using the integral equation technique *Geologian tutkimuskeskus, Tutkimusraportti 73.* 20—25.

Two numerical methods are given for solving the electrical potential problem. In the first method, the electric field is represented by Fredholm's integral equation of the 2nd kind; and in the second, the electric potential is represented by Fredholm's integral equation of the 1st kind. The latter method requires that the conductivity of the anomalous bodies is at least two orders of magnitude higher than the conductivity of the environment. The practical advantages of the methods are discussed briefly.

Key words: electrical methods, electrical potential, numerical analysis, equations, mise-à-la-masse, anomalies

Эскола, Л. № Элоранта, Э., 1986. Цифровое вычисление модельных аномадий метода заряда с использованием методики интегрального уравнения
Геологический центр Финляндии, Рапорт исследования 73. 20—25.
Приводятся два цифровые метода для решения задачи электрического потенциала. С применением первого метода электрическое поле изложено в виде интегрального уравнения фредгльма 2-го рода; с использованием второго метода электрический потенция представлен интегральным уравнением фредгольма I-го рода. Последний метод предполагает, что удельная проводимость аномальных тел по крайней мере на 2 порядка превышает удельной проводимости окружающей среды. Коротко рассматриваются практические возможности применения методов.

Introduction

When the mise-à-la-masse method is applied, one of the current electrodes is earthed directly in the conductor to be surveyed and the other at a distance so long as not to affect the potential pattern to be measured. The mise-à-la-masse anomalies can be calculated as the solution of a potential problem like all the other galvanic anomalies.

The potential problem can be solved by analytical methods only for some simple structural models, and thus numerical methods are required. Of these, the differential equation methods are particularly suited to the solution of potential problems when the structure of the model is very complicated. However, the application of these methods requires that the numerical values of the function to be solved be calculated for each poit of definition of the model. This means that numerical calculations for a three-dimensional model become impossible in practice as the model increases in size.

Integral equation methods are suited to the solution of potential problems for models with simple structures. A typical model consists of one or two anomalous bodies situated in a homogeneous or layered half space. The advantage of these methods is that the region of solution can be restricted to the boundaries of the anomalous bodies. This makes it possible to treat also three-dimensional problems.

The present paper is confined to the consideration of integral equation methods. Two different formulations are given for the solution of the electrical potential problem. In the former, we follow Eskola (1979), who solved the problem by using Fredholm's integral equation of the 2nd kind. The latter formulation is given analogously with Eloranta (1984), who solved the problem by using Fredholm's integral equation of the 1st kind. A similar solution based on the integral equation of the 1st kind has been developed and programmed also in Amalgamation "Rudgeofizika" in the Soviet Union. The applicability of these formulations in computing mise-à-la-masse anomalies is discussed briefly.

Fredholm's integral equation of the 2nd kind

Let us consider a linear half-space composed of a homogeneous environment with the electrical conductivity g_o and a finite number of homogeneous bodies i within it with conductivities g_i. A direct current is emitted into the half-space by an electrode earthed within either the host medium or any of the anomalous bodies. The current generates charge distributions on the boundaries of the bodies. The potential of the current system can be written (Stratton 1941, pp. 183—184):

$$U(\bar{R}) = U_p(\bar{R}) + (1/4\pi\epsilon_o) \int_S G(\bar{R},\bar{R}_s)\, \sigma(\bar{R}_s)\, ds, \qquad (1)$$

where σ is the surface charge density on the boundaries S_i of the anomalous bodies i. G is half-space Green's function for the potential:

$$G = 1/|\bar{R}-\bar{R}_s| + 1/|\bar{R}-\bar{R}_s'| \quad , \qquad (2)$$

where $\bar{R}$ is the calculation point and $\bar{R}_s$ the source point. $\bar{R}_s'$ is the mirror image of $\bar{R}_s$ in relation to the (plane) surface of the half-space. The integration region S is the sum of all the boundaries S_i of the anomalous bodies i. U_p is the primary potential

$$U_p = (I/4\pi g_j)(1/|\bar{R}-\bar{R}_p| + 1/|\bar{R}-\bar{R}_p'|) \tag{3}$$

where $\bar{R}_p$ is the earthing point of the current electrode and $\bar{R}_p'$ the mirror image of $\bar{R}_p$ in relation to the surface of the half-space. g_j is the conductivity of the medium (j) in which the current electrode is located.

The field strength is obtained from the potential as follows:

$$\bar{E} = -\text{grad } U, \tag{4}$$

where the differentiation is performed at the calculation point. Using (4), eq. (1) takes the form

$$\bar{E} = \bar{E}_p + (1/4\pi\epsilon_o) \int_S (-\text{grad } G)\, \sigma \, dS, \tag{5}$$

where $\bar{E}_p = -\text{grad } U_p$.

To determine σ in eqs. (1) and (5), we use the following two boundary conditions on the surfaces S_i:

$$\epsilon_o(E_{on}-E_{in}) = \sigma \tag{6}$$

$$j_{on}-j_{in} = 0 \tag{7}$$

and Ohm's law

$$\bar{j} = g\bar{E}. \tag{8}$$

In eqs. (6) and (7), n denotes the normal component with a positive direction out of the anomalous bodies. The indices o and i indicate that the field vectors are expressed in the host medium o and in the anomalous medium i, respectively.

We can now write for σ:

$$\sigma = \epsilon_o(1-(g_o/g_i))\, E_{on}. \tag{9}$$

Substituting (9) into (1) and (5), we obtain for U and $\bar{E}$

$$U = U_p + (1/4\pi) \int_S (1-(g_o/g_i))\, G\, E_{on} dS \tag{10}$$

$$\bar{E} = \bar{E}_p + (1/4\pi) \int_S (1-(g_o/g_i))(-\text{grad } G)\, E_{on}\, dS. \tag{11}$$

As the next step, the unknown quantity E_{on} is solved numerically by discretization of integral equation (11). The surfaces S_i of the anomalous bodies i are divided into subareas s_{ij} so small that the field strength within each of them can be considered as constant. Requiring that the normal component of the field strength satisfies (11) in the centre of each subarea s_{ij}, we obtain

$$E_{on}(ij) = E_{pn}(ij) + (1/4\pi) \sum_k (1-(g_o/g_k))(\sum_{l(k)} (-\partial\bar{G}(ij, s_{kl})/\partial n)\, E_{on}(kl)), \tag{12}$$

where (ij) and (kl) denote the centre of the calculation subarea s_{ij} and the source subarea s_{kl}, respectively.

Green's function $\bar{G}$ is defined by

$$\bar{G}(ij,s_{kl}) = \int_{S_{kl}} G(ij,\bar{R}_s)\, dS. \tag{13}$$

Green's function of the field strengt for the singular subarea (i.e., i = k and j = l) is:

$$\lim_{(ij) \to (kl)} \partial\bar{G}(ij,s_{kl})/\partial n = -(1/2)(1-(g_o/g_i)). \tag{14}$$

Equation (12) denotes a set of algebraic equations. The number of unknowns E_{on} and the number of equations equal the total number of subareas. After solving the set (12), the quantities E_{on} on each subarea are known. Consequently, the potential and the field strength can be calculated at any point $\bar{R}$ of the half-space by using the discretized forms of eqs. (10) and (11) as follows:

$$U(\bar{R}) = U_p(\bar{R}) + (1/4\pi) \sum_i (1-(g_o/g_i)) \sum_{j(i)} G(\bar{R},s_{ij})\, E_{on}(ij) \tag{15}$$

$$\bar{E}(\bar{R}) = \bar{E}_p(\bar{R}) + (1/4\pi) \sum_i (1-(g_o/g_i)). \sum_{j(i)} (-\text{grad}\, \bar{G}(\bar{R},s_{ij}))\, E_{on}(ij). \tag{16}$$

Geological structures are often elongated in one direction. These are the very structures that are most unfavourable for numerical modelling. It is because the number of subareas grows rapidly with the length of the model.

The direction of elongation is often horizontal, in which case the model can be considered as 2 ½-dimensional. By a 2 ½-dimensional model, we mean a cylindrical model with a strike length so large as compared with the other dimensions that the effect of the end faces in field calculations can be omitted. In the following are given the basic ideas of the 2 ½-dimensional approximation in solving 3-dimensional integral equations. A more detailed description of the approximation is given by Eskola and Hongisto (1981), and Eskola (1984). Let the point current electrode be located at y = 0. Parallel to the y axis (direction of the strike), the field component normal to y is represented by the Fourier series between $-L/2 \leq y \leq L/2$:

$$\bar{E}(x,y,z) = \sum_{n=1}^{N} \bar{E}^n(x,z) \cos(2\pi ny/L), \tag{17}$$

where L is the strike length, n the degree of the harmonic term, and $\bar{E}^n$ the nth harmonic of the field strenth component normal to the y axis. Applying expansion (17) surface integral equation (11) reduces to a series of line integral equations, the integration region being the projection of the boundaries on plane y = 0. Each line integral equation is solved numerically by approximating the integration lines by a succession of line segments (subsections) and by assuming the field strength as constant (or linearly varying) over each subsection. Each line integral equation reduces now to a set of algebraic equations. The harmonic components of the field strength over the subsections are obtained as the solution of the sets of equations. Finally, the field strength and potential can be calculated at any point of the half-space in region $-L/2 \leq y \leq L/2$ by using the expansions (10,17) and (11,17).

Fredholm's integral equation of the 1st kind

Let us consider a linear half-space where a finite number of conducting bodies with conductivity g_i are located in a homogeneous environment with conductivity g_o. Let the conductivity contrast g_i/g_o be so high (at least one hundred) that each body can be considered as an equipotential region.

The potential of the current system can be expressed by eq. (1), where G is given by eq. (2) and U_p by eq. (3). Using the boundary conditions (6) and (7), we obtain for the potential

$$U(\bar{R}) = U_p(\bar{R}) + (1/4\pi) \int_S (1/g_o - 1/g_i)\, G(\bar{R},\bar{R}_s)\, j_n\, dS, \tag{18}$$

where $j_n = j_{1n} = j_{2n}$.

The following is confined to the mise-à-la-masse problem of ideal conductors, i.e., for each conductive body $g_i \geq 100 \cdot g_o$. For this case, each conductor i can be considered as an equipotential region:

$$U_i = U_i^{const}. \tag{19}$$

In the mise-à-la-masse method, the primary current electrode is earthed in one of the conducting bodies. According to eq. (3), the primary potential is inversely proportional to the conductivity (g_i) of the medium in which the current electrode is located. Consequently, the term of the primary potential in eq. (18) is very small in relation to the secondary potential. By applying the constraint of equipotentiality to eq. (18), we now obtain:

$$U_i^{const} = (1/4\pi g_o) \int_S G\, j_n\, dS. \tag{20}$$

Eq. (20) represents Fredholm's integral equation of the 1st kind. Since in (20) both U_i^{const} and j_n are unknown, they have to be solved with supplementary equations derived from the equation of continuity (Stratton 1941, pp. 222—223):

$$I = \int_{SI} j_n\, dS, \tag{21}$$

where S_I is the surface of the body that houses the current electrode and I is the current strength fed into the body. For other bodies (without current earthing)

$$0 = \int_{S(no\ I)} j_n\, dS. \tag{22}$$

By dividing the boundaries S_i of the conducting bodies into subareas s_{ij} so small that the current strength within each of them can be considered as constant and requiring that eq. (20) be valid at the centre (ij) of each subarea s_{ij}, we obtain the following set of algebraic equations:

$$\begin{cases} U_i^{const} = (1/4\pi g_o) \sum_k \sum_{l(k)} \bar{G}(ij,s_{kl})\, j_n\,(kl) \\ I = \sum_{l(k)} j_n\,(kl)\, s_{kl} \text{ for each body k with current source} \\ 0 = \sum_{l(k)} j_n\,(kl)\, s_{kl} \text{ for each body k without current source.} \end{cases} \tag{23}$$

Green's function $\bar{G}$ is given by eqs. (2) and (13). No particular consideration is needed for singularity, because Green's function of the potential is non-singular when i = k and j = l.

The unknown quantities $j_n(ij)$ are solved from the set (23) and the values obtained are substituted into the equation

$$U(\bar{R}) = (1/4\pi g_o) \sum_k \sum_j \bar{G}(\bar{R}, s_{ij})\, j_n(ij) \qquad (24)$$

derived from eq. (20) by discretization. Eq. (24) allows the calculation of the potential at any point in the half-space.

Discussion

Some specific comparisons of the results obtained by using different modelling methods are presented by Eskola, Avdevich, Hongisto and Vdovichenko in this issue. Here we shall content ourselves with making some general conclusions about the two calculation methods presented in the foregoing.

In the calculation of galvanic anomalies by using the integral equation of the 2nd kind, no restrictions are needed concerning the choice of the conductivity values of the model. However, in the application of this formulation in the calculation of mise-à-la-masse anomalies for models with high conductivity contrast values, one has to use the reciprocal electrode configuration. This implies that the integral equation has to be resolved for each calculation point, which increases the computational effort. The computational drawbacks in the ''direct solution'' of the mise-à-la-masse anomalies are due to the location of the primary source inside the conductor, which makes the primary field very low and thus the problem ill-posed.

In the application of the integral equation of the 1st kind, it is assumed that each anomalous body of the model forms an equipotential region. For this to be valid, the conductivity values of the bodies are required to be at least two orders of magnitude higher than that of the environment. Conductivity contrasts of one hundred are fairly common in nature, and it is these very models with a high conductivity contrast that are particularly suited to mise-à-la-masse surveys. The solution of galvanic problem based on the integral equation of the 1st kind is thus relevant in most cases of mise-à-la-masse modellings encountered in practical applications. The supplementary eqs. (21) and (22) facilitate the numerical solution and accelerate the convergence. They quarantee the right amount of total surface charge on the boundary of the model.

It can thus be concluded that the high speed and accuracy achieved in the calculation make the solution based on the integral equation of the 1st kind better suited in the calculation of mise-à-la-masse anomalies if the conductivity contrast between the anomalous bodies and the environment is high (at least one hundred). If the conductivity contrast is low, the solution based on the integral equation of the 2nd kind should be applied.

References

Eloranta, E., 1984. A method for calculating mise-à-la-masse anomalies in the case of high conductivity contrast by the integral equation technique, Geoexploration 22, 77—88.

Eskola, L., 1979. Calculation of galvanic effects by means of the method of sub-areas, Geophysical Prospecting 27, 616—627.

Eskola, L., 1984. Addendum to ''The solution of the stationary electric field strength and potential of a point current source in a 2 ½-dimensional environment'' by L. Eskola & H. Hongisto, Geophysical Prospecting 32, 510—511.

Eskola, L. & Hongisto, H., 1981. The solution of the stationary electric field strength and potential of a point current source in a 2 ½-dimensional environment, Geophysical Prospecting 29, 260—273.

Stratton, J. A., 1941. Electromagnetic theory, McGraw-Hill, New York, 615 p.

THEORETICAL BASIS FOR ANALOG MODELLING OF POTENTIAL ELECTRIC FIELDS

by

M.M. Avdevich and A.Ph. Fokin

Avdevich M.M. & Fokin A. Ph., 1986. Theoretical basis for analog modelling of potential electric fields. *Geologian tutkimuskeskus, Tutkimusraportti 73.* 26—29.

The principles of modelling potential electric fields in the operative quantitative solution of electrical prospecting problems (the methods of direct current, induced polarization and self potential) are described. The method of electric modelling is based on the combined use of physical and mathematical modelling and opens up the possibility of solving the problems of electrical prospecting by taking into account the true geoelectric environment right in the field.

Key words: electrical methods, electrical field, physical models, mathematical models, theoretical studies

Авдевич М.М. № Фокин А.Ф., 1986 Теоретические основы аналогового моделирования потенциальных электрических полей. Геологический цептр Фирляндии, Рапорт исследования 73. 26—29.

Изложены принципиальные основы элекиро-моделирования потенциальных электрических полей при оперативном численном решении задач электроразведки (методы постоянного тока, вызванной поляризации, естественного электрического поля). Способ электромоделирования основан на совместом использовании физического и математического моделирования и позволяет решать задачи электроразведки с учетом реальной геоэлектрической обстановки непосредственно в условиях полевых партий и экспедиций.

Potential electric fields are considered to be the fields that in a first approximation satisfy Laplace's equation. These are: direct current electric field, self-potential field and induced polarization field.

The electric field obtained by geophysical measurement with direct current is the sum of two fields: the primary field generated by current electrodes in the uniform, infinite host medium and the anomalous field induced by polarizable electrical heterogeneities present in the primary field. The primary and anomalous fields in any point of the half-space outside the polarizable heterogeneities are summed according to the principle of superposition (Tamm, 1956).

The potential and the intensities of the primary and anomalous fields are as follows:

$$U_o = \frac{\varrho}{4\pi} \frac{I}{R} \tag{1}$$

$$\bar{E}_o = \frac{\varrho}{4\pi} \frac{I\bar{R}}{R^3} \tag{2}$$

$$U_a = \frac{1}{4\pi} \int_V \frac{\bar{P}_e \cdot \bar{R}}{R^3} dV \tag{3}$$

$$\bar{E}_a = \frac{1}{4\pi} \int_V \left(\frac{3\bar{P}_e \cdot \bar{R}\bar{R}}{R^5} - \frac{\bar{P}_e}{R^3}\right) dV, \tag{4}$$

where ϱ is the resistivity of the host medium, I the current strength at the transmitting electrode, and R the distance between the field source and the observation point. $\bar{P}_e$ is the electric dipole moment for a unit volume of polarizable heterogeneity (the electric polarization) related to the primary field by:

$$\bar{P}_e = C_e\bar{E}_{in} = C_e\bar{E}_o/(1 + NC_e). \tag{5}$$

In (5), C_e is the electric susceptibility factor of polarizable heterogeneity, and N is the shape factor for the polarizable body, which has a specific value at every point of the heterogeneity. $\bar{E}_{in}$ is the field intensity inside the heterogeneity at the point where $\bar{P}_e$ is determined.

When the induced polarization (IP) field or the natural electric potential field (SP) is being examined, it suffices to insert $\bar{P}_{IP}$ and $\bar{P}_{SP}$ instead of $\bar{P}_e$ in (3) and (4). Correspondingly, in the determination of the IP vector $\bar{P}_{IP}$, the IP-polarization susceptibility factor C_{IP} should be substituted for C_e in (5). The problem involves essentially the determination of the polarization vectors, which act as sources of the anomalous fields.

In real conditions for bodies of arbitrary forms in the presence of various distorting factors (conducting overburden of variable thickness, curvature of the earth-air interface, anisotropy, conducting zones which are not the research targets, etc.), the electric fields are extremerely complicated and the determination of the polarization vectors by analytical methods is very difficult. At the same time, if in modelling provision is made for the similarity between boundary conditions in nature and on the model, then also the field which is "primary" in relation to the object examined and the anomalous field of this object on the model and in nature will be similar (Alpin, 1966).

In modelling the direct current electric field, use is made of the physical similarity of the boundary conditions in nature and in the model. The primary field is generated by physical modelling. To determine the anomalous field, it is possible to use both physical and mathematical modelling. In the latter case, the polarizable object is replaced by an aggregate of direct current dipole sources (Avdevich and Phokin, 1978).

In physical modelling as well as in nature, the summary field is examined. The equivalence of summary fields in nature and in the model is valid only when the similarity factor has one and the same value for the primary and the anomalous fields. The analysis of the eqs. (1) through (4) as applied in nature and in the model shows that this equivalence is provided when the current strength in the model is as follows:

$$I_m = I_n \varrho_n / \varrho_m K, \tag{6}$$

where I_m and I_n are respectively the current strength values in the model and in nature, and ϱ_m and ϱ_n are the resistivities of the host media in the model and in nature. K is the modelling scale ratio (the ratio of dimension in nature to dimension in the model).

When the mathematical modelling is being worked out, the polarization P_e may be substituted by the dipole moment jl, which is an approximation to the direct current source strength of a unit volume of electric heterogeneity (Avdevich and Phokin, 1978). The similarity factors between the respective components of an anomalous field in mathematical modelling are determined by:

$$K = U_n/U_m = P_e K/\varrho_m jl \tag{7}$$

$$K' = E_n/E_m = P_e/\varrho_m jl. \tag{8}$$

As the mathematical modelling of the anomalous field should be related with the physical modelling of the primary field, the factors K and K' should be equal to unity. The polarization vector is determined by eq. (5). For this purpose, the inner field is measured in the heterogeneity of the model simulating the heterogeneity in nature. The electrical susceptibility of the model equals the susceptibility in nature in accordance with:

$$C_e = (\varkappa_2 - \varkappa_1)/\varkappa_1, \tag{9}$$

where $\varkappa_1$ and $\varkappa_2$ are the electrical conductivity values of the host medium and the heterogeneity.

Further, the dipole moment values of the direct current sources are determined by eqs. (7) and (8) and the mathematical modelling of the anomalous electric field is then performed (Avdevich and Phokin, 1978).

In analog modelling, it is possible to use different approaches to IP field determination, but all of them are based on the formal similarity between the polarizability and the fictitious increase of the resistivity of the medium (Komarov, 1980) expressed by:

$$\varkappa^* = \varkappa(1-\eta) \tag{10}$$

where $\varkappa$ is the conductivity of the medium in a non-polarized state, η is the IP polarizability, and $\varkappa^*$ is the conductivity of the medium in a polarized state. This means that the polarization is taken into account in modelling by replacing the true conductivity $\varkappa$ with the fictitious one. So, for the anomalous IP field, only the mathematical modelling is performed. The effects of the conductance of the body and the electrical heterogeneities of the host medium may be taken into account both by mathematical and by physical modelling. The physical and mathematical modelling in this case are accomplished simultaneously (Avdevich and Phokin, 1978).

The mathematical modelling techniques discussed in the foregoing may be applied to self-potential studies if the resistivity of the polarized objects differ slightly from the resistivity of the host medium.

In exploration geophysics, the cases in which the electrical resistivity of a natural polarizable body is much lower than the resistivity of the host medium are of great interest.

The emf of natural galvanic elements is determined by natural geoelectrochemical factors, and in this case it is a stable value for any geoelectrical situation. Indeed, a change in the situation may change the behaviour of the current passing through the polarized object which is caused by the interaction of these objects and with other electrical inhomogeneities. These currents are foreign to the given body and they are not caused by any particular geoelectrochemical situation. However, as the resistivity of the naturally polarizable bodies is low, these currents will not cause any substantial potential loss over the body and consequently its emf will remain unchanged.

At the same time, the foreign currents bring about a redistribution of charges σ on the surface of the polarizable body and therefore the dipole moment of the body changes by the relation (Ovchinikov, 1971):

$$P_{SP} = \int_S \sigma \, dS \tag{11}$$

where σ is the surface charge density, and S the surface of the polarizable body. The moment of the naturally polarizable body is thus the function of geoelectrochemical as well as geoelectrical situations. Consequently, when the quantitative interpretation of the self-potential field is performed, both these phenomena should be taken into account.

Applying the electrotechnical analogy, let us consider the naturally polarizable body with low resistivity as a regulated voltage supply. Its inner resistance is known to be about zero. Therefore, to model the naturally polarizable body, it is necessary to replace it by two groundings. The regulated voltage supply with given emf is connected between these groundings. The conditions of physical modelling are now effected and the field of naturally polarizable conductor assemblage with regard to the effects of arbitrary electrical heterogeneities can be modelled. So the fields in the model and in nature will be equal.

The principal bases of volume potential field modelling are discussed in the foregoing. The modelling theory examined for the three-dimensional field is directly applicable to a two-dimensional field, provided that the primary field is also two-dimensional field. Investigating the three-dimensional field in a two-dimensional model is not generally possible. However, in some cases, it is possible to extract regions in the boundaries where the field at the first approximation can be examined by using a two-dimensional model. Besides, there are some techniques that make it possible with satisfactory accuracy to solve practical three-dimensional problems with two-dimensional modelling (Avdevich et al., this issue; Semenov and Avdevich, this issue).

REFERENCES

Avdevich M.M., Phokin A.Ph., 1978. The electromodelling of potential geophysical fields, 99 p. (Электромоделирование потенциальных геофизических полей). Nedra, Leningrad.

Alpin L.M. 1966. The field theory. (Теория поля). Nedra, Moscow, 312 p.

Komarov V.A. 1980. Induced polarization electrical prospecting, p. 390. (Электроразведка методом вызванной поляризации). Nedra, Leningrad.

Ovchinikov I.K. 1971. The field theory, 312 p. (Теория поля). Nedra, Moscow.

Tamm I.E., 1956. The foundation of the electricity theory, 620 p. (Основы теории электричества). Gostechizdat, Moscow.

COMPARISON OF VARIOUS MODELLING METHODS IN ELECTRICAL PROSPECTING BY CONSIDERING AN EXAMPLE OF A LONG, PERFECTLY CONDUCTING BODY IN THE FIELD OF A POINT CURRENT SOURCE

by

L. Eskola, M. Avdevich, H. Hongisto and Y. Vdovichenko

Eskola, L., Avdevich, M., Hongisto, H. & Vdovichenko, Y. 1986 Comparison of various modelling methods in electrical prospecting by considering an example of a long, perfectly conducting body in the field of a point current source. *Geologian tutkimuskeskus, Tutkimusraportti 73.* 30—36, 5 figs.

Comparisons are made between potential anomalies of perfectly conducting bodies obtained by using three different modelling methods. The methods are: a) electromodelling on the ohmic resistance grid, b) numerical solution of Fredholm's integral equation of the 1st kind, and c) numerical solution of Fredholm's integral equation of the 2nd kind. The results obtained by using the resistance grid (method a) are taken as reference system, which is used for evaluating the modelling results obtained by the numerical methods (b and c). It is verified that method b) is more appropriate than method c) in solving resistivity problems for models with high conductivity contrasts.

Key words: electrical methods, electrical potential, conducting materials, resistivity, numerical analysis, models

Эскола, Л., Авдевич, М.М., Хонгисто, Х. и Вдовиченко, Ю.Я., 1986 Геологический центк Финляндии, Рапорт исследования 73. 30—36, Идд. 5.

Сравительное изучение разлих методик моделирования в электроразведке применительно к случаю удлиненного полностью проводящего тела в поле точечного источинка тока.

Проведено сравительное изучение аномалий сопротивления от полностью проводящих тел с применением трех различных методик моделирования: а/ электромоделирования на сети омических сопротивлений, б/ числового решения интегрального уравнения фредгольма 1го рода, и в/ числового решения интегрального уравнения фредгольма 2го рода. Данные, полученные с помощью омической сети/методка **а**/ прияты за опорную систему для оценки результатов моделирования по цифровым методикам /**б**/ и **в**/. Показано, что методика **б** более приемлима чем методка **в** при решении задач с высоким контрастами проводимости.

Introduction

The electric field studied in electrical prospecting is determined by the primary field structure and intensity and geoelectrical environment of the area investigated (Avdevich, Phokin, in this issue). Solving the electric field problem is generally difficult. Moreover, the accuracy of the solution obtained is often difficult to estimate.

A very important exploration problem is that of determining the shapes and connections of highly conducting bodies. Suitable for solving such problems are the resistivity methods, among which we can also count the mise-à-la-masse method. (In the mise-à-la-masse method, one of the current electrodes is earthed into one of the bodies). Consequently, for the interpretation of resistivity measurement results, the problem of finding the electric potential of an assemblage of perfectly conducting bodies with arbitrary shapes located in a uniform isotropic conductive half-space in the field of a point current source is of practical interest.

In this paper, comparisons are made between modelling results obtained using three different methods for solving the electric potential problem. The methods are as follows:

a) electromodelling on the ohmic resistance volume grid,
b) numerical solution of Fredholm's integral equation of the 1st kind for the potential, and
c) numerical solution of Fredholm's integral equation of the 2nd kind for the field strength.

The modelling work applying methods a) and b) was done in the Soviet Union, and the work applying method c) in Finland.

A description of the two numerical modelling methods (b and c) is given by Eskola and Eloranta in this issue.

Previous comparisons

Comparisons between apparent resistivity profiles over highly conductive 3-dimensional prisms as calculated by using methods b) and c) were made in the course of Eloranta's work (Eloranta 1984). He found that the solutions obtained by using method b) were generally more rapidly converging than those obtained by using method c). If the number of sub-areas used in the calculations sufficed, the solutions obtained by these two different methods were similar. In the comparison of mise-à-la-masse anomalies of 3-dimensional prisms obtained by using methods b) and c), the amplitude values given by method c) were considerably lower than those given by method b). This phenomenom persisted even with the highest possible number of sub-areas (about one thousand for the VAX 11/780 computer of the Geological Survey of Finland).

This can be explained by the fact that, in the "direct" solution of the mise-à-la-masse problem using method c), the location of the primary source is inside the conductor. The primary field strength that is proportional to the resistivity of the medium in which the source is located is thus only a small fraction of the total field strength to be solved. This makes the problem ill-posed. On the other hand, in method b), the equations of continuity (Eskola and Eloranta, in this issue) facilitate the numerical solution and accelerate the convergence. They guarantee the right amount of total surface charge on the boundaries of the model. Contrary to method c), method b) is thus well suited for the direct solution of mise-à-la-masse problems.

Method c) was also used for calculating mise-à-la-masse anomalies by replacing the true electrode configuration by its reciprocal configuration. This made the primary field strength sufficiently strong and the calculated anomalies were well comparable with the anomalies obtained by using method b).

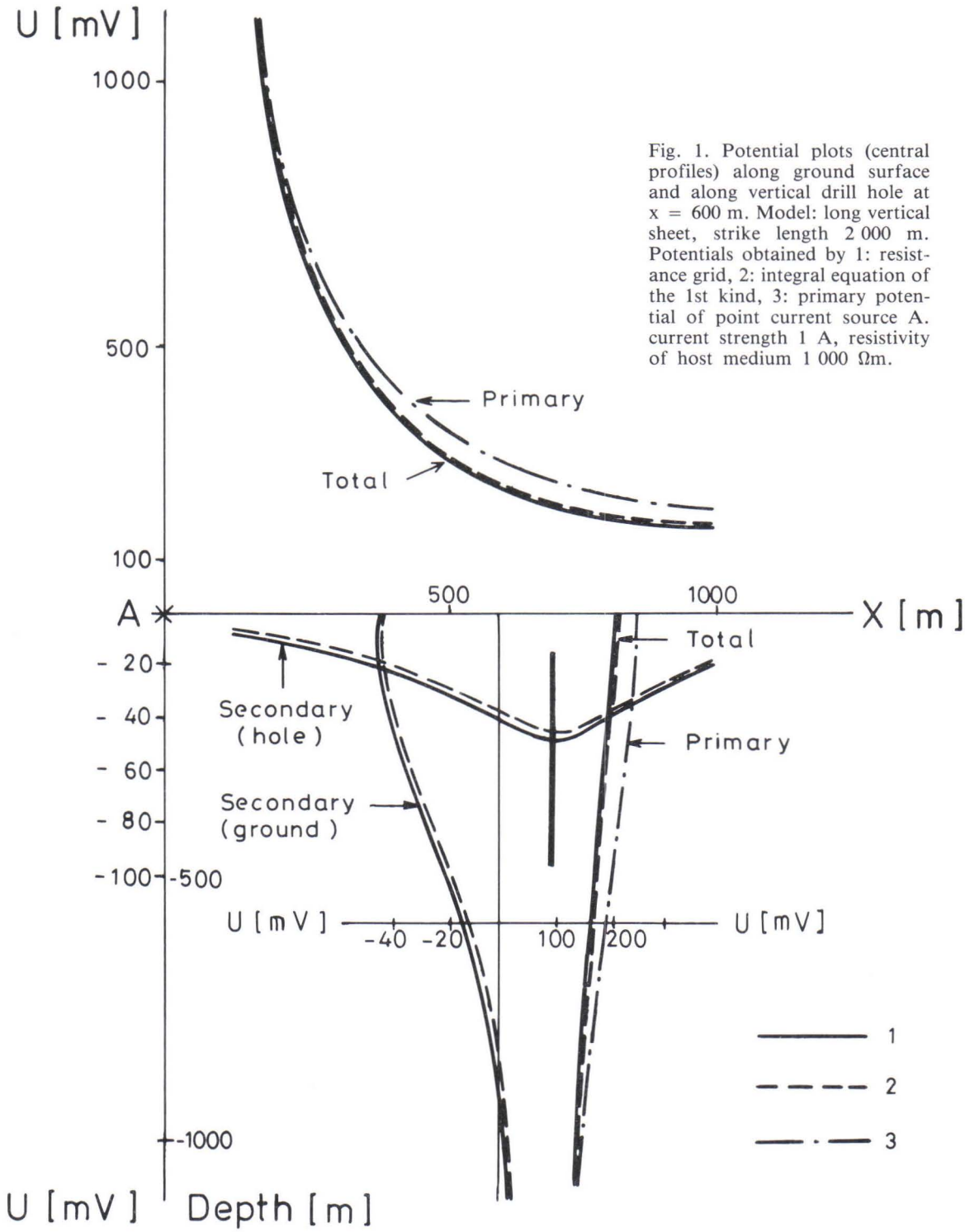

Fig. 1. Potential plots (central profiles) along ground surface and along vertical drill hole at x = 600 m. Model: long vertical sheet, strike length 2 000 m. Potentials obtained by 1: resistance grid, 2: integral equation of the 1st kind, 3: primary potential of point current source A. current strength 1 A, resistivity of host medium 1 000 Ωm.

M. Avdevich determined model anomalies for a 3-dimensional, long horizontal cylinder, as illustrated in Fig. 4 by applying method a). H. Hongisto calculated numerical anomalies for the same model by the 2 ½-dimensional approximation in method c) (Eskola and Eloranta in this issue). The numerical anomalies given by method c) were again lower in intensity than those given by method a). The loss in intensity is

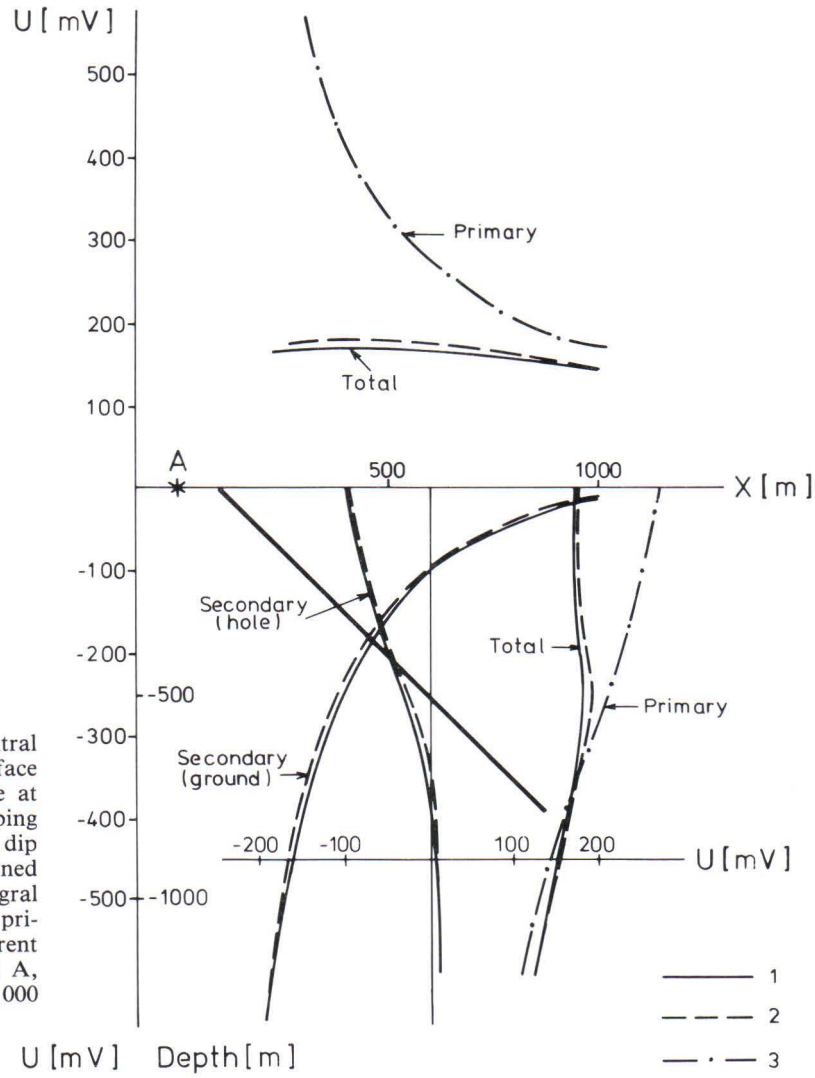

Fig. 2. Potential plots (central profiles) along ground surface and along vertical drill hole at x = 600 m. Model: outcropping sheet, strike length 2 000 m, dip angle 45°C. Potentials obtained by 1: resistance grid, 2: integral equation of the 1st kind, 3: primary potential of point current source A. Current strength 1 A, resistivity of host medium 1 000 Ωm.

partly explained by the same effect as in connection with the pure 3-dimensional solution. An additional error was also caused by the application of the 2 ½-dimensional solution itself, where the end faces were omitted in the calculations.

Comparison of modelling results for long horizontal bodies

In the following our previous comparisons, reported in the foregoing, are supplemented by choosing the ohmic resistance volume grid (method a)) as the reference system. It is used for checking the correctness and accuracy of method b) and the 2 ½-dimensional approximation in method c) in solving resistivity problems for long, 3-dimensional, highly conductive bodies in the field of a point current source. This model is particularly difficult to use in numerical modelling because, in the discretized approximation of the region of solution, the number of elements rapidly grows with the length of the strike.

Fig. 1. illustrates the primary, secondary and total potentials along central profiles on the ground surface and in a vertical drill hole, obtained by using modelling methods a) and b). The model is a long vertical sheet excited by a point current source located at x = z = 0. The secondary and total potentials obtained by different methods do not differ from each other more than 5 %. Similar conclusions can be drawn also by inspection of the potentials for a dipping sheet and an assemblage of three sheets in Figs. 2. and 3.

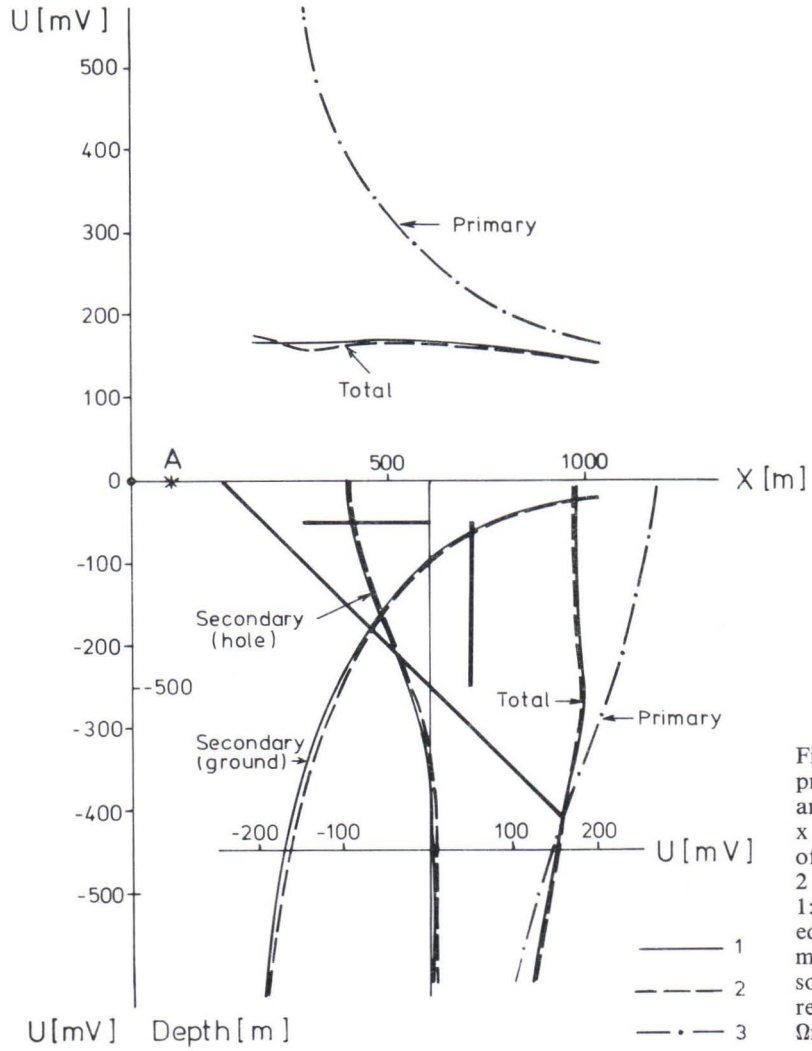

Fig. 3. Potential plots (central profiles) along ground surface and along vertical drill hole at x = 600 m. Model: assemblage of three sheets with strike length 2 000 m. Potentials obtained by 1: resistance grid, 2: integral equation of the 1st kind, 3: primary potential of point current source A. Current strength 1 A, resistivity of host medium 1 000 Ωm.

Secondary potential profiles along a ground surface and along two vertical drill holes for a perfectly conducting horizontal cylinder in the field of a point current source are shown in Fig. 4. The potentials are obtained by the resistance grid and by the integral equation of the 1st kind. For cylinders with various strike lengths (1000 m, 3000 m and 6000 m), the potential curves vary in amplitude and shape, but in all cases the potentials obtained by different modelling methods differ from each other no more than 5 %.

Fig. 5. illustrates the secondary potentials along a ground surface and along two vertical drill holes for a highly conductive horizontal cylinder in the field of a point current source (the same model as in Fig. 4.) The potential is solved by using the 2 ½-dimensional approximation in method c) (integral equation of the 2nd kind). Comparison between Figs. 4. and 5. shows that, for the model with a strike length of 6000 m, the shapes of the potential curves of Fig. 5. are highly similar to the shapes of the corresponding curves in Fig. 4. However, when the strike length of the model decreases, the similarity of the curves also decreases. Moreover, the reference levels of the potentials in Fig. 5. are considerably lower than those in Fig. 4.

The increase in similarity between the potential curves with increasing strike length is for the most part a consequence of the basic characteristic of the 2 ½-dimensional approximation, i.e., by the fact that the effect of the end faces of the model be omitted in calculations. Consequently, when the strike length grows in relation to the dimensions of the end faces, the quality of the approximation improves.

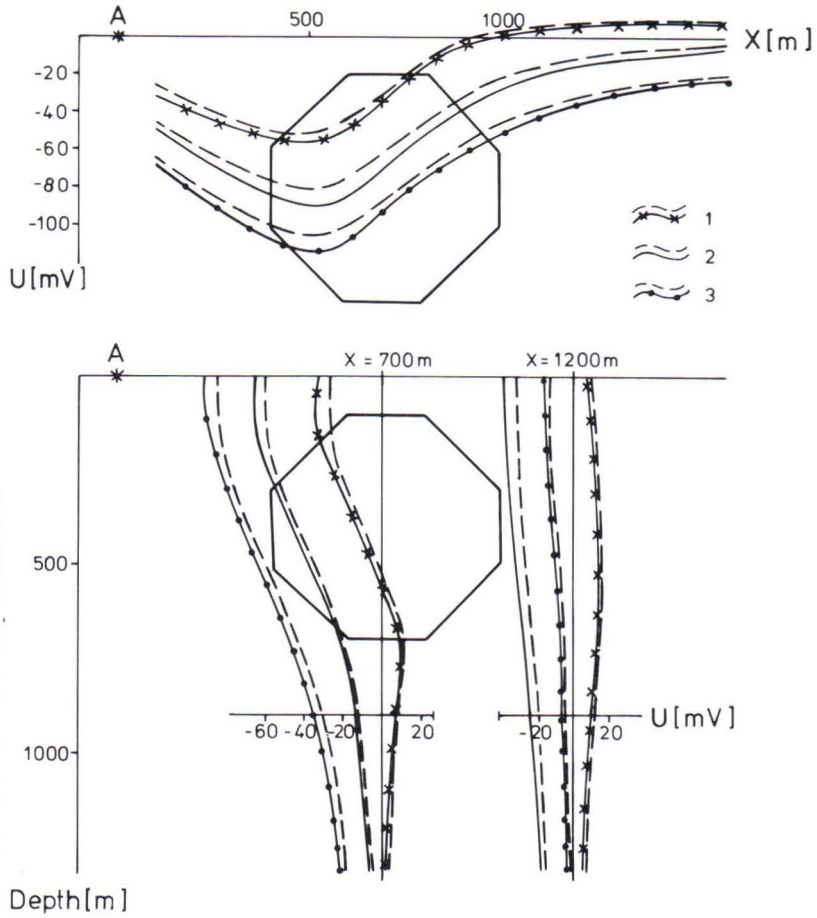

Fig. 4. Secondary potentials (central profiles) along ground surface and along vertical drill holes at x = 700 and x = 1 200 m, obtained by resistance grid (solid) line and by integral equation of the 1st kind (dashed line). Model: perfectly conducting cylinder with polygonal cross section, strike length 1: 1 000 m, 2: 3 000 m, 3: 6 000 m. Point current source A at x = z = 0. Current strength 1 A, resistivity of the host medium 680 Ωm.

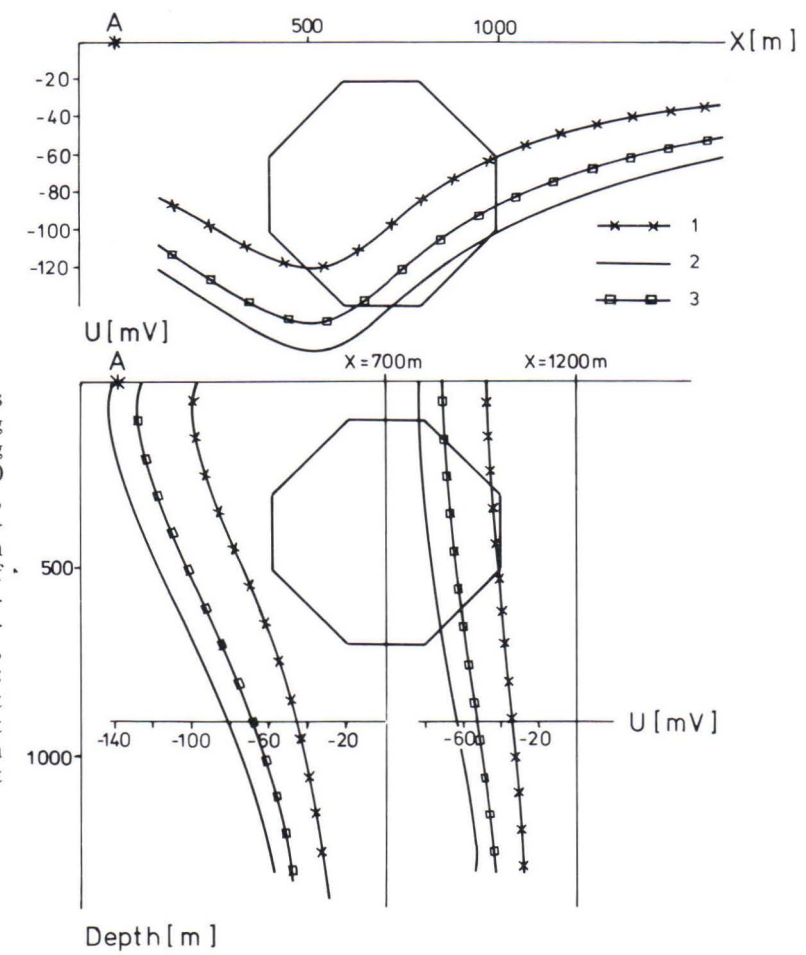

Fig. 5. Secondary potentials (central profiles) along ground surface and along vertical drill holes at x = 700 m and x = 1 200 m, obtained by using 2 ½-dimensional approximation in solving integral equation of the 2nd kind. Model: cylinder with polygonal cross section, resistivity 0.0068 Ωm, strike length 1: 1 000 m, 2: 3 000 m, 3: 6 000 m. Point current source A at x = z = 0. Current strength 1 A, resistivity of the host medium 680 Ωm.

The inaccuracy in reference level of the potential can be understood by remembering that the potential is a line integral of field strength taken from infinity to the point of calculation. In the integration, even a small systematic inaccuracy in field strength may accumulate to a considerable inaccuracy in the level of the potential. Consequently, in calculating the potential by using the 2 ½-dimensional approximation, the potential value at an arbitrary distant point (still finite) should be used as the reference level of the potential.

Conclusions

From the foregoing considerations, we can conclude that the solution of the electric potential problem on the basis of Fredholm's integral equation of the 1st kind is well suited for models where perfectly conducting bodies are located in a moderately conducting environment. The method based on Frendholm's integral equation of the 2nd kind can also be used to solve the electric field problem for the model with a high conductivity contrast if the primary source is located in a host medium (i.e., the problem is not a mise-à-la-masse problem) and the solution is made by using a complete 3-dimensional model. Owing to its faster convergence, the solution based on the integral equation of the 1st kind is, however, more appropriate for this model.

The 2 ½-dimensional approximation in solving 3-dimensional electric field problems on the basis of Fredholm's integral equation of the 2nd kind is not very suitable for models involving perfect conductors, unless the strike length is very large as compared with the other dimensions of the model. Moreover, in calculating potential anomalies, the potential value at a distant point should be used as the reference level for the potential in the anomalous region. It should also be noted that the 2 ½-dimensional approximation considered in the foregoing was originally developed for the calculation of induced polarization anomalies for long disseminated ore bodies with moderate conductivity contrasts (at most, twenty). Various test calculations have shown that, for such models, the 2 ½-dimensional approximation is a useful completion of solution methods, especially when the model is too long for a reasonably accurate solution by the complete 3-dimensional model.

References

Eloranta, E., 1984. A method for calculating misa-à-la-masse anomalies in the case of high conductivity contrast by the integral equation technique, Geoexploration 22, 77—88.

Semenov M.V., Sapojnikov V.M., Avdevich M.M., Golikov J.V., 1984. The electrical prospecting for ore bearing fields by the charge method. 216 p. (Электрорахведка рудных полей методом заряда). Nedra, Leningrad.

POSSIBILITIES OF ANALOG AND DIGITAL COMPUTERS USED FOR THE INTERPRETATION OF VERTICAL ELECTRICAL SOUNDING DATA FOR ORE DEPOSIT AREAS HAVING A COMPLEX GEOLOGICAL STRUCTURE

by

M.M. Avdevich, M.V. Semenov and N.A. Ochkur

Avdevich, M.M., Semenov, M.V. & Ochkur, N.A., 1986. Possibilities of analog and digital computers used for the interpretation of vertical electrical sounding data for ore deposit areas having a complex geological structure. *Geologian tutkimuskeskus, Tutkimusraportti 73.* 37—44, 7 figs.

The given apparaturs for interpreting the vertical electrical sounding (VES) data obtained in regions with a horizontally stratified structure is used with some difficulty for interpreting data obtained in ore regions with complex geological structures. The pattern of VES diagrams obtained in various conditions may be quite different. The possibility of interpret VES diagrams quantitatively by using analog computers (MUSG-1 unit) is described. Recommendations are given for completing the modelling with digital computers when performing operative VES data interpretation.

Key words: electrical methods, electrical sounding, ore bodies, resistivity, models, automatic data processing, USSR

Авдевич М.М., Семенов М.В., Очкур Н.А., 1986. Возможности аналоговой и цифровой вычислительной техники при интерпретации данных ВЭЗ в рудных районах со сложным геологическим строением. Геологический центр Финляндий, Рапорт исследования 73. 37—44, Идд. 7.

Существующий аппарат интерпретации данных ВЭЗ, полученных в районах с горизонтально-слоистым стоением, затруднительно применят при интерпретации материалов, полученных в рудрых районах, характеризующися сложным геоэлектрическим строеннем. Форма графиков ВЭЗ, полученных в разных условиях, может быть принципиально различной. Рассматривается возможность количественной интерпретации графиков ВЭЗ с использованием аналоговой вычислительной техники (установка МУСГ-1) и даются рекомендации по комплексированию ее с цифровой вычислительной техникой при оперативной интерпретации данных ВЭЗ.

The method of vertical electrical sounding with direct current (VES) is widely and succesfully used in oil-bearing regions which as a rule have a horizontal bedding structure. For the interpretation of VES curves obtained in such conditions, well-developed software is available. Besides, programs for the reliable solution of forward and reverse VES problems are prepared (Pylaev, 1968; Kolesnikov, 1981).

Ore-bearing regions have as a rule a block structure distorted by fractures, ore bodies are of limited size and they have an arbitrary geometrical form, etc. In such an environment, it is impossible to interpret the VES data using the software mentioned.

Even for an ideally conducting horizontal sheet of rather large size along the strike, but of limited size across the strike, lying in the homogeneous isotropic half space, the plot of apparent resistivity differs considerably from that of the infinite sheet at the same depth (Fig. 1). Moreover, this difference is exceedingly apparent when studying the field produced by ore bodies of limited size. It should be noted that a geoelectrical cross section produced according to VES diagrams along the profile over the ore body provides no information concerning the form of the body.

Therefore, in order to interpret VES data obtained in ore-bearing regions, it is necessary to solve forward problems of electrical prospecting taking into account the true geoelectrical environment.

At present, there is no technique that could be used to solve these tasks efficiently and in full scope. Discussed here is the possibility and expediency of solving such tasks by means of analog modelling on the MUSG-1 device.

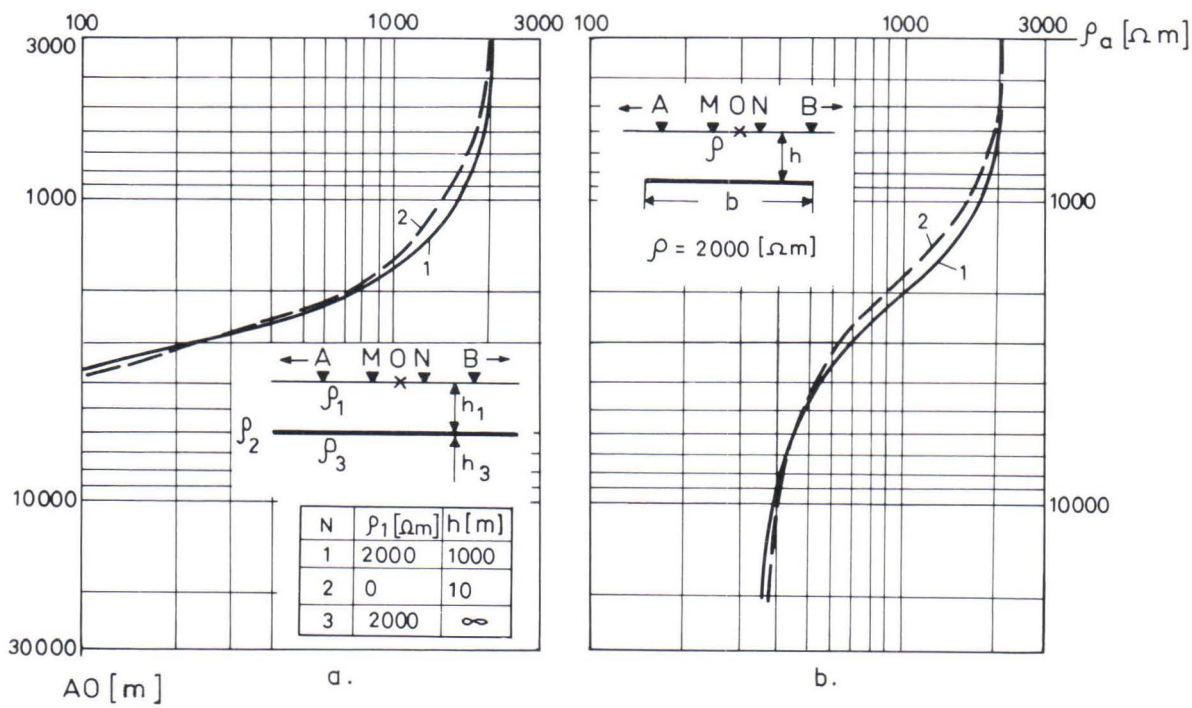

Fig. 1. VES plots over the horizontal ideally conducting sheet. a) the layer is infinite, b) the width of the layer across the strike (b) is equal to 3.4 km. Wenner array. Plots obtained 1) on the computer, 2) on the MUSG-1.

The MUSG-1 device is intended for solving two-dimensional geophysical problems. Strictly speaking, this device should not be used for studying fields caused by point-current sources. However, modelling problems may be solved with sufficient accuracy for practical purposes if certain assumptions are made. It is therefore necessary to conduct some special studies.

Particularly, VES data obtained by theoretical computer calculations were compared with VES data obtained by modelling on the MUSG-1 device. This comparison was performed for equipotential objects located in a homogeneous isotropic conductive half-space and also for a horizontally layered medium. Ves diagrams for the models mentioned may be obtained with a computer and serve as standards for checking the correctness of modelling by the MUSG-1. Some examples of such a comparison are given in the following.

Fig. 1 shows VES diagrams obtained with a computer and the MUSG-1. The diagrams shown differ from each other with a range of 5—10 %.

The same modelling error was encountered also when solving VES problems for the horizontally layered medium. Figs. 2—4 show VES apparent resistivity diagrams obtained by modelling with the computer and with the MUSG-1 for a horizontally layered medium containing a varying number of layers. The exception is the case where the substratum of a two-layer medium has an infinitely high resistivity. Here the modelling error may be as high as 20—25 % (Fig. 2c).

Fig. 5 shows the apparent resistivity plots obtained on the computer and the MUSG-1 along the profile across the body strike for the following cases: a) 2500 m long vertical bar; b) vertical sheet with dimensions of 1000 m along the strike and 2500 m along the dip.

When modelling the apparent resistivity of the vertical bar, the diagrams obtained with the computer and the MUSG-1 differ no more than by 15 % (Fig. 5a). The diagrams obtained for the vertical sheet with relatively great strike lengths (Fig. 5b) differ considerably. The reason is that in this case the polarization vectors in nature and in two-dimensional modelling differ markedly in the direction of the strike (Avdevich and Phokin, 1978). Consequently, such a case is mostly unfavourable for modelling on the MUSG-1.

The examples considered show that, with the help of two-dimensional analog modelling, it is possible in some cases to solve numerically VES problems with a margin of error up 10—15 %. This accuracy is quite sufficient for solving practical problems.

This conclusion is of great value for the solution of problems when true geoelectrical conditions are taken into account. As in analog modelling any geoelectrical environment is taken into account by the simple provision of the geometrical and physical similarity of nature and model (Avdevich and Phokin, 1978), it may be supposed that when modelling the field caused by complicated earth sections, the error of the solution will not increase in comparison with the cases described.

Let us analyze some examples of the practical use of analog modelling in the interpratation of VES data. In particular, it is advisable to analyze one of the vertical sections of apparent resistivity obtained by the method of three-electrode VES over a sulphide deposit in Kola Peninsula (Fig. 6). The sulphide ores of the vein type have resistivities of 1—10 Ωm and occur among relatively homogeneous rocks with a resistivity of 10000 Ωm. The form of the ore body is sufficiently well studied by drilling. The results of modelling on the MUSG-1 actually coincide with the results of the field observations. Here one may notice that the form of the section of the object being examined is not reflected on the pattern of apparent resistivity isolines.

In the case given the results of interpreting VES data with the help of electrical modelling on the MUSG-1 showed that the field observed is entirely explained by the known structure of the deposit and that the search for undiscovered ore bodies in the immediate vicinity of this deposit is useless.

The next example of quantitative interpretation of VES data is related to another type of sulphide deposit.

Ore objects having the form of a sheet stretched along the strike and having limited dimensions across the strike occur in conformity with host rocks. The latter is

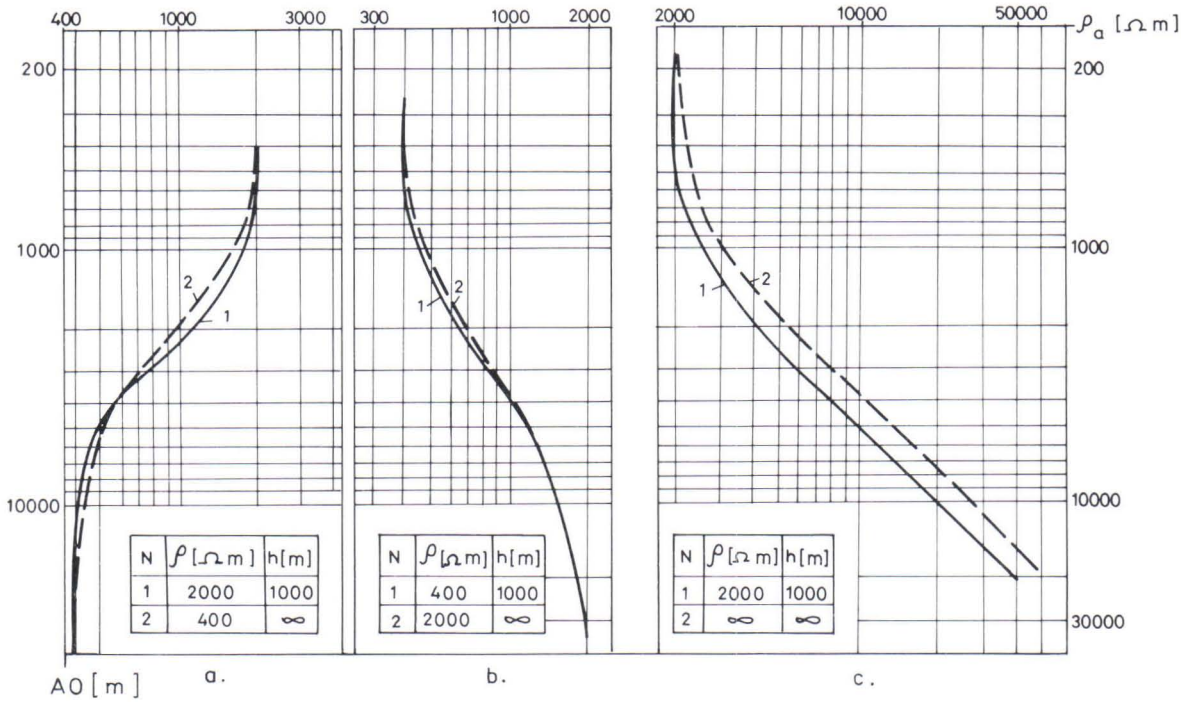

Fig. 2. VES plots over various types of two-layer media. Legends in Fig. 1.

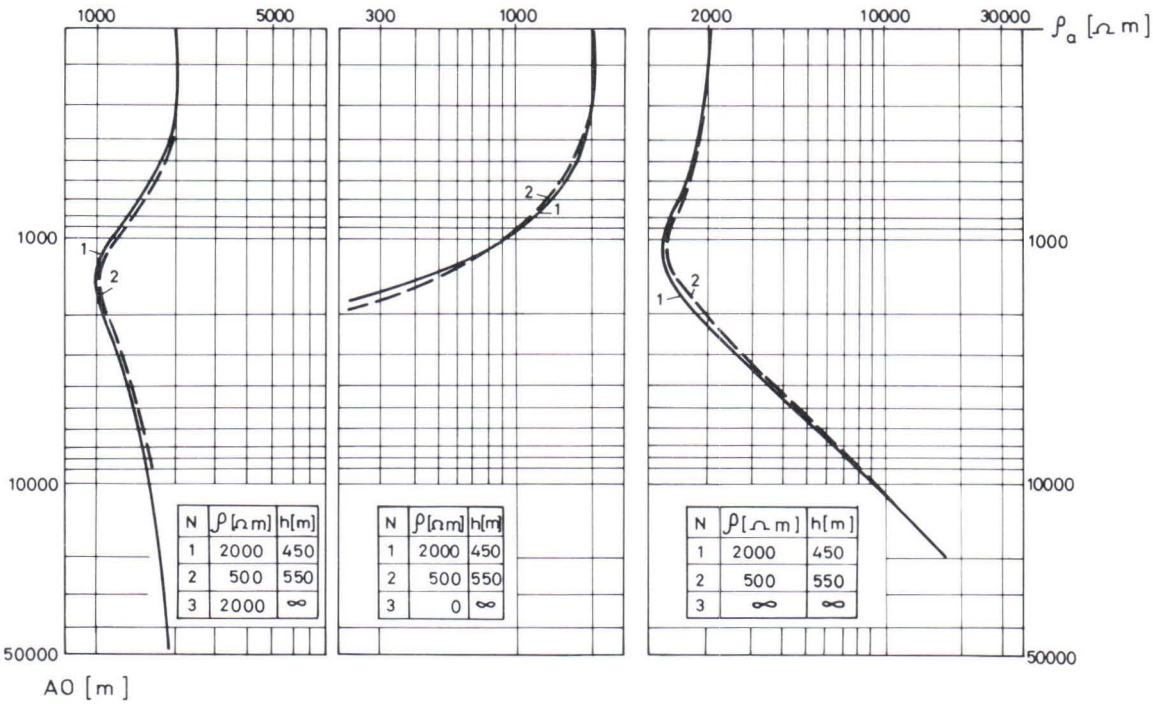

Fig. 3. VES plots over various types of three-layer media. Legends in Fig. 1.

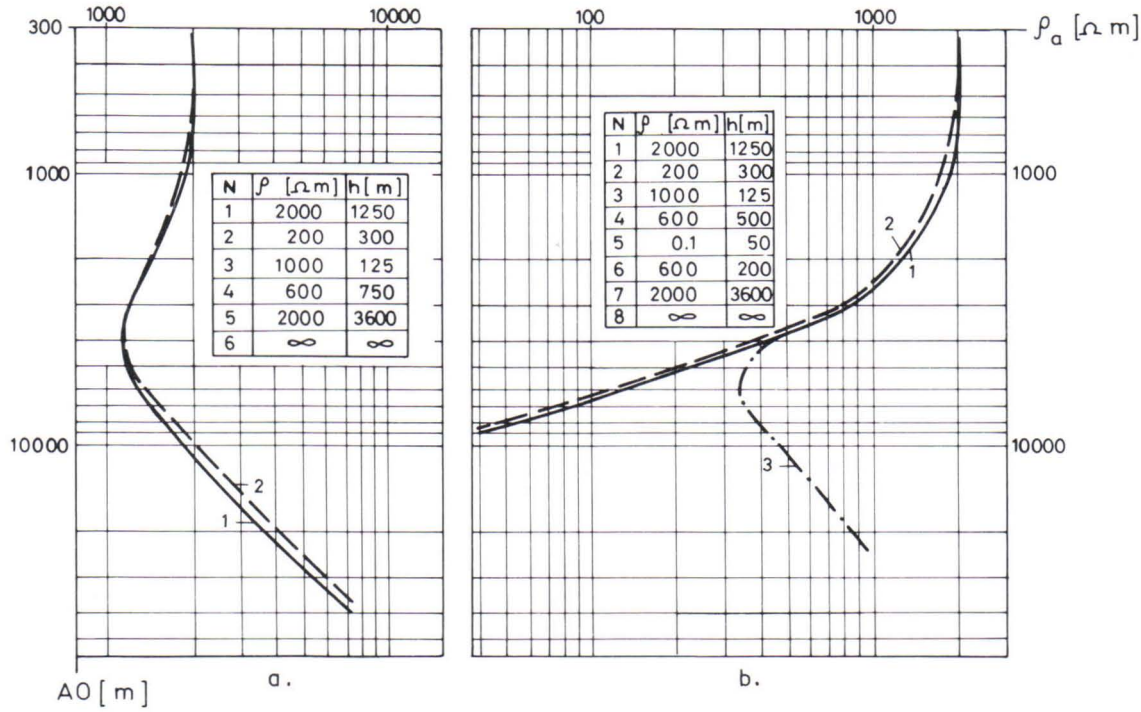

Fig. 4. VES plots over the multilayer medium. a) six-layer section, b) eight-layer section. Plots obtained 1) on the computer, 2) on the MUSG-1, 3) on the MUSG-1 (the width of the conducting layer across the strike 10 km).

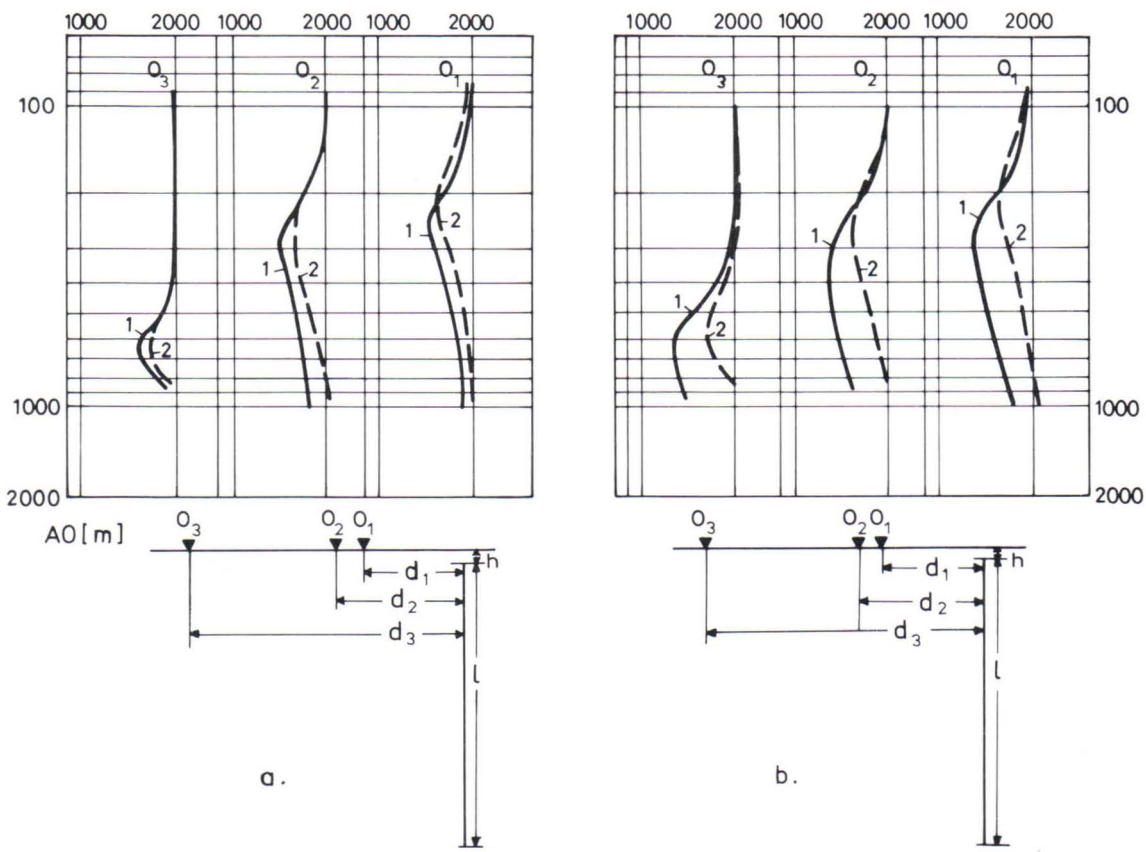

Fig. 5. VES plots over the vertical ideally conducting a) bar, b) sheet with the parameters: h = 25 m, l = 2 500 m, d_1 = 200 m, d_2 = 250 m, d_3 = 550 m. The length of the sheet along the strike L = 100 m. ϱ_a plots obtained 1) on the computer, 2) on the MUSG-1. 0_1, 0_2 and 0_3 are location points of the fixed electrode of the pole-pole array.

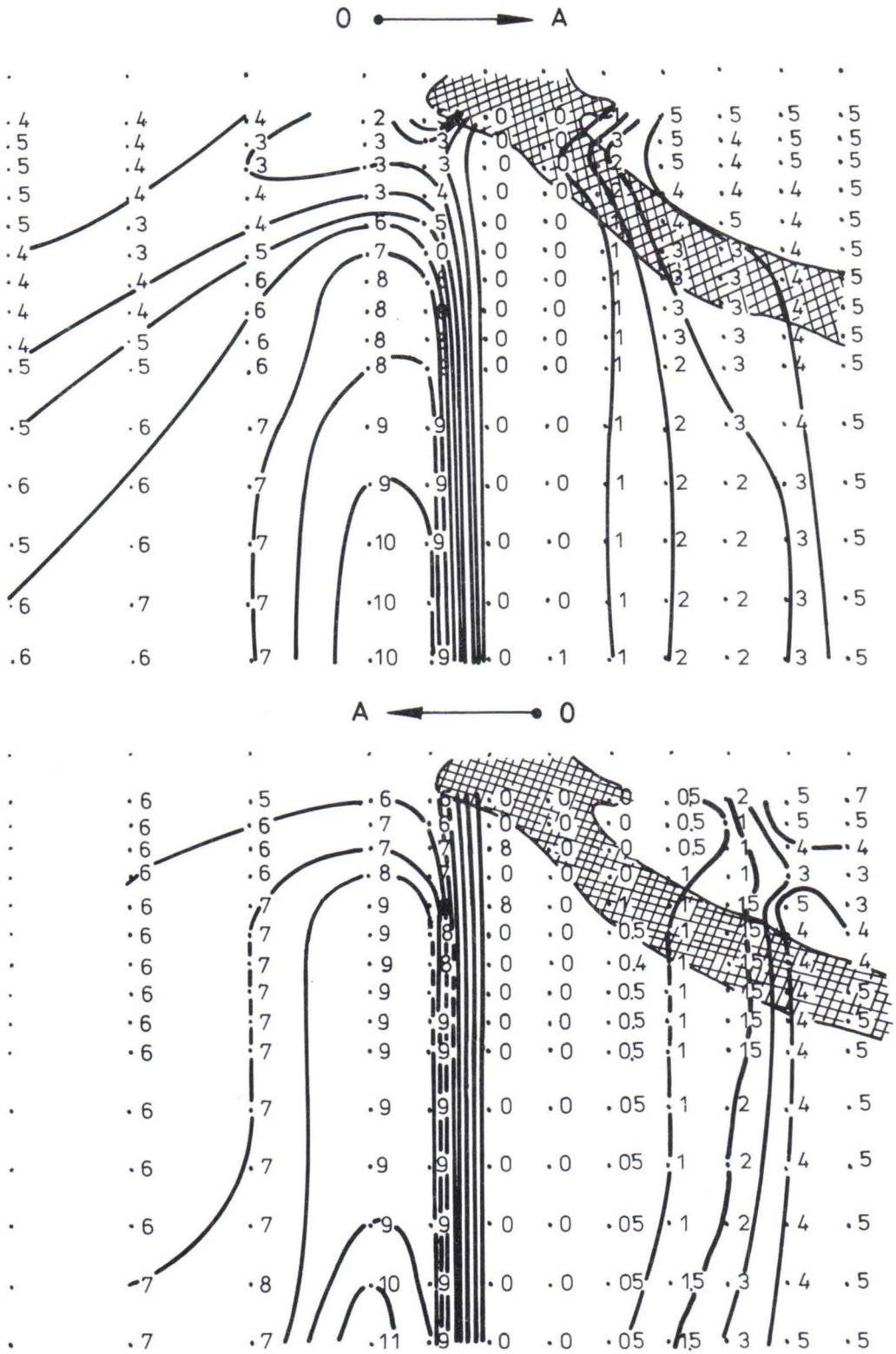

Fig. 6. The vertical section of VES apparent resistivities data at one of the sulphide ore deposits. 1) ϱ_a isolines, 2) ore body, 3) movement direction of the potential electrode.

represented by horizontally layered "puff pustry," the specific electrical resistivity of its layers differing considerably. Moreover, the block structure of the region investigated is evident, i.e., certain rock blocks have shifted relative to one another in a vertical direction along the fracture zones. The application of analytical methods for calculating the field in such conditions is impossible.

Actually, even if the sheet-shaped ore body (about 10 km) with a limited dimensions across the strike does not lie very deep (about 2 km), it cannot be considered as an infinite sheet. The apparent resistivity diagrams for a horizontally layered medium obtained by computer and by MUSG-1 for the true medium of the model differ in essence (Fig. 4b). Similar diagrams obtained in the absence of ore bodies in locations remote from fracture zones coincide with an error that does not exceed 10 %.

The main interpretation was performed by means of two-dimensional modelling on the MUSG-1. The known geological situation was fixed on the model and remained unchanged during the interpretation, but the location, size and elements of the ore body were chosen. Naturally, the anomalous field of the fixed part of the section also varied at each replacement of the model, and the result obtained was determined by the effect of the whole geoelectrical section reflected in the given model.

So all the VES data measured in the field were interpreted and the geological structure of the deposit studied was determined more accurately.

Fig. 7 illustrates the case showing that if the whole medium is assumed to be composed of horizontal layers, then the results of interpretation may be far from the truth. Diagram 2 was obtained by the MUSG-1 over the true six-layer section, where at the depth of 2100 m there lies an ideally conducting horizontal sheet (ore body). The width of the sheet across the strike (b) is 3800 m. According to this diagram, the section

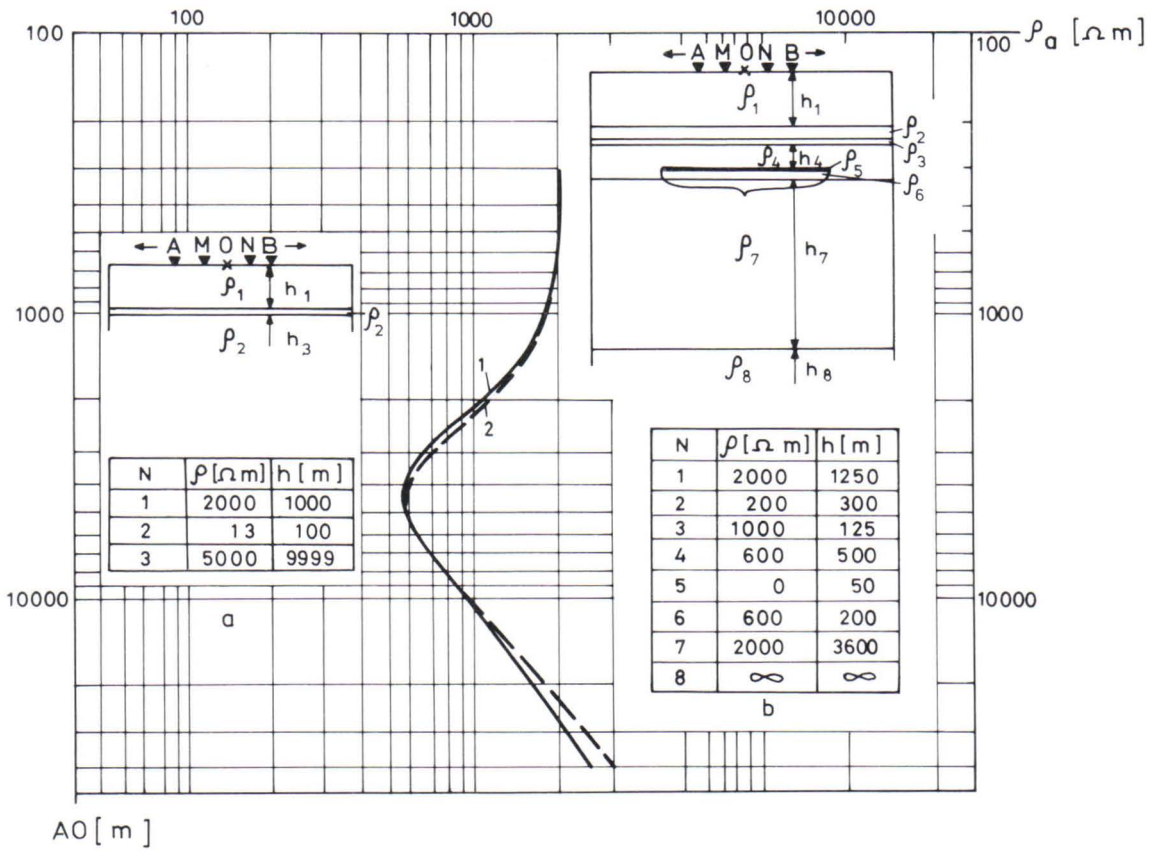

N	ρ [Ω m]	h [m]
1	2000	1000
2	13	100
3	5000	9999

N	ρ [Ω m]	h [m]
1	2000	1250
2	200	300
3	1000	125
4	600	500
5	0	50
6	600	200
7	2000	3600
8	∞	∞

Fig. 7. The results of VES data interpretation using analog and digital computers: a) the horizontal layer section chosen by computer-assisted interpretation, b) the section modelled on the MUSG-1; the width of the ideally conducting sheet across the strike, $\delta = 3\ 800$ m. ϱ_a plot obtained: 1) on the computer, 2) on the MUSG-1.

was chosen in conformity with the information available. The authors asked Mr. E. Lakanen, the scientific worker of the Outokumpu Company, Finland, to make the interpretation on the basis of the horizontal layer model with the use of desktop computer HP 9845. ϱ_a diagrams agreed very well, but the geoelectrical section differed in essence from the correct one (Fig. 7b). As a result of such and interpretation, the anomaly obtained could be explained by a conductive layer (non-ore) bedding much nearer to the surface of the earth than the true ore body and so false geological recommendations could be given.

The following conclusions concerning the VES data can thus be made.

At first stage, it is necessary to perform an interactive interpretation of the VES data on the relatively ''quiet'' zones where the distorting effect of the objects studied or the geoelectrical heterogeneity is not large. The aim of this interpretation is the choice of ''host medium'' where the object is located.

The following interpretation by the trial-and-error method, where the main geoelectrical heterogeneities are taken into account (relief, overburden with various thickness, fracture zones, various resistivity rock block contacts, etc.) must be performed by means of analog modelling. The aim of this interpretation is the determination of the location, size and peculiarities of the object studied.

Such a combination of digital and analog computer methods gives the rather simple possibility of accomplishing an efficient quantitative interpretation of VES data collected in areas having a complicated geological structure and to obtain reliable results.

References

Avdevich, M.M., 1977. The modelling of an electrical field on electrical conducting paper used in the geological interpretation of vertical electrical sounding curves (VES). (Моделирование электрического поля на электропроаодной бумаге при геологическом истолковании кривых вертикальных электрических зондирований (ВЭЗ). Prospecting methods and engineering (Методика и техника разведки). No 116 VITR. Leningrad, 42—45.

Avdevich M.M. & Phokin A.Ph., 1978. Electromodelling of potential fields. (Электромоделирование потенциальных полей). Nedra, Leningrad, 99 p.

Kolesnikov V.P., 1981. Computer, — assisted processing and interpretation of vertical electrical sounding data. (Обработка и интерпретация результатов вертикального электрического зондирования с помощью ЭВМ). Nedra, Moscow, 141 p.

Pylaev A.M., 1968. Manual for the interpretation of vertical electrical soundings. (Руководство по интерпретации вертикальных электрических зондирований). Nedra, Moscow, 132 p.

THE BEHAVIOUR OF APPARENT IP SPECTRA OF MODELS WITH THE RESISTIVITIES OBEYING THE COLE-COLE DISPERSION MODEL

by

Heikki Soininen

Soininen, H., 1986. The behaviour of apparent IP spectra of models with the resistivities obeying the Cole-Cole dispersion model. *Geologian tutkimuskeskus, Tutkimusraportti 73.* 45—49.

In the case of one body with Cole-Cole polarization embedded in an unpolarizable half-space the phase spectrum of apparent resistivity resembles quite closely in functional form the true petrophysical Cole-Cole phase spectrum. The apparent spectra shift on the log-log scale downward, and toward lower frequencies.

Of the apparent Cole-Cole parameters inverted from the anomaly spectra the apparent chargeability is noticeably smaller than the chargeability of the petrophysical spectrum. The apparent frequency dependence, on the other hand, is very close to the value of the true frequency dependence. The shift of the apparent phase spectrum toward lower frequencies partly compensates for the decrease in the apparent time constant caused by attenuation of the spectrum. The apparent time constant is thus close to the true time constant.

The effect of a polarizable half-space may be handled by simply adding the phase spectrum of the half-space to the apparent phase spectrum due to the body.

The apparent spectrum of several polarizable bodies builds up in a complex fashion. Nevertheless, by measuring the spectra at a number of points along a profile crossing over formations differing in time constants, the various components can be discriminated from the apparent spectra even if the difference in time constants is small. As the conductivity contrast decreases, the share of the spectrum of the body in the apparent spectrum increases. Likewise the body with the smaller time constant is in more advantageous position than the body with the greater time constant.

Key words: electrical methods, induced polarization, resistivity, infrared spectra, models

Соининен, Х., 1986. Поведение кажущихся вп спектров моделей с удельными сопротивлениями соотвестствующими модели кол-кол. Геологический центр финлянлии, Рапорт исследования 73. 45—49.

В случае одного тела с поляризацией Кол-Кол в неполяризуемом полупространстве фазочастотный спектр кажушегося удельного сопротивления функционально сходны с фактическим петрофизическим фазочастотным спектром Кол-Кол. Кажущиеся спектры перемещаются вниз в логарифмической шкале, к более низким частотам.

Из кажущися параметров Кол-Кол обращенных из спектров аномалий кажущаяся поляризуемость гораздо ниже поляризуемости петрофизического спектра. Кажущаяся зависимость от частоты, однако, близка к значению фактической зависимости от частоты. Смещение кажущегося фазочастотного спектра к более низким частотам частью компенсирует уменьшение кажущейся постоянной времени вызванное затуханием спектра. Следовательно кажущаяся постоянная времени близка к фактической постоянной времени.

Эффект поляризуемого полупространства будет решен прибавлением фазочастотного спектра полупространсева к кажущемуся фазочастотному спектру тела.

Кажушийся спектр некоторых поляризуемых тел составлен комплексным образом. Измерение спектра в некоторых точках вдоль профиля через формации с различными постоянными времени позволяет отделит разнообразные составляющие от кажущихя спектров даже в случае небольших разностей в постоянных времени. С уменьшением различия по удельной проводимости доля спектра тела в кажущемся спектре увеличивается. Тело с более низкой постаянной времени находится в более выгодном положении чем тело с высокой постаянной времени.

Introduction

The objective in spectral induced polarization (IP) method is to determine the distribution of resistivity of the earth at a wide frequency band (e.g., 1/1024) ... 4096 Hz). Principally owing to differences in mineral textures, the petrophysical resistivity spectra of rock types differ from each other, and hence the spectra can be used for such purposes as identification of mineralization types (Pelton et al., 1978).

In field measurements, however, the frequency spectrum of the petrophysical resistivity is not measured, but rather the apparent spectrum dependent upon the electrode array and the geometry of the targed body. In the application of the spectral IP therefore, one must know how the petrophysical spectrum transforms into an apparent spectrum. The reduction of the apparent IP spectrum into the true spectrum has often been done with the 'dilution factor' (Pelton et al., 1978). Description of the frequency-dependent complex system with such a frequency-independent constant is wrong, however, and leads in practice to erroneous spectral behavioural relations (Soininen, 1984a). The reductions between the anomaly and the original spectrum must thus be based on theoretically correct considerations.

In this paper the behaviour of the apparent spectrum is summarized first in the case of a polarizable body situated in an unpolarizable host rock, second of a polarizable prism situated in a polarizable half-space and finally of two polarizable prisms joined together in a unpolarizable half-space (Soininen, 1984b, 1985). The examinations were done in the frequency domain; this is more advantageous than the time domain for both theoretical treatment and practical spectral measurements (Soininen, 1984c). The frequency dependent resistivity of the medium is depicted by means of the Cole-Cole dispersion model.

Cole-Cole dispersion model

On the basis of the laboratory and in-situ measurements it has been observed that in linear regime the frequency-dependent resistivity of a rock can be described well by the Cole-Cole dispersion model (Pelton et al., 1978, Hallof and Klein, 1982a,b). The Cole-Cole dispersion model

$$Z(\omega) = R_0 \left(1 - m\left(1 - \frac{1}{1 + (i\omega\tau)^c}\right)\right), \tag{1}$$

where

$Z(\omega)$ = the complex impedance,
R_0 = the value of $Z(\omega)$ at zero frequency,
m = the chargeability,
c = the frequency dependence,
τ = the time constant,
ω = the angular frequency, and
i^2 = -1

provides a good basis for the analysis of spectral IP measurements, because the characteristic features of a spectrum can be represented solely by means of the four parameters R_0, m, c and τ.

R_0 is highly variable and depends on porosity, groundwater conductivity and the presence of interconnected or veined conductive minerals. The chargeability m is a measure of the magnitude of IP effect. It is proportional to the volume percent of conductive minerals. It is restricted to the range $0.0 \leq m \leq 1.0$ by the definition of Seigel (1959). The requirement for a complex resistivity to be a function whose

amplitude decreases with increasing frequency (relaxation) restricts c to the range $0.0 < c \leq 1.0$. For mineralization with a single grain size, c is equal to or greater than 0.5, if grain size is distributed about some mean value typical value of c is 0.25 (Pelton et al., 1978). The time constant τ is related to the frequency at which the main IP effect occurs and is dependent on the grain size and texture of metallic minerals present. It ranges from 10^{-3} s to 10^{+4} s. The time constant is a crucial parameter for mineral discrimination for example the time constant of sulfides is generally up to four decades smaller than that of graphite (Pelton et al., 1978).

The Cole-Cole phase spectrum is symmetrical on a double logarithmic scale and its positive and negative asymptotic slopes are equal to the frequency dependence c. The frequency f at which the phase angle peak occurs is

$$f = \frac{1}{2\pi\tau\,(1 - m)^{1/2c}} \cdot \tag{2}$$

If the resistivity spectrum of the medium is described with the Cole-Cole dispersion model two questions will arise; first, is it possible to invert the apparent parameters from the anomaly spectra and second, how do the inverted spectral parameters stand in relation to the original petrophysical parameters?

One polarizable body in an unpolarizable half-space

Let us first discuss the behaviour of the apparent spectrum in the case of a polarizable body in an unpolarizable environment. Soininen (1984b) examined the forming of the apparent spectra by numerical modelling. The computations were done using the integral equation technique (Eskola, 1979). The frequency dependent resistivity of the three-dimensional prism model was depicted by means of the Cole-Cole dispersion model (1). The values of the Cole-Cole parameters were varied in such a way that the chargeability had values between 0.35 and 1.0. With each chargeability value, the anomalies were calculated with the values of frequency dependence $c = 0.15$, 0.32, and 0.60. The ratio of the resistivity of the environment to the resistivity of the prism at direct current was 5 and 20. Both the gradient array and dipole-dipole array were used.

According to the model calculations it can be stated that the essential behavioural relations of the spectra are independent of a particular electrode array used.

The phase spectra of apparent resistivity resemble quite closely in functional form the original petrophysical phase spectra of the Cole-Cole dispersion model. The phase angle anomaly is always smaller than the true phase angle of resistivity of the rock and that is why the apparent phase spectra shift on the log-log scale downward. Important is that they shift also to left toward lower frequencies.

The apparent Cole-Cole parameters have been inverted from the apparent spectra using Levenberg-Marquardt algorithm. The apparent chargeability m_a is generally noticeably smaller, owing to the geometric attenuation, than the chargeability of the original petrophysical spectrum. The apparent frequency dependence c_a, on the other hand, is very close to the value of the true frequency dependence.

The values of apparent time constant τ_a, remain smaller than their petrophysical value. They are closer to it with high values of frequency dependence and low values of chargeability. The apparent time constants deviate, however, almost invariably less than one decade from the value of true time constant.

Keeping the apparent time constant close to the time constant of the petrophysical spectrum is helped by the fact that as the spectrum attenuates it also shifts toward the lower frequencies. This can be easily understood on the basis of following analysis. Let us solve the time constant τ_a from equation (2). We can then see that the diminishing of m_a tends to diminish τ_a. At the same time, however, the spectrum shifts toward the left, upon which f diminishes and therefore τ_a increases. τ_a remains now close to its petrophysical value. It is possible in principle to obtain by direct inversion from an apparent spectrum measured in the field a reasonable estimate of the frequency dependence and time constant of the true spectrum of a polarizable body.

One polarizable body in polarizable half-space

Soininen (1985) calculated anomaly spectra for a vertical, rectangular, polarizable prism situated in a polarizable half-space. The effect of the conductivity contrast and of the difference in time constants and chargeabilities between the prism and environment was studied.

As the difference in time constants increases, the spectrum of the prism becomes increasingly differentiated from that of the environment in the apparent spectrum. Further, as the conductivity contrast is reduced the share of the spectrum of the prism in the apparent spectrum increases. On the contrary, as the chargeability of the environment increases, the apparent spectrum approaches the petrophysical spectrum of the environment in shape.

It is possible to represent the apparent resistivity spectrum in the case of a polarizable prism in a polarizable environment (both with Cole-Cole dispersion) by the product of two Cole-Cole dispersion models (i.e. the sum of the dispersion model phase spectra) even if the environment is highly polarizable.

The phase spectrum of the half-space contributes almost unattenuated to the apparent spectrum and thus the apparent spectral parameters describing the half-space are close to the parameters of the petrophysical spectrum in value. Of the inverted parameters describing the spectrum of the prism, the apparent chargeability m_a remains smaller than the chargeability of the petrophysical spectrum owing to the attenuation of the spectrum. The reduction in the share of the prism spectrum in the apparent spectrum at large conductivity contrast values is manifested as a reduction in m_a as the conductivity contrast grows. The frequency dependence c_a is very close to its true value; likewise the time constant τ_a, for its natural range of variation is close to the time constant of the petrophysical spectrum.

Several polarizable bodies

The use of the spectral IP method as an aid to identifying mineralization is generally based on the difference in the time constants of the resistivity spectra of the mineralization types. Hence, in the case of several polarizable bodies, the problem is the discrimination of the components with different time constants from the apparent spectrum measured. Soininen (1985) examined how an apparent spectrum is built up in the case of two vertical, rectangular prisms joined together, and polarizable with different dispersion. The spectra were calculated at two points at the surface above the center of prisms.

The apparent phase spectra produced by two polarizable prisms are built up in a complex fashion from the petrophysical spectra of prisms. This is because the apparent spectra are affected not only by the petrophysical spectra of the prisms but also by their geometry and mutual attitude. The apparent spectrum is not simply the sum of the apparent phase spectra of the prisms, and therefore we do not get with direct inversion an estimate for the values of the petrophysical spectral parameters of a model of several bodies. Some qualitative behavioural relations can, however, be stated.

By measuring the spectra along a profile crossing over the prisms, formations differing only from their time constants can be distinguished from each other even if the difference in their time constants is small. The spectra calculated above the center of each prism do not have the same shape even though the petrophysical spectra, time constants excepted, do. The spectrum calculated over the prism with smaller time constant is closer in shape to the original petrophysical spectrum than is the spectrum over the prism with larger time constant.

When the resistivity of the prism with larger time constant reduces (the conductivity contrast increases) the share of the spectrum of that body in the apparent spectrum diminishes. The trend is similar when the conductivity contrast of the body with larger time constant increases; the share of the spectrum of the formation in the apparent spectrum diminishes as the conductivity contrast grows. Nevertheless, the body with the smaller time constant can be perceived more readily than the body with the

larger time constant. This is attributed to the fact that as the spectra differ from each other only in the time constant, the relaxation models at all frequencies always give higher absolute values of resistivity to the body with the smaller time constant than to the body with greater time constant. Hence the effective conductivity contrast of the body with the smaller time constant is lower, and its impact on the total spectrum is greater than that of the body with the greater time constant.

Summary

The functional form of the Cole-Cole spectrum of a polarizable body situated in an unpolarizable environment preserves well in a potential-theoretic transformation to the apparent spectrum. For this reason, the Cole-Cole dispersion model can also be fitted into an apparent spectrum. Of the parameters inverted from apparent spectra, the apparent frequency dependence c_a preserves well its petrophysical value. The apparent time constant τ_a remains somewhat smaller (generally, however, less than a decade) than the petrophysical time constant. From the practical standpoint of mineral discrimination, however, the apparent time constant is generally sufficiently close to its true value.

The effect of a polarizable environment on an apparent phase spectrum can be readily approximated by summing the petrophysical phase spectrum of the host medium with the apparent phase spectrum caused by the model in a unpolarizable environment. Thus we obtain the spectral parameters by inversion from the apparent phase spectrum by fitting into it the sum of two Cole-Cole phase spectra.

In the case of several polarizable bodies, the apparent spectrum is built up in a complex way, and it depends on the mutual attitude of the bodies as well as the electrode configuration used. The apparent phase spectrum can no longer be described simply as the sum of the spectra of its components. We can, however, draw some qualitative conclusions concerning the behavioural relations of the spectra. The aim of spectral measurements may be the mapping of different parts of a formation that differ in their time constant. By making measurements at various points along a profile crossing over the formation, the components that differ in time constant are discriminated form the apparent spectra, even if there is only a small difference in the time constants.

In a system with two polarizable bodies, the spectrum of the body with the smaller conductivity contrast tends to be dominant. Likewise, it is easier to distinguish a formation with a smaller time constant adjacent to a body with a larger time constant than it is to distinguish a body with a larger time constant. This behaviour is an advantage in the identification of sulfide mineralizations if we remember that the time constant of sulfides is generally up to four decades smaller than that of graphite.

References

Eskola, L., 1979. Calculation of galvanic effects by means of the method of sub-areas: Geophys. Prosp., 27, 616—627.

Hallof, P.G. & Klein, J.D., 1982a. Electrical parameters of volcanogenic mineral deposits in Ontario: Presented at the 52nd Annual International SEG Meeting, Dallas.

Hallof, P.G., & Klein, J.D., 1982b. Electrical parameters of nickel-copper ores at Sudbury, Ontario: Presented at the 52nd Annual International SEG Meeting, Dallas.

Pelton, W.H., Ward, S.H., Hallof, P.G., Sill, W.R. & Nelson, P.H., 1978. Mineral discrimination and removal of inductive coupling with multifrequency IP: Geophysics, 43, 588—609.

Seigel, H.O., 1959. Mathematical formulation and type curves for induced polarization: Geophysics, 24, 547—565.

Soininen, H., 1984a. Discussion on "Mineral discrimination and removal of inductive coupling with multifrequency IP" by Pelton, W.H., Ward, S.H., Hallof, P.G., Sill, W.R., and Nelson, P.H.: Geophysics, 49, 1556—1557.

Soininen, H., 1984b. The behavior of the apparent resistivity phase spectrum in the case of a polarizable prism in an unpolarizable half-space: Geophysics, 49, 1534—1540.

Soininen, H., 1984c. Inapplicability of pulse train time-domain measurements to spectral induced polarization: Geophysics, 49, 826—827.

Soininen, H., 1985. The behavior of the apparent resistivity phase spectrum in the case of two polarizable media: Geophysics, 50, 810—819.

Galvanic methods and equipments

REVIEW OF THE LATEST GALVANIC METHODS AND EQUIPMENT USED IN FINLAND

by

E.Lakanen

E. Lakanen 1986. A Review of the latest galvanic methods and equipment used in Finland. *Geologian tutkimuskeskus, Tutkimusraportti 73.* 52—59, 3 tables.

The four main galvanic methods and their variants are briefly discussed. Some of the instruments most frequently used today in Finland are specified. Self-potential is seldom used. Resistivity is quite important with the commonly used variants of logging and sounding. IP has many applications and more research is under way. Mise-à-la-masse is a valuable method for detailed investigation. Instruments are much alike, because the basic parameter, voltage, is measured in all of them. Thanks to modern electronics some progress has been made in their use.

Key words: electrical methods, self-potential methods, resistivity, induced polarization, mise-à-la-masse, instruments, review, Finland

Лаканен, Э., 1986. ОБзор последних гальванических методов и аппаратур применяемых в Финляндии. Геологический центр Финляндии, Рапорт исследования 73. 52—59.

Коротко описываются чентре главных гальванических методов и их варианты. Специфируются некоторые употребляемые в Финляндии сеголня инструменты. Потенциал самопроизвольной поляризации редко применяется. Удельное сопротивление играет значительную роль вместе с обыкновенно применяемыми вариантами каротажа и зондирования. ВП имеет много применений и дальнейшее исследование проводится. Метод заряда являеися важным методом при детальном изучении. Инструменты довольно сходные, так как основной параметр, напряженые, измеряется всеми инсирументаме. Благодаря современной электронике прогресс достигнут в их пользовании.

Introduction

The following is a short description of the galvanic methods and equipment currently used for ore prospecting in Finland.

There are four main methods: self-potential (SP), resistivity, induced polarization (IP) and charged potential (CP) or mise-`a-la-masse. Their overall importance is illustrated by the fact that they account for roughly 20 per cent of the entire volume of ground geophysics in ore prospecting in Finland. The most popular of the four methods is IP. CP and in situ resistivity are also used quite often, but SP is applied very seldom. The number of resistivity soundings (vertical electric soundings) is increasing.

SP is the only passive (without controlled source) method. The basic parameter measured in all these methods is potential (voltage). Therefore their principles and modes of utilization are similar and the equipment is interchangeable. Resistivity can be divided into three variations: mapping or profiling, sounding and combined. By in situ resistivity is meant logging and drill core analysis. Table 1 gives some information about these methods and Tables 2 and 3 specifications of the equipment commonly used, receivers and transmitters respectively.

Methods

Self-potential (SP)

SP is the most feasible galvanic method. The voltage between one fixed and one moving electrode is measured using non-polarizable electrodes. Unfortunately it does not give too much information and so it is very rarely used in Finland nowadays; it was more popular during the seventies. It is used more often in drill holes than for ground survey. There are rough wide anomalies and non-stable peaks, but only the former can be used reliably for mapping large conductors and sometimes for estimating the depth extension of a conductive body. Its correlation with some geochemical anomalies has been observed, but not useful application has been devised.

Resistivity

Resistivity has been used more for geotechnical purposes. Determination of overburden thickness using soundings has become increasingly popular, even in ore prospecting. Improved equipment and interpretation have boosted resistivity sounding at the expense of refraction seismics. Only in a few cases has it been used to locate bedrock conductors. Some success has been achieved in follow-up studies of gently dipping conductive horizons down to 300 m depth. In situ resistivity determinations with special logging probes and small electrodes are as common as susceptibility measurements.

The only equipment that is needed is a current source and two all-purpose meters; one measures the current, other the voltage. Manual SP compensation has made the instrument suitable for special purposes. For the past seven years more sophisticated microprocessor-controlled devices with authomatic rejection of linear SP and drift have been available. Stacking has improved resolution. Both DC and low-frequency (about 1 Hz) current is used. Non-polarizable electrodes are no longer necessary.

The most commonly used electrode configuration in the sounding method is the Schlumberger, also called the central gradient configuration. Sometimes the half-Schlumberger or Hummel method is used. The fraction of the current pentrating the deeper levels increases with the electrode separation. At least six current electrode

Table 1. The galvanic methods used in Finland.

Method	Target	Site surveyed	Configuration	Parameter	Epuipment
CP	Follow-up and connections between conductors	Ground and borehole	Potential	Voltage DV/A	Gefinex 100
IP	Locating weak conductors and disseminations	Cround and borehole	Dipol-dipole, Gradient and Pole-dipole	Chargeability mV/V Frequency effect and Phase %, mrad	Scintrex IPR-10 Systal R DHIP-2
Spectral IP	Investigated				
Resistivity profiling	Delineation of conductors (by-product of IP)	Ground	,,	Apparent resisstivity Ωm	Same as IP
mapping sounding	Determination of overburden thickness and tracing of gently dipping conducting sheets	Ground	Schlumberger and Half-Schlumberger	,,	AMEM SAS-300 Gefinex 100
combined	Determination of overburden thickness and delineation of conductors	Ground	,,	,,	,,
in situ	Logging	Borehole	Wenner	,,	PROM-2 RRK-10
SP	Mapping larger conductors and estimation of their depth extensions	Ground and borehole	Potential		
Voltage mV	Geonics SP-19				

Table 2. Specifications of the galvanic equipment used in Finland, receivers.

Model	Gefinex 100 CPRS 2062	Terrameter SAS-300	IPR-10	Syscal-R	RROM-2
Company	Outokumpu Oy, Finland	ABEM, SWEDEN	Scintrex Ltd., CANADA	BRGM, FRANCE	Rautaruukki Oy, Finland
In use	since 1981	1981	1978	1982	1979
No. of units	5	7	4	1	7
Method	CP	Resistivity	IP/time domain	IP/time domain	Resistivity/Wenner array
Other	Resistivity and SP	SP and CP (with Booster)	Resistivity and SP	Resistivity and SP	a = 318 mm, ø 40 mm
Displayed parameter	In-phase and guadrature components of potential divided by current, mV/A	Resistance, Ω	Chargeability, mV/V	Chargeability, mV/V	Resistivity, Ωm
Range	15 automatically selected maximum voltage 6640mV	1, 100, 10k, 1MΩ	150 mV/V maximum	0-8V, 6 ranges automatically selected by √10 step	1-400000 Ωm, logarithmic output
Resolution	0.01 mV/A	0.0005 Ω	0.1 mV/V	0.03 mV	0.1 mV/cm, 2V/decade
Accuracy	1 % of reading at 20°C	2 % of reading	3 % of reading		
Input impedance	20 M Ω (1 Hz)	10 M Ω minimum	3 M Ω	10 M Ω	
Display	LED, 5 digits	LCD, 4 digits	LCD(LED) 4 digits	LCD	Analog recorder RRAR-3
Compensation	Automatic, SP and linear drift	Automatic, SP	Automatic, SP	Automatic, SP	(Data logger option, KTP-84)
Noise rejection	80dB 50Hz	95dB 50Hz, 85dB 16—20Hz	50dB 50Hz	24dB/octave (low pass) 50/60Hz	
Operating temperature	—20° ... +50°C	—10° ... +70°C	—30° ... +60°C		—20° ... +50°C
Humidity	Splash-proof	Splash-proof	Splash-proof		Max. working pressure of probe 10 MPa
Power supply	Dry Pb rechargeable batteries, 12V 2.5 Ah	NiCd rechargeable batteries, 12V	4 D cells, 6V	7 C cells, 10 V	Recorder Pb rechargeable batteries, 12V
Weight	9.7 kg incl. batteries	5.6 kg incl. batteries	3.6 kg incl. batteries	7.5 kg	Recorder 18 kg
Dimensions	420 x 370 x 180 mm	325 x 300 x 105 mm	310 x 170 x150 mm	350 x 300 x200 mm	460 x 310 x 210 mm
Portability	One man	One man	One man	One man	One man
Other features	Background noise level measuring mode Stacking Built-in test circuit Automatic overload indication Electrode resistance measured from 1 to 500 kΩ	Selectable cycle time and total averaging period Automatic check-up procedure	Six channels, means: 130, 260,...780 msec Drill hole option, DHIP-2	Microprosessor, PMOS 4 bits Data acquisition system 8 AD channels, 2000 pts: CMOS	Includes depth transducer Depth scales 1:100, 1:200, 1:500 and 1:1000

Table 3. Specifications of the galvanic equipment used in Finland, transmitters

Model	Gefinex 100 CPTS 2061	Terrameter SAS-300	IPC-8 (IPC-7)	Syscal-R	RROM-2
Company	Outokumpu Oy, FINLAND	ABEM, SWEDEN	Scintrex Ltd., CANADA	BRGM, FRANCE	Rautaruukki Oy, Finland
In use	since 1981	1981	1978	1982	1979
Units	5	7 (1)	4 (1)	1	7
Receiver	Gefinex 100 CPRS 2062	Receiver in the same box (Booster option)	IPR-10	Receiver in the same box	Receiver electronics in the same probe
Power supply	Dry Pb rechargeable batteries, 12V, 5Ah	NiCd rechargeable batteries, 12V	Dry Pb rechargeable batteries, 24V, 12Ah	7 C cells, 10V, 60mA	3 x 6V batteries consumption 3.2W
Frequency	1 Hz, sinusoidal	DC pulses	DC pulses, 1, 2 and 4 sec (8)	DC pulses, 1.5 ... 24 sec.	20 Hz
Output power	150W maximum	3W (200W)	250W (25W)	1500W	
Output current	0.1 ...1.5A peak	0.2 ... 20mA (500mA)	1.5A max	3A mac	10mA
Output voltage	12.5, 25, 50, 75 and 100V peak	160V max (400V)	850V max	500V max	
Operating temperature	—20° ... +50°C	—10 ... +70°V	—30° ... +70°C		—20° ... +50°C
Connected to receiver by	Optocoupler	Galvanically	Galvanically	Galvanically	Galvanically
Humidity	Splash-proof	Splash-proof	Splash-proof		Max. working pressure of probe 10MPa
Weight	12.1 kg incl. batt.	5.6 kg incl. batt.	15.5 kg (5 kg) incl. batt.	7.5 kg with receiver and incl. batt.	2.5 kg
Dimensions	420 x 370 x180 mm	325 x 300 x 105 mm	460 x 300 x 140 mm	350 x 300 x 200 mm	1570 x 42 x 42 mm
Portability	One man	One man	One man	One man	Manual winch, cable 1000 m Two men
other features	Transmitter on controlled by receiver 500 single cycle measuremets per charge	3500 (800) single cycle measurements per charge Option SAS LOG 200 (1 in Finland)		Controlled by receiver	RRK-10 for inductive conductivity determination

separations are taken per decade, normally 3, 4, 5, 6, 8, 10, 12, 16, 20, 26, 32, 40, 50, 60, 80, 100, 120, 160 and 200 m. More are taken if needed, but seldom those exceeding 2000 m. The potential electrode separation depends on the signal intensity (voltage), but it should be less than one fifth of the corresponding current electrode separation. The values normally used are 1, 4, 10, 20, 40 and 80 (100) m. The half-Schlumberger procedure can only be used for smaller current electrode separations, because the remote electrode, which is usually on the same line, must be at a distance that is longer at least by a factor of seven. Adjacent soundings are generally 50 m apart, but 20 m has also been used; sometimes only selected stations (scattered) are measured. Small walkie-talkies (VHF or UHF band) are necessary for communication when long separations (over 100 m) are surveyed.

Outokumpu Oy has recently started using the Offset-Wenner system for shallow depths (less than 50 m). This method, which eliminates the errors of lateral variations, has been described by Barker (1981). Mapping is usually a by-product of IP survey and therefore dipole-dipole or gradient configuration is used. Special focusing systems have sometimes been used when locating lateral variations accurately. Although the merits of combined profiling are recognized, the procedure is slow and therefore seldom used in ore prospecting.

For in situ resistivity the one point method was used to determine the grounding resistance in drill holes until the advent of RROM-2 made by Rautaruukki Oy (Tables 2 and 3), which has a Wenner-type configuration with 318 mm electrode separations. High conductivity values must be measured inductively, which is possible with the susceptibility probe of the RRK-10. Various small four-electrode systems have been designed for drill core and layman samples (irregular specimens).

The data gathered with sounding methods are plotted onto log-log normal paper in the field to check that the readings are correct. A pocket calculator is needed when using the Offset-Wenner system to estimate all the intermediate readings and statistics. There is no special data processing scheme for resistivity results.

Interpretation of sounding results is a straightforward task with layered earth modelling, 1D. Interactive computer programs with optimization and graphics are available. Even desktop calculators can handle these programs fast enough. The algorithm is based on the theory of linear filters, and the coefficients have been calculated by Johansen (1975). The optimization method commonly used is a simple hyperparabola minimization developed by Lakanen (1982). Model curves and the auxiliary point method are used only occasionally if no computer is at hand. Numerical modelling programs for 2D or 3D resistivity contrast bodies are only used by the few experts dedicated to this time-consuming task.

Induced polarization (IP)

Induced polarization (IP) was first used in Finland in 1961 by Outokumpu Oy. The first equipment purchased from the USA measured the frequency effect (FE). In the 1970s Finnprospecting Ky made phase-IP equipment under license from Boliden Ab, Sweden. The first pulse-IP (time domain) was constructed by the same company in 1973. In 1978 Outokumpu Oy bought new instruments, an IPR-10 (time domain receiver) and IPC-7 and 8 (transmitters) from Canadian Scintrex Ltd. The University of Oulu received a French Syscal R in 1982. Geological Survey bought the Scintrex equipment in 1983.

The electrode conficuration most commonly used is dipole-dipole (D-D). The electrode spacing is usually 20 m, although 40 m has frequently been used. The separation of the dipole centres varies from 2 to 6 times (n-value) the spacing. When only one n-value is surveyed, the most common number is n = 3. The gradient system has also been used to a certain extent. Though the latter is faster, it suffers from the drawback that separate parts of the survey area are not in the same position with regard to the current electrodes and so the anomalies are not comparable. Its resolution is also poorer. The dipole-dipole system with multielectrode separations has been used for drill hole logging.

The parameter recorded has depended on the instrument used. The frequency effect was the main parameter until 1978, when it was replaced by pulse-IP and chargeability. The phase angle measurements have been done in the lesser measure. Primary voltage and current are also recorded and apparent resistivity is calculated. The IPR-10 has six channels, but normally the value of the middle channel (no. 3) and extreme variation are observed. The Syscal R has a greater time range, but it is not a real spectral IP either. For drill holes, the time domain is more advantageous because of the smaller coupuling effects. Therefore an IPR-10 receiver and only a 25 W IPC-7 transmitter have been used.

There are no special data processing for IP results. Recorded readings are written out and fed into a computer's memory. Resistivities are calculated by the computer. Any time results can be plotted as profiles or contoured maps on the scale and with the colours required. The pseudosections, which are profiles with different n-values as the vertical scale, are also drawn. Some organizations still contour all their maps manually.

Most of the results are used in a qualitative sense. The basis of all interpretations is comparison with petrophysical determinations of IP. Some model curves of a simple dyke model are available. The program of the Geological Survey can be used in calculating anomalies for simple prism models. It requires much memory capacity of the computer. An interpretation program for routine use by field geophysicist must be sufficiently fast and usable. A recent algorithm of an ellipsoid model made by Outokumpu Oy comes close to this demand.

IP is not used in Finland as much as inductive methods such as Slingram (HLEM). One reason is that it is more expensive. With IP three men can survey 2 km in one day but with Slingram two men can cover at least 6 km. IP is useless in areas where there are many parallel good conductors. But for more resistive and disseminated sulphides, which do not respond inductively enough, IP is the only method. Copper, zinc, lead and occasionally nickel and even gold indirectly have been searched by using IP. Magnetite causes spurious anomalies; so do saline clays, but inland clays only reduce the amplitude (masking effect). Polarizable material right at the surface generates a negative IP response, because the secondary current is in the opposite direction to the primary one. Resistive areas have their own trouble, high electrode resistance, but high-power transmitters have not been considered necessary.

IP is especially sensitive for low grade disseminations. Only about half a per cent of sulphides may cause a distinct anomaly, if the minerals are fine grained and the host rock is resistive. This is further accentuated in drill holes which seem to be anomalous all over. 0.1 per cent of sulphides has been noticed to give a chargeability anomaly of 80 mV/V. Nevertheless, IP was not sensitive enough for a molybdenite deposit grading 1 per cent of molybdenum in some places. Only one ore deposit being exploited in Finland was found by IP. The annual number of points measured varied from 20 000 to 30 000.

Charged potential (CP)

Charged potential (CP) (or miseà-la-masse) is the method used most for detailed investigations of established conductors. The current is fed directly to the conductor and the remote electrode is located many kilometers away. Potential is measured between a fixed electrode and a moving electrode. Measurements are carried out as much on the ground as in drill holes. Good results have also been obtained from the mines under exploitation.

Almost any resistivity equipment could be used, but Outokumpu Oy has costructed a device specifically for this purpose, the Gefinex 100.

Contoured maps and cross sections are drawn from the results, and the connections of the conductive bodies between intersections are established mainly by qualitative interpretation. Some geometry and estimates of volume can be extracted from the results. The conductivity contrast should be clear, that is, more than one order of magnitude. Poor conductors can be studied, but then the point source character

should also be taken into account. Some subjective ways can be devised for filtering the effect of homogeneous ground, but they are seldom satisfactory. More sophisticated calculations can be used with numerical algorithms, but as with resistivity and IP they are just not feasible enough for a routine scheme.

All the galvanic measurements are laborious in winter when the ground is frozen. Drill holes and smaller areas are surveyed, however, when necessary, but larger areas are saved for summer. This is in contrast to other geophysical methods, which are used increasingly in winter.

Acknowledgements

Thanks to Aimo Hattula and others, who assisted in collecting the specifications and gave valuable suggestions.

References

Barker, R.D., 1981. The Offset system of electrical resistivity sounding and its use with a multicore cable. Geophysical Prospecting 29, 128—143.

Johansen, H.K., 1975. An interactive computer/graphic-display-terminal system for interpretation of resistivity soundings. Geophysical Prospecting 23, 449—458.

Lakanen, M.E., 1982. Interactive and automatic model interpretation. Tech. Lic. thesis, Helsinki University of Technology (in Finnish), 133 p.

A REVIEW OF THE PRESENT STATE OF THE TECHNIQUE AND INSTRUMENTATION OF CALVANIC EXPLORATION METHODS IN THE USSR

by

A.Ph. Fokin, H.N. Mikhailov and M.V. Semenov

Fokin, A.Ph., Mikhailov, H.N. & Semenov, M.V., 1986. A Review of the Present State of the Technique and instrumentation of Galvanic Exploration Methods in the USSR. *Geologian tutkimuskeskus, Tutkimusraportti 73.* 60—66.

Owing to its high efficiency, electrical prospecting is applied in the USSR at all stages of geological exploration.

The main prospecting operations are performed using five principal galvanic methods: the induced poralization, resistivity, vertical electrical sounding, natural electrical field and mise-à-la-masse methods. All the electrical prospecting techniques call for the use of sets of equipment. The technique selected depends on the conditions of its application and on the nature of the prospects being investigated. For geological mapping and ore prospecting, complex procedures involving electrical prospecting and providing solutions to the main problems have been devised. The basis for the engineering reequipment of electrical prospecting is its reduction to one multiparametric method that incorporates all the advantages of the separate methods existing at present, with hardware in the form of an integrated complex of electrical prospecting techniques and involving the broad use of the computer for the automation of the collecting and processing of data and their geological interpretation.

Key words: electrical methods, induced polarization, resistivity, electrical sounding, electrical field, mise-à-la-masse, review, USSR

Фокин А.Ф., Михайлов Г.Н., Семенов М.С., 1986. Обзор современного состояния методики и аппаратуры гальванических методов рудной электроразведки в СССР Геологический центр Финляндии, Рапорт исследования 73. 60—66.

Рулная электроразведка, благодаря своей высокой эффективности, применяется в СССР на всех стадиях геологоразведного процесса.

Основные обьемы работ выполняются на стадии поисков месторождений, в основном пятью кондуктивными (гальваническими) методами: вызванной поля и заряда. Все методы электроразведки обеспечены серийной аппаратурой. Методика работ зависит от условий их проведения и особенностей искомых обьектов. Для геологического картирования, поисков рудных месторождений и их разведки отработаны комплексы методов, включаюгщие электроразведку, обеспечивающие решение основных задач. В основу технической политики в области перевооружения рудной электроразведки положен подход к ней, как к единому многопараметровому методу, обьедияющему в себе достоинства существующих пока порознь методов, имеющему аппаратурное обеспечение в виде агрегатированного комплекса электроразведочной техники и с широким применением ЭВМ для автоматизации работ при сборе и обработке информации, а также при геологической интерпретации полученных данных.

Introduction

Owing to its high efficiency, electrical prospecting holds a dominant position among geophysical methods and is employed at all the stages of geological exploration: for geological mapping and ore prospecting. Nowadays, the singificance of electrical prospecting is increasing also in the solution of problems involving engineering geology, water supply, etc. From the standpoint of costs, electrical prospecting has for many years occupied first place in ore geophysics, accounting for about one quarter of the expenditures for all ore-prospecting geophysical operations. The efficiency of electrical prospecting, judged on the whole, may be characterized by the fact that up to 70 % of the new ore deposits in the USSR have been discovered by electrical prospecting methods.

The main bulk of the operations (up to 60 %) performed with electrical equipment is done at the prospecting stage. Out of the large number of well-known electrical prospecting methods and their modifications — which differ from each other as regards the geoelectrical parameters, the technique of receiving and generating electromagnetic fiels, and the behaviour of the fields in the time and frequency domains —, only five galvanic methods, accounting annually for up to 80 % of all electrical ore prospecting, have been widely developed. These are employed in combination with induction methods in addition to geological and geochemical methods, drilling and excavations. In the following, the present state of the galvanic methods and the equipment used in their application are described.

The galvanic methods

The dominant position of galvanic methods is explained by the fact that in the USSR the largest number of electrical prospecting operations are performed on the ground. To a lesser extent, downhole and shaft methods are used, in addition to still less often, airborne electrical prospecting. This is due to the limited areas of Precambrian shields and the great extent of the surficial deposits forming a very thick cover in the main ore provinces.

For geological mapping in areas with low resistivity contrasts and under favourable grounding conditions, use is made of various modifications of galvanic resistivity profiling (gradient array, combined and dipole, more often symmetrical) and vertical electrical sounding (VES) methods. In direct current operations, an AB-72 millivoltmeter is employed: dry cell batteries or ERDU-71, SCE-72 motor generators of 14 kW (Electrical ..., 1980) are used as current sources.

Fos ac operations, a lightweight portable AHCH-3 apparatus with increased noise immunity and sensitivity supplies the output (Electrical ..., 1980).

When grounding conditions are poor and the resistivity contrast of the geological formations being mapped is high, profiling induction methods are preferable.

The basic method used for prospecting massive and disseminated conducting ores as well as for the single-valued definition of the conductivity of the occurrence is the induced polarization method. Pulse and frequency modifications of this method, both with the galvanic generation of the polarizing field, are applied.

A rather wide range of instruments used for IP pulse transient measurements in the time range from tens of milli-seconds to tens of seconds is produced. This equipment is manufactured as truck-mounted electrical prospecting stations (VP-62, VPS-63, SVP-74) (Electrical ..., 1980; Komarov et al. 1981; Instruction ..., 1984).

The instruments used in the IP method in the frequency domain are much fewer. The VP-F instrument is being produced, and the production of the EVP-203 apparatus has begun (Electrical ..., 1980; Instruction ..., 1984; Solovjev et al. 1978).

To a lesser extent, in prospecting orebodies with electronic conductivity and in the geological mapping of graphitized and pyritized rocks, the natural electrical field method is applied.

When performing operations for the purpose of estimating the economic value of a deposit (especially examining its flanks and deep horizons) and searching for nearby ore occurrences, the mise-à-la-masse method is used. This approach includes the whole complex of methods used in studying the direct current (low frequency) electrical and magnetic fields on the day surface, in boreholes and openings, generated by the ''charged'' conductor or point current source located on the day surface or downhole. All the operations are performed using electical prospecting stations of the ERSU-71, SVP-74, EVP-302 type or with the ANCH-3 portable apparatus (Electrical ..., 1980; Borehole ..., 1971; Instruction ..., 1984). The mise-à-la-masse method is used also for searching and tracing ore bodies between boreholes and openings. It is used in combination with the radio-wave shadowing method.

The annual expenditures involved in electrical prospecting by calvanic methods can be broken down as follows: the IP method 34 %, various direct current and low frequency current profiling modifications 26 %, the vertical electrical sounding method 15.5 %, the natural electrical field method 10.7 %, the mise-à-la-masse mathod in different variants 4.5 %.

The electrical prospecting technique and the tasks being performed are determined by the geological environment and by the physical parameters of the occurrences being investigated. Newly surveyed regions are superficially studied, and as a rule the terrain is rough. Basically for economic reasons such electrical prospecting is conducted mainly in limited areas with the aim of finding, tracing and estimating the mineralized sulphide zones and ore occurrences situated at depths of 50 to 100 m. Regions with producing mines and deposits under industrial exploitation are studied in detail by a complex of gephysical methods and drilling down to 100—300 m — in some ore fields down to 1—2 km. Geophysical research in such regions is mainly concentrated on prospecting for orebodies at the flanks of known deposits; the aim is to discover new ore deposits at great depths (500—1500 m).

In prospecting activity, besides economic deposits, non-economic occurences are also discovered, the estimation of which by drilling requires heavy expenditures and much time. Therefore ore prospecting is complicated by the necessity of checking out non-economic occurrences. In these connections, most of the work is performed by electrical prospecting methods.

Let us analyze the application of the electrical prospecting technique to one of the most widespread sulphide pyrite deposits. Deposits of this type occurring in bedrock at a depth of 50 m or under loose deposits 10—15 m thick are successfully located by all the known electrical prospecting methods. However, to minimize the emergence of non-ore anomalies, only the geologically most efficient methods are used. As a rule, these are the induced polarization method (IP), and the transient electromagnetic method (TEM) (in combination with lithogeochemistry according to the secondary haloes of metal dissemination, with gravity and magnetic prospecting). The IP method is used on the scale of 1:25,000—1:10,000 with gradient or combined profiling arrays. The TEM method is used in massive ore prospecting on the scale of 1:10,000 and more in the loop version. The exploratory and estimation work on ore prospects is conducted in conjunction with drilling boreholes, which are employed in making downhole investigations by the IP, mise-à-la-masse, natural electrical field and dipole electromagnetic profiling (DEMPS) methods. The mise-à-la-masse method is applied in tracing orebodies along the strike as well as in prospecting nearby ore occurrences. The natural electrical field method is used in combination with the IP method for prospecting the metallization in borehole spaces and for estimating the depth of mineralizations.

In tracts probed to depths of 100—300 m or covered by very thick surficial deposits prospecting on the ground for pyrite-polymetallic deposits is very difficult as

the depth peneration of the IP and TEM methods is reduced by the screening effect of conductive overlying deposits and the greater depth at which the ore lies. The IP method is applied in areas where the thickness of the conductive overburden does not exceed 100—150 m, or open areas where pyrite-polymetallic metallization occurs at a depth of 300—350 m. In such an environment, the prospecting targets are not separate orebodies but large zones of hydrothermally altered rocks with a sulphide dissemination. All the operations are carried out with the gradient array used in combination with the VES—IP system. This technique is successfully used in the Urals, the Altai and Kazakhstan (Instruction ..., 1984). For the estimation of the thickness of the conductive overburden, good results were obtained by TEM soundings, which were successfully followed up by high precision gravity prospecting. This technique made it possible to discover in the Altai, at a depth of 250 m, pyrite ores that occur beneath an overburden 160 m thick.

For prospecting pyrite polymetallic deposits occurring at depths of 300 m and more, where all ground electrical prospecting methods are ineffective, downhole electrical prospecting methods are widely used (Borehole ..., 1971). The depth of metallization in periborehole and interborehole spaces can be determined only by deep drilling. For this purpose, the drilling is done in two rounds. The boreholes of the first round are drilled with 500—1,000 m spacing and they make it possible to carry out electrical prospecting. When the supply grounding is inserted into the borehole, the electrical potential observations made on a scale of 1:100,000—10,000 by the mise-à-la-masse method are carried out over areas of some tens of square kilometers in accordance with the profile system on the surface as well as in deep boreholes. In addition to geological mapping, this technique allows one to judge the morphology of ore-control zones and to locate rationally the boreholes for the second round. To ascertain the ore content of the anomalies registered, the IP method is also used to determine the sulphide dissemination and the TEM method to discover massive ores. The exploration of the flanks and deep horizons of deposits is carried out only by means of downhole electrical prospecting and, more often, by the mise-à-la-masse method. Under complex geologic circumstances, when difficulties are met with in grounding, ac magnetic field measurement is preferable. In the Altai, polymetallic orebodies were discovered using the mise-à-la-masse method at depths ranging from 150 to 1,200 m. In the Kola Pensinsula, rich copper-nickel ores were discovered by the mise-à-la-masse method while measuring the magnetic field at depths up to 400 m among phyllite shales with high conductivity. In the South Urals, in an area covered by barren rocks not less than 400 m thick, copper pyrite ore discovered by drilling to dephts of over 500 m were contoured afterwards by the mise-à-la-masse method. Different logging techniques, downhole versions of the IP and TEM methods, and radio-wave shadowing are widely used in carrying out the foregoing operations.

The variety of ore types affects the electrical prospecting technique and the final results. Pyrite-polymetallic, copper-nickel and certain other deposits represented by sulphide ores with a high electrical conductivity and chargeability are the direct targets of electrical prospecting, whereas tin, antimony, mercury and certain other ores cannot be observed directly with these methods owing to their low metal contents or unfavourable electrical properties. In such cases, electrical prospecting is applicable for indirect searching and locating of sulphide mineralization zones, favourable structures, ore control horizons, etc., associated with metallization. The search for antimony-mercury ores of the interformation type in Kirghizia may serve as an example. It has been observed that in sedimentary rocks situated close to occurrences of ore the pyrite and organic contents are not very high but increase substantially with the development of hydrothermal processes in the proximity of the ores. The distribution of chargeability in these zones has proved to be proportional to the antimony-mercury satellite element concentration. It has made it possible to interpret the IP data toward predicting blind occurrences, tracing the contours of ore zones and discriminating the zones of antimony-mercury metallization prospects. The IP method has occupied the dominant position in the complex of geological-geophysical methods and facilitated the discovery of new antimony and mercury deposits.

Recently, the significance of electrical prospecting has increased substantially in the solution of geological problems attending ore exploitation. It has been enhanced by various theoretical, experimental and methodological investigations as well as by the development and commercial production of different types of shaft-mine electric prospecting equipment: stations for complex logging in boreholes of underground drilling, multipurpose apparatus for investigations by the radio-wave method in shafts and downhole, and instruments used in investigations made by the IP method in quarries and boreholes (Solovjev et al., 1978; Lebedev et al. 1983). The methods of shaft-mine electrical prospecting enable us to check the data on the geological structure of certain explored and exploited areas, to ascertain the ore reserves at the stage of close exploration and the exploitation of deposit, and to cut down the degree of shaft-sinking operations and drilling in barren tracts. The data obtained by these methods make it possible to correlate ore connections in openings and boreholes, and contribute to the reduction of losses in mineral resources during exploitation. The main methods employed in combination with drilling and the sinking of openings in underground conditions are the direct-current or low-frequency mise-à-la-masse method and the radio-wave shadowing mehtod (in the frequency range 156 kHz to 36 MHz); to these methods can be successfully added the electromagnetic logging of dry boreholes drilled underground, and electromagnetic induction profiling. To investigate ore technological grades in quarries, use is made of besides geological mapping and sampling, a complex of electrical prospecting methods, including the IP method and dipole induction profiling and frequency sounding method, having an operating frequency range of 20 kHz to 2.5 MHz. All the methods and instrumentation are provided with manuals and data-interpretation techniques. The application of the shaft-mine electrical prospecting methods is of great value to the Soviet Ministries of Ferrous and Non-Ferrous Metals, the effectiveness of their use during the last 5 years having amounted to savings of some tens of millions of roubles. Recent scientific investigations are the basis of the extension of the spheres of application of electrical prospecting for the increase of depth penetration, resolution and capacity, and finally for the increase of the geological and commercial efficiency of the method. Scientific advances in the field of electrical prospecting have been made by a number of research institutions of the Ministry of Geology, the Academy of Sciences of the USSR and the republics, and certain schools of higher education.

In the sphere of resistivity methods, the theoretical basis and the technique of natural electrical and electromagnetic fields of application for geological mapping have been developed, making it possible to work without a generator and perform operations under difficult conditions (Antonov et al., 1980).

An electrical field non-contact measurement method has been devised in which galvanic groundings are replaced by capacitive groundings. This method is of particular importance to geological mapping and prospecting under difficult conditions or in the winter time (Sapozhnikov, 1973).

Close attention is paid to the determination of the geological nature of anomalies. The theoretical and methodical investigations carried out make it possible to determine the dimensions and texture of electronically conductive inclusions and to solve the problems involved in distinguishing streaky and massive ores among disseminated pyrite, graphite and other electronically conductive mineral impregnations by examining the IP time responses, expecially in the early stage (from tens to thousands of μs), as well as the non-linear IP responses.

The frequency-domain IP employed to increase the capability and efficiency of the method in an industrial noise environment has been further developed (Electrical ..., 1980). The field of application of the IP method is also extended — the prospects of applying the method in the search for gas and diamonds are shown. The measurement of the IP magnetic field are confirmed theoretically and performed experimentally.

For prospecting the flanks of explored and exploited deposits by the mise-à-la-masse method, small-scale techniques for modelling electric and magnetic mise-à-la-masse anomalies have been worked out. Also the technique or numerical modelling has been developed for the geological interpretation of mise-à-la-masse data, the model

anomalies being obtained by means of a computer and MUSG-1 device. The mise-à-la-masse method applied in small-scale measurements has been successfully used in the Altai, the Urals, the Norilsk region and the Kola Peninsula.

The main geological tasks of electrical prospecting for the coming decade are: geological mapping and prospecting for ore in difficult geological circumstances and in districts with a high level of industrial noise, the increase of depth penetration up to 500 and then to 2000 m, and the transition from detecting anomalies to assessing and classifying predicted reserves of ore minerals.

As it is necessary to probe greater depths, the targets of electrical ground prospecting will change. If currently the targets of direct electrical prospecting are orebodies, then in the future they will be mineral deposits and ore fields. It is necessary to be prepared for using the special borehole array. The increase in investigation depth requires high accuracy or sensitivity of the equipment used and high power of the current sources. It also increases the possibilities of applying the natural and industrial noise electromagnetic field (power transmission line fields included). Apparently, some redistribution of the electrical operations at different stages of geological exploration will take place. The bulk of the methods used for deep geological mapping, estimating the geological nature of electrical prospecting anomalies, and evaluating predicted ore reserves is to be increased.

The complication of geological tasks solved with the electrical prospecting method will result in the nearest future in a sharp increase in the volume of information to be processed. In this connection it has become necessary to automate all these processes. The development of the hardware and software of electrical prospecting methods is being pursued in the USSR in cooperation with the other countries belonging to the Council for Mutual Economic Aid. In the nearest years ahead, it is planned to prepare the following scheme of information collection, quality estimation of field measurements, data processing, and qualitative and quantitative geological interpretation, which consists of four main stages:

1) recording field observations directly across the profile onto the playback carrier (magnetic tape, solid-state memory);

2) preliminary processing of measurement data (correlation, elimination of coarse errors, etc.), the computation of geological and geophysical parameters to estimate the quality of field observations. These operations are performed directly in the field;

3) computation of geophysical parameters, their plotting on the display or plotter, preparation of data for interpretation (filtering, etc.), qualitative geological interpretation with approximate consideration of the geoelectrical effects, involving analogue and digital modelling. This work is done by field crews and expeditions;

4) specifying the solutions obtained at the previous stage by complex algorithms and detailed analysis of the true geological and geophysical effects. The work is done by expeditions and geological institutions.

Summary

As already mentioned, electrical prospecting in the USSR is done nowadays with a one-method specialized apparatus. This results in a variety of apparatus types, which complicates unification of procedures and creates technological problems for the manufacturers. In connection with all these circumstances, the technique of electrical prospecting (ACET) is being developed as an aggregated complex in our country. The ACET should provide the basic electrical ground prospecting methods in the frequency range of 0 to 10 kHz or in the adequate transient process time range. The ACET of field electrical prospecting includes 4 types of generator devices, differing in power, and 7 types of measuring devices.

It is proposed to limit the complex of digital measuring devices to 3 types of pulse meters in the time domain applied for recording the early, middle and late stages of the electromagnetic transient as well as 3 types of frequency domain meters, for low

(up to 78 Hz), middle (up to 1250 Hz) and high (up to 10,000 Hz) frequencies. Besides, the ACET includes two magnetometers with a high sensitivity magnetometer used for recording magnetic fields in pulse and frequency mode.

The ACET is provided with the capability of packaging the generator, measuring devices and auxiliary equipment in the form of three different types of electrical prospecting stations mounted on one or two trucks.

In conclusion, it can be stated that the basis of the engineering reequipment of electrical ore prospecting is its reduction to one multiparameter method that incorporates all the advantages of the methods existing separately at present, with hardware in the form of an integrated complex of electrical prospecting equipment involving automation on broad lines of the work of collecting, processing, and geologically interpreting data.

The implementation of this task will require greaf effort and the coordination of many scientific research and production organizations of the USSR and member countries of the Council for Mutual Economic Aid interested in enhancing the efficacy of electrical prospecting.

References

Electrical prospecting. Geophysicist's handbook. Moscow, Nedra, 1980. 518 p. (Электроразведка. Справочник геофизика, 1980. 518 с.)

Komarov V.A., Dubman V.V., Joffe L.M. et al. The SVP-74 secondary fields station. — Geophysical apparatus, No. 74. Leningrad, Nedra, 1981, p. 33—74. (Станция вторичных полей СВП-74. — Геофизическая аппаратура, 1981. No 74, с. 33—44).

Borehole ore geophysics. Leningrad, Nedra, 1971. 536 p. (Скважинная рудная геофизика. Ленинград, Недра, 1971. 536 с.).

Intruction on electrical prospecting. Leningrad, Nedra, 1984, 378 p. (Инструкция по электроразведке. Ленинград, Недра, 1984, 378 с.).

Solovjev S.S., Savitsky A.P., Shefer V.R., Lebedev V.Ph. "Galenite" apparatus used for logging boreholes of underground drilling by electrical methods. — Geophysical apparatus, No. 63. Leningrad, Nedra, 1978, p. 114—119. (Аппаратура "Галените" для каротаза скважин подземного бурения электрическими методами. — Геофизическая аппаратура, 1978, No. 63, с. 114—119).

Lebedev V.Ph., Strelov N.K., Trufanov A.M. et al. "Lazurite" prospecting and exploration equipment. — Geophysical apparatus, no. 74. Leningrad, Nedra, 1983, p. 60—65. (Поисково-разведочная аппаратура "Лазурит". — Геофизическая аппаратура, 1983, No. 77, с. 60—65).

Antonov G.K., Eliseev A.A., Somov G.M. Some peculiarities of the apparatus applied for electrical prospecting by ac electrical fields with various operating frequencies. — In: The application of electrical prospecting methods for geological mapping while prospecting mineral deposits. Leningrad, NPO "Rudgeofysika", 1980, p. 3—14. (Особенности аппаратуры для электроразведки методом ПЭП с использованием нескольких рабочих частот. — В кн.: Использование электроразведочных методов для геологического картирования при поисках месторождений полезных ископаемых).

Sapozhnikov B.G. The apparatus and procedure employing gradient array with the ungrounded receiving line. — Geophysical apparatus, No. 52. Leningrad, Nedra, 1973, 31—40. (Аппаратура и методика срединного градиента с незаземленной приземной линией. — Геофизическая аппаратура, 1973, No. 52, с. 31—40).

Interpretation of galvanic data

RESULTS OF INTERPRETING DATA OBTAINED BY THE MISE-À-LA-MASSE METHOD USING ANALOG AND DIGITAL COMPUTERS

by

M.V. Semenov and M.M. Avdevich

Semenov, M.V., & Avdevich, M.M., 1986. Results of interpreting data obtained by the mise-à-la-masse method using analog and digital computers *Geologian tutkimuskeskus, Tutkimusraportti 73.* 68—72, 3 figs.

The efficiency of the mise-à-la-masse method in investigating geological structures is markedly enhanced if quantitative interpretation methods are used. The optimal manner of quantitative interpretation is the trial-and-error method, which makes it possible to take into consideration the influence of the true geoelectrical conditions in the area investigated. It is understandable that the quantitative interpretation should be done by combined use of an analog modelling device and the digital computer. The quantitative interpretation of mise-à-la-masse data received for a copper-pyrite deposit is discussed as an example.

Key words: electrical methods, mise-à-masse, automatic data processing, ore bodies, models, USSR

Семенов М.В., Авдевич М.М., 1986. Интерпретация данных метода заряда с использованием аналовой и цифровой выцислительной техники. Геологический центр Финляндии, Рапорт исследования 73. 68__72, Идд. 3.

Существенное повшение геологической эффективности метода заряда достигается при проведении количественной интерпретации получаемых при этом данных. Оптимальным способом интерпретации является метод подбора, при котором численное решение задач производится с учетом влияния реальных геоэлекрических услосий исследуемого участка. При этом целесообразно комплексировать аналоговую и цифровоую вычислительную технику. Рассмотрен пример количественной интерпретации данных метода заряда, получеррых на одном из медноколчеданных месторождений.

Introduction

The mise- à-la-masse method is widely used for the prospecting and exploration of highly conductive ore formations. Recently, in connection with considerable advanced made in quantitative interpretation techniques, the efficiency of the mise- à-la-masse method has been considerably increased, particularly when the investigations are made over a vast territory (Semenov et al., 1984). A considerable difficulty in enhancing the efficiency of the quantitative interpretation of mise- à-la-masse data is the complexity of the numerical solution of the electric potential problem when it is necessary to take into account the effect of the true geoelectrical environment on the potential.

The best approach to the rapid quantitative interpretation of mise- à-la-masse data is the trial-and-error method. The essence of the method is as follows. The interpreter constructs the supposed model of the deposit investigated and checks its conformity with the natural object by comparing the potentials produced by the model and by the natural object. If the potentials do not coincide, he modifies the model and repeats the solution until the potentials agree with a given accuracy. It should be noted, however, that the agreement of the potentials does not as a rule provide the single-valuedness of the solution found; it must be considered as one of the proper alternatives. Here the solution is performed with the computer and the conclusion as to the completion of the interpretation is made by the geophysicist-interpreter.

Usually, in the course of the trial-and-error process, it is necessary to calculate the potential anomalies caused by various models with regard to the true geoelectrical environment. The computer makes it possible to perform the calculations in some particular cases very fast. The modelling on analog computers in three-dimensional or two-dimensional cases is more tedious but gives the possibility of obtaining a reliable solution also in the case of the true geoelectrical environment. It is thus reasonable to perform the quantitative interpretation of the electrical prospecting data by combined use of analog and digital computers. As an example of such an approach, a quantitative interpretation of mise-à-la-masse data obtained over a copper-pyrite deposit is described in the following (Semenov et al., 1984).

Interpretation of mise- à-la-masse data

The primary material for the work of interpretation is the geological map and sections around the known part of the deposit, and the mise- à-la-masse measurement data on the grid 100 m x 50 m, obtained in a survey with the groundings in the ore body at the depth of 470 m (Fig. 1). The known ore body is a plate dipping at an angle of 45°. The length of the plate is 850 m in the direction of the dip, and 250 m in the direction of the strike. The presence of an overburden with a thickness of 1 m and resistivity of about 100 Ωm is possible. The resistivity of the host rock is 680 Ωm, the resistivity of the altered rock zone is about 200—300 Ωm, and the ore bodies are actually equipotential conductors.

The preliminary interpretation was accomplished by modelling on the MUSG-1 (Avdevich and Phokin, 1978). Fig. 2 illustrates the modelling results for various structural types of the deposit. As the strike length of the body is limited, comparison of plots obtained by measurement in the field and by two-dimensional modelling is possible only on the short central part of the profile (Avdevich, Menshutina and Phokin, 1981). The initial model for simulating was a conducting rectangular plate with dimensions of 800 m x 250 m (Fig. 2a). This model produced the maximum potential value of 64 mV (without overburden) and 50 mV (with overburden) relative to the reference electrode.

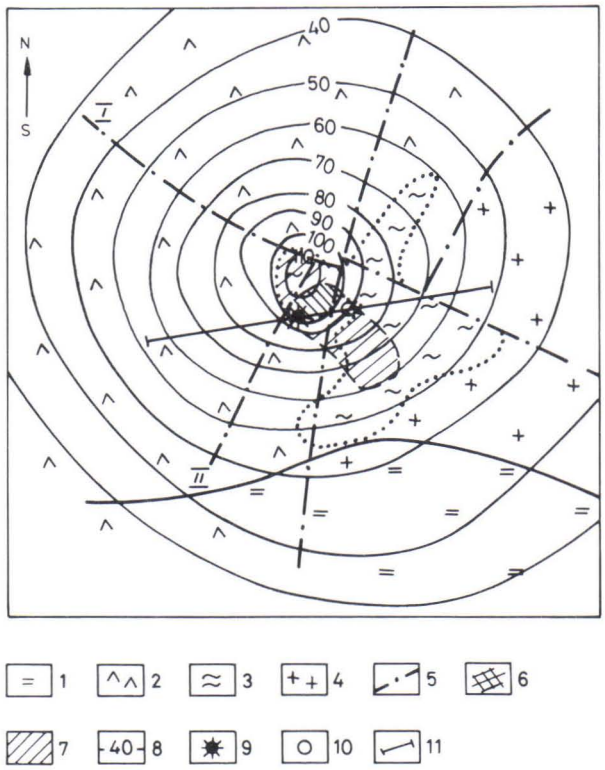

Fig. 1. A schematic geological map of the area explored and the mise-à-la-masse potential isolines. 1: tuff-sandstones, 2: porphyrites, 3: hydrothermally altered rocks, 4: granites, 5: fractures, I — principal, II — IV — feathering, projections of mineralization zone contours on the day surface, 6: explored, 7: supposed according to the interpretation, 8: mise-à-la-masse potential isolines (mV/A), 9: the projection of the current source on the day surface, 10: the checking borehole, 11: section line.

At the same time, the respective magnitude of the plot obtained in the field is equal to 18 mV. So it is concluded that, in the modelling, the size of the body was taken as being appreciably smaller than in nature. It is therefore necessary to localize the regions where subsidiary mineralization zones may occur. Various types of deposit models with a meaningful geological structure were prepared on the basis of available geological information analysis. The position of the explored mineralization zone is controlled by the subvolcanic porphyritic intrusion tongue sole (Figs. 1 and 3). To the west of the fracture II (Fig. 1), this intrusion, which is impermeable to ore-bearing solutions, spreads in all directions. Geological data suggest that, in the plane of fracture II, there is a "window" filled with ore-hosting, altered and brecciated effusive sedimentary deposits, which are permeable to the solutions. Through this "window", ore-bearing solutions can rise from the bottom to the top along fracture II. The intersection of fracture I with the bottom of fracture II is the assumed mineralizing channel. It was supposed that the subsidiary mineralization zone may occur in the plane of fracture II and have a nearly vertical dip down to 1500—2000 m. The upper dipped part of this zone represents the known explored body of the deposit with a length of 850 m along the dip.

The correctness of this geological model of the deposit was verified by the repeated modelling on the MUSG-1. In this work, many geologically meaningful structural versions of the deposit were examined. Some of these solutions are illustrated in Figs. 2 b and c.

In the course of the interpretation, it was found that the morphology of the body does not allow satisfactory agreement between the potential plots obtained by modelling and by field measurements, as the model plot illustrates the branch asymmetry that is absent on the field plot. Satisfactory agreement between the plots may be obtained provided that the deposit model is supplemented with one more mineralization zone bedding below the explored part of the ore body and being at the depth electrically connected with the supposed main mineralization zone (Figs. 2 d—f). At the

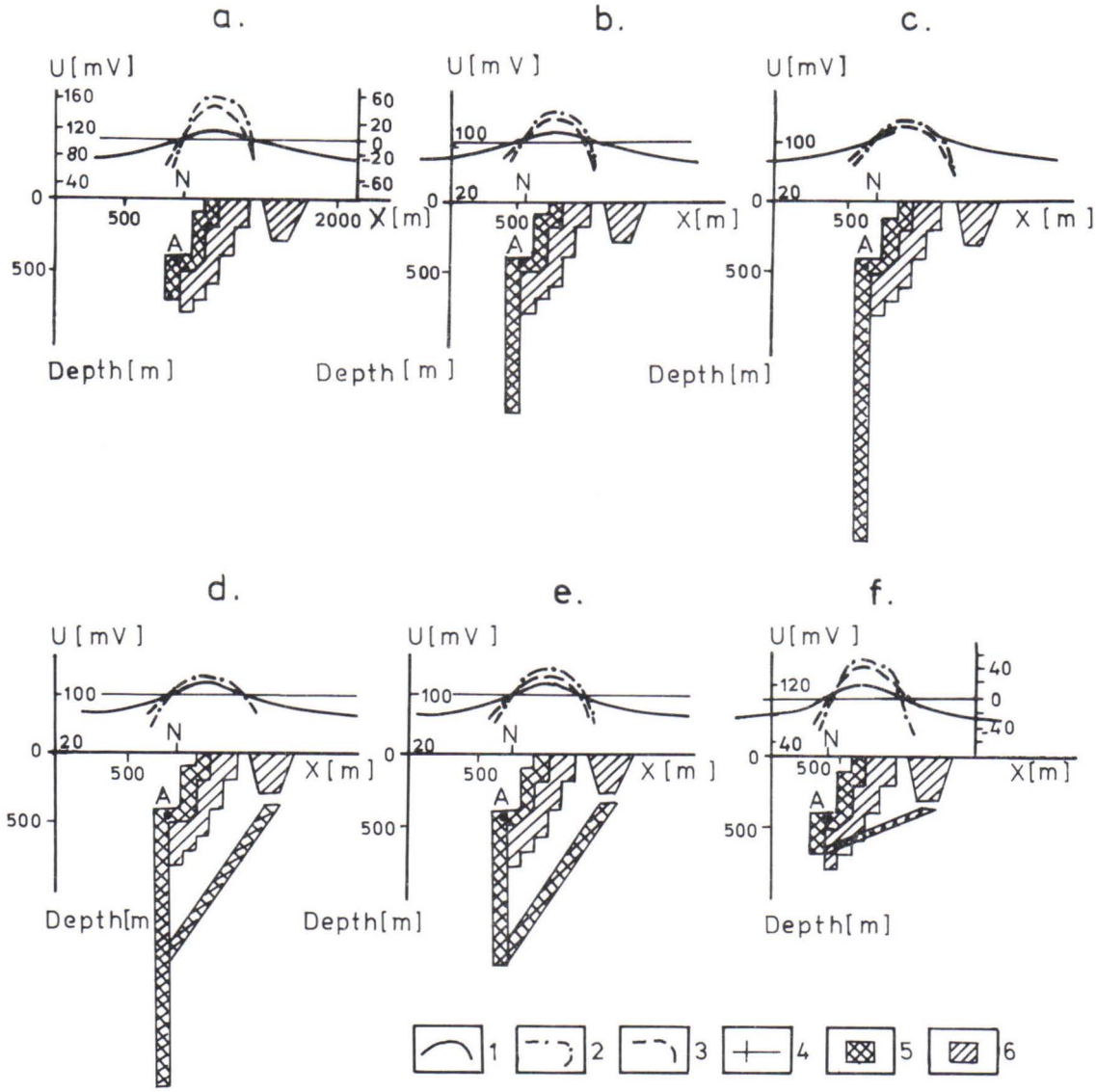

Fig. 2. The results of mise-à-la-masse data interpretation by electormodelling on the MUSG-1 devide. a—f: various versions of deposit texture. Potential plots obtained 1: in the field, 2: on the MUSG-1 without the oberburden effect, 3: on the MUSG-1 with the overburden effect, 4: the zero level in relation to the potential of the reference electrode, 5: ore zones, 6: altered rock zones.

same time it is supposed that the steeply dipping root part of the main ore zone stretches to a depth not less than 2 km from the day surface. The depth to the top of the subsidiary dipped body is 300—400 m. This body is hosted in the known big zone of altered rocks, which lies to the east of the explored part of the deposit and is separated from it by the second tongue of unaltered intrusive porphyrites (Fig. 3).

The conclusions made as a result of the efficient quantitative interpretation on the MUSG-1 were confirmed by modelling on the volume ohmic resistance grid and by computer-assisted calculations (Semenov et al., 1984).

On the basis of the interpretation accomplished, projected maps and sections reflecting the position of the supposed part of the main ore zone and the new mineralization zone in the space have been produced. The projected section along one of the exploration lines is shown in Fig. 3. The geological column of the borehole drilled for checking the conclusions made in the foregoing on the basis of the quantitative

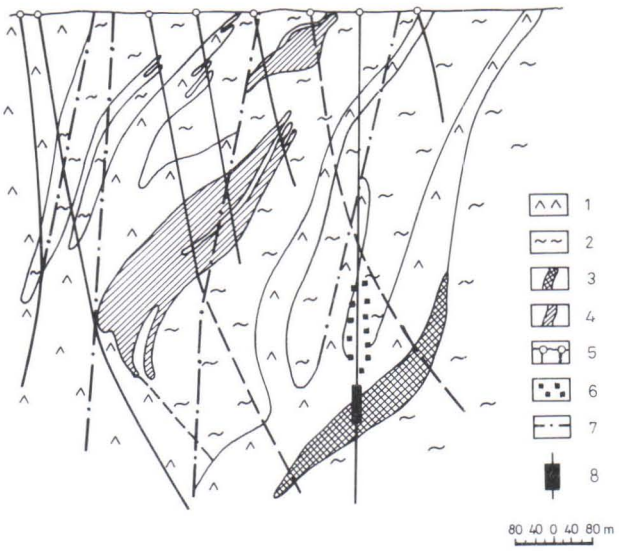

Fig. 3. The projected geological section of the deposit. 1: porphyritic intrusions, 2: hydrothermally altered effusive sedimentary rocks, 3: the ore body assumed according to the quantitative interpreatation of mise-à-la-masse data, 4: the known ore bodies, 5: the boreholes, a) drilled, b) recommended for checking the interpretation results, 6: pyritization in the checking borehole, 7: fractures, 8: the interval with the interbeds of massive pyrite ores intersected by the checking borehole.

interpretation carried out is shown in the same figure. The borehole has revealed the predicted lower mineralization horizon under the second porphyritic intrusion tongue at a depth of more than 700 m. Amid the zone of altered rocks with rich pyritization at a depth of 733—791 m, the borehole has intersected the massive pyrite ore interbeds up to 3 m thick. Actually, the position of the predicted zone has been fully confirmed. According to the calculations, the upper and the lower ore zones must be connected at the depth behind the section plane shown in Fig. 3.

Conclusion

It should be noted that the high reliability in the quantitative interpretation of mise-à-la-masse data became possible thanks to the fact that the interpretation was performed in close connection with the geolocial studies of the structure of the deposit. The potential calculation has been made only for geologically meaningful deposit models produced on the basis of detailed studies of the geological structure and taking into account the effect of true geoelectrical heterogeneity on the measured potential.

References

Avdevich M.M., Phokin A.PH. 1978. The electromodelling of potential geophysical fields. (Электромоделирование потенциальных геофизических полей). Nedra, Leningrad, 99 p.

Avdevich M.M., Menshutina L.E., Phokin A.Ph. 1981. The quantity solution of the charge method tasks by the electromodelling on the MUSG-1 device. (Численное решение задач Метода заряда с помощью электромоделирования на уснановке МУСГ-1). The collection of articles ''Methods of exploration geophysics.'' Tr. Amalgamation ''Rudgeofyzika,'' Leningrad, 37 p.

Semenov T.V., Litvina I.M. 1980. Methodical recommendations for computer assisted geological interpretation of small scale charge method materials. (Методические рекомендации по геологической интерпретации материалов метода мелкомасштабного заряда с использованием ЭВМ). Amalgamation ''Rudgeofyzika,'' Leningrad, 37 p.

Semenov M.V., Sapojnikov V.M., Avdevich M.M., Golikov J.V. 1984. The electrical prospecting of ore fields by the charge method. (Электроразведка рудных полей методом заряда). Nedra, Leningrad, 216 p.

RESULTS OF ELECTRICAL AND ELECTROMAGNETIC MEASUREMENTS IN VAARALAMPI-NIITTYLAMPI, RANUA

by

T. Rekola

Rekola, T., 1986. Results of electrical and electromagnetic measurements in Vaaralampi—Niittylampi, Ranua. *Geologian tutkimuskeskus, Tutkimusraportti 73.* 73—84, 10 figs, one table.

Outokumpu Oy and Lapin Malmi (1982—) have been searching for an economic ore deposit in the Suhanko-Pekkala area in northern Finland already for almost twenty-five years.

The present paper deals with some of the geophysical electrical methods, their results and the interpretations applied in connection with these exploration activities. Many of the survey methods, such as Sirotem and borehole EM logging, were used as test surveys but not in the following-up studies.

The application of several electrical methods has resulted in a reliable structural interpretation of the layered intrusion and the pyrrhotite orebodies.

Key words: electrical methods, electromagnetic methods, copper ores, nickel ores, pyrrhotite, ore bodies, layered intrusions, Proterozoic, Finland, Ranua, Vaaralampi, Niittylampi

Рекола, Т., 1986. Результаты электрических и электромагнитых измерений в районе Вааралампи-Нииттюлампи, Рануа. Геологический центр Финляндии, Рапорт исследования 73. 73—84, Идд. 10.

А/О Оутокумпу и Лапин Малми (1982—) проводят разведку месторождений экономических руд в районе Суханько-Пеккала в северной Финляндии почти 25 лет.

В статье рассматриваются некоторые геофизические электрические методы, их результаты и интерпретации применяемые при разведке. Многие разведочные методы, как например Сиротем и скажиный электромагнитый каротаж, использовались в качестве контрольного испытания но не при разведке.

Доставерное толкование текстур расслоенных интрузий и пирротиновых рудных тел является результатом применения электрических методов.

Introduction

Since the 1960s Outokumpu Oy has been searching for an economic ore deposit in the Suhanko-Pekkala area, some 40 km south of Rovaniemi (Fig. 1). Geologically, the area is part of the Peräpohja schist zone, in which there are occurrences of massive pyrrhotite, often with some copper and nickel, in the contact of layered intrusions with the old gneissose granite basement. Studies undertaken recently have also revealed metals of the platinum group in the layered intrusions. The largest of the pyrrhotite occurrences is called Vaaralampi-Niittylampi.

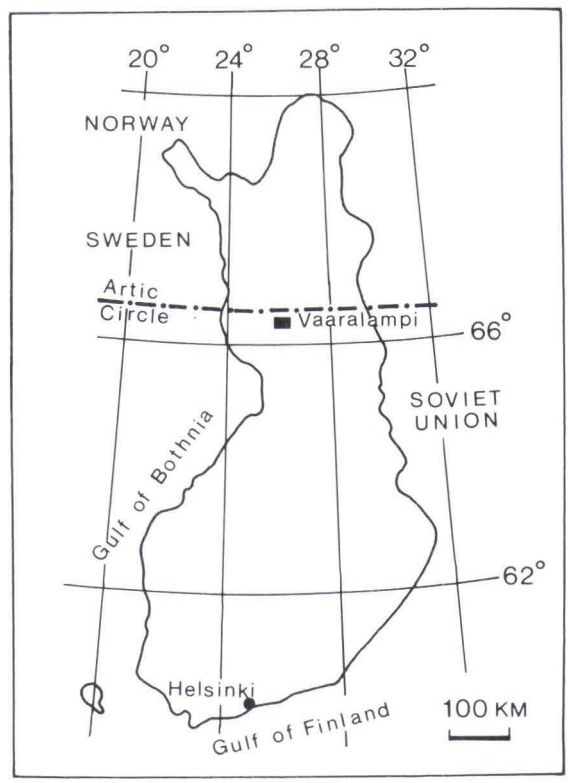

Figure 1. Location of Vaaralampi—Niittylampi project.

Geology

The survey area can be devided geologically into two units in terms of age and lithology, Fig. 2 (Vuorelainen et al. 1982). The older unit consists of Archean granitoids that have undergone polyphase metamorphism. North of them there are younger Proterozoic Svecokarelian metasediments and metavolcanics. The whole pile of schists dips north at 30°—50°. Layered intrusions are encountered between the schists and the basement over a distance of 270 km from Tornio on the Swedish border eastwards to Näränkävaara on the Soviet border. Associated with these rocks are the chromite and PGE deposits at Kemi and Penikat, the vanadium-bearing iron occurrences at Koillismaa and the sulphide and PGE occurrences in the Suhanko-Pekkala area as well as in the various blocks of the layered intrusions at Koillismaa. Stratigraphically, the sulphide

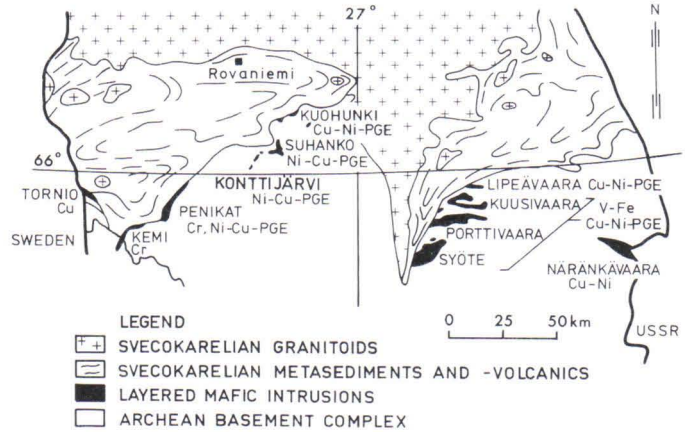

Fig. 2. Location of the layered mafic intrusions in northern Finland. (Vuorelainen et al. 1982)

occurrences are usually at the contact between the layered intrusions and the basement whereas the PGE showings are encountered in both the layered intrusions and the underlying basement (Lahtinen 1983).

Geology of the Vaaralampi—Niittylampi area

The plough-shaped intrusion at Suhanko, some 20 km^2 in surface area, is the largest of the layered intrusions in the study area (Reino 1978). The Vaaralampi and Niittylampi Cu-Ni mineralizations are located in the southeastern corner of this intrusion (Fig. 3).

A section A-A' (Fig. 3) drawn across the southeastern part of the intrusion on the basis of drilling data shows a basin-like structure in which the layers dip at 20°—30° near the surface. The basin plunges towards northwest (section B-B', Fig. 3) and, provided the whole intrusion plunges at the same angle, it can be assumed to be c. 1 km at its thickest, as suggested by gravity and AMT surveys.

The layered intrusion is composed mainly of monotonous gabbro. Ultramafic rocks, predominantly peridotites, occur at the base of the intrusion, in the contact with the gneissose granite of the basement.

Electrical and electromagnetic measurements

Geophysics played a decisive role in studies on the ores in the Suhanko layered intrusion. The area is very poorly exposed and the depth of the overburden varies from 5 to 10 m. The absence of graphite schists and black schists facilitates the application of electrical methods and the interpretation of results.

The area was submitted to a low-altitude airborne survey in 1974 using a protone magnetometer and a wingtip Slingram. This survey provided a big boost to exploration, and numerous aeroelectrical anomalies, all of which were due to the pyrrhotite chalcopyrite occurrences, were localized and tested on the ground.

The ground Slingram survey was followed by mise-à-la-masse measurements, SIROTEM measurements, AMT, resistivity and VLF-R surveys and, finally, borehole EM measurements. The measurements contributed decisively to establishment of the structure of the mineralizations and the layered intrusions.

The apparent resistivity was determined in situ in the drill holes in the area by means of the 4-electrode system/RROM-2 of Rautaruukki Oy to test the viability of the various electrical methods and to interpret the results. Table 1. gives the average apparent resistivities for various rock types.

The measuring data show that the rock types differ from each other in apparent resistivity by 1—2 orders of magnitude for the pyrrhotite mineralization, being up to $\varrho a \sim 10^{-2}$ Ωm.

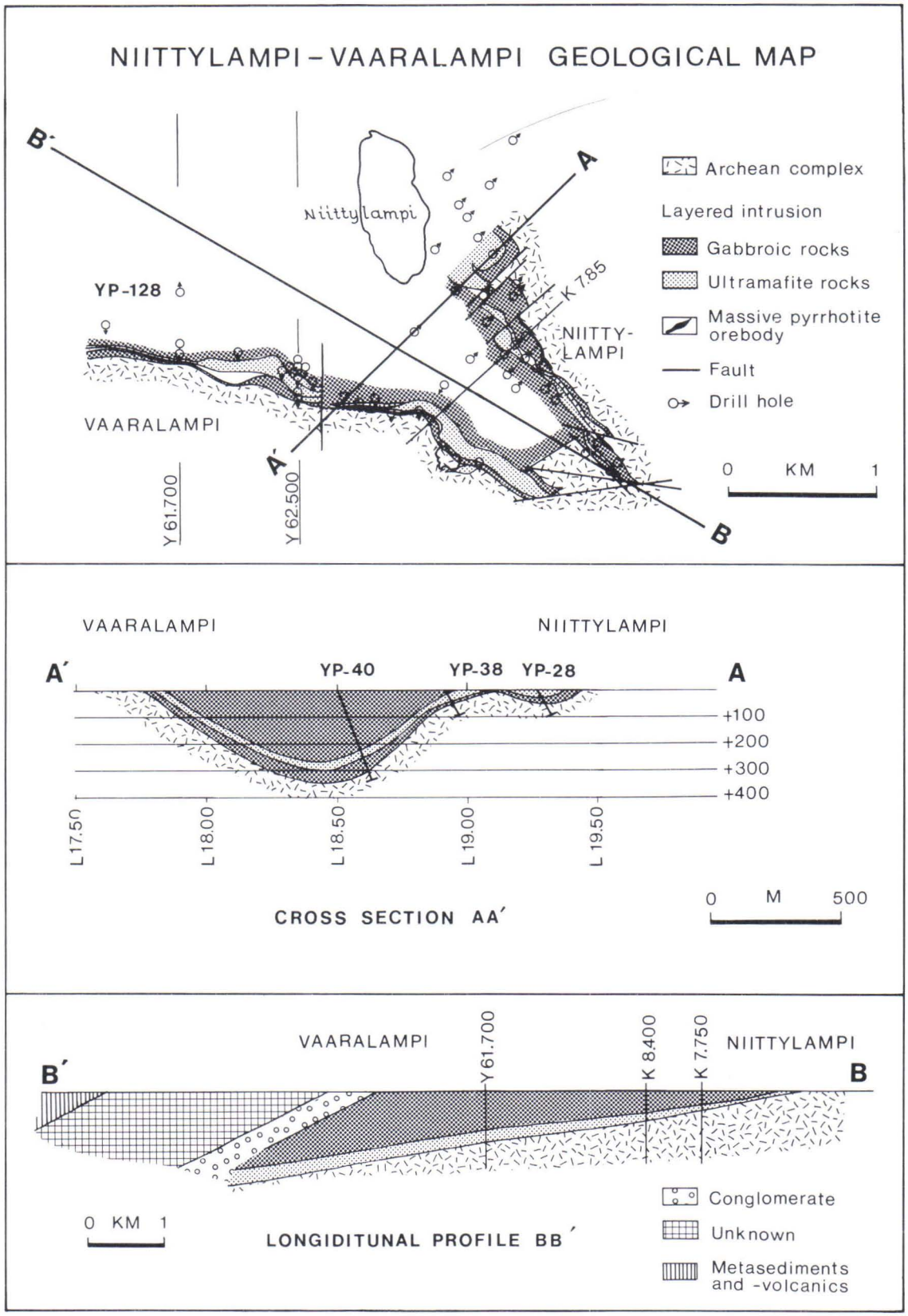

Figure 3. The geology of the study area. (Lahtinen 1983)

Table 1. The average apparent resistivities of rocks in the Vaaralampi—Niittylampi area

Rock Type	ϱa (Ω_m)
Archaean complex	100 000
Gabbroic rocks	40 000—400 000
Ultramafic rocks	100—4 000
Massive pyrrhotite orebody	$4—10^{-3}$

Slingram surveys

The whole contact of the layered intrusion with the gneissose granite basement at Vaaralampi—Niittylampi was covered with a Slingram survey with a = 60 m and f = 1 775 Hz. The objective of the survey was to localize the outcropping pyrrhotite orebodies covered by overburden.

Figure 4 illustrates the plane interpretation of the survey data based on small-scale modelling (Ketola & Puranen 1967). Also marked in the figure is the inferred pyrrhotite orebody projected to the surface.

The Slingram survey localized the outcrop of the sulphide orebody covered by overburden in the eastern part of the area and part of its southern contact within the limits of the depth penetration of the method. Figure 4 also gives the conductors classified according to the conductivity parameter W = $\sigma\mu\omega$ ad deduced from interpretation. The bulk of the sulphide orebody is classified as a good conductor: W > 10.

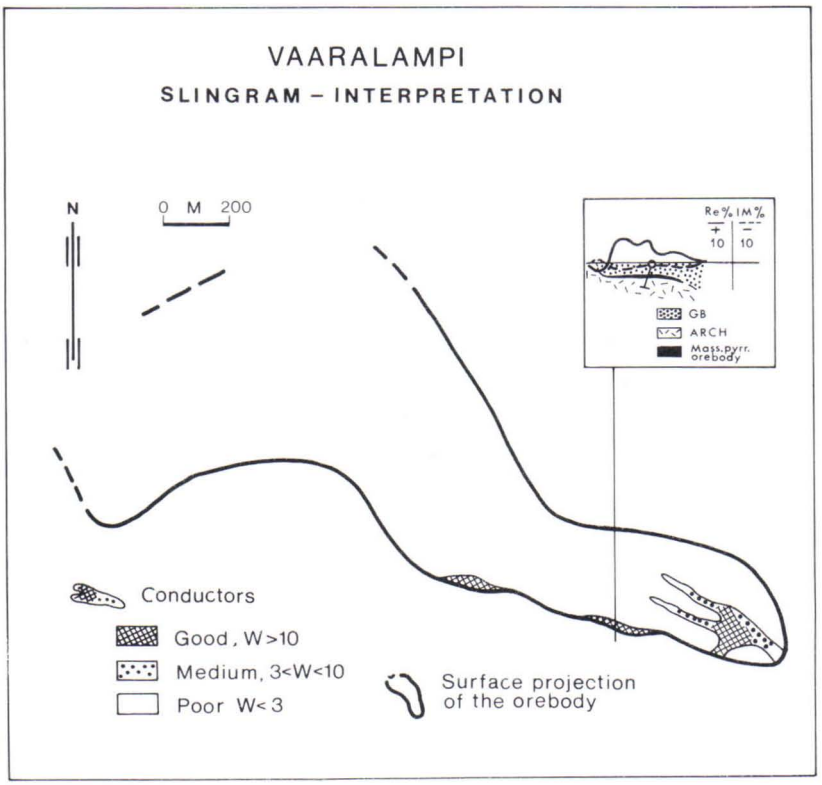

Fig. 4. Plane interpretation of the Slingram survey.

Mise-à-la-masse measurements

Early drilling at Vaaralampi demonstrated that the pyrrhotite orebody was highly conductive ($\sigma_a \leqq 1$ Ωm). It was therefore decided to undertake a mise-à-la-masse survey with the aim of establishing the possible westward continuation of the sulphide orebody.

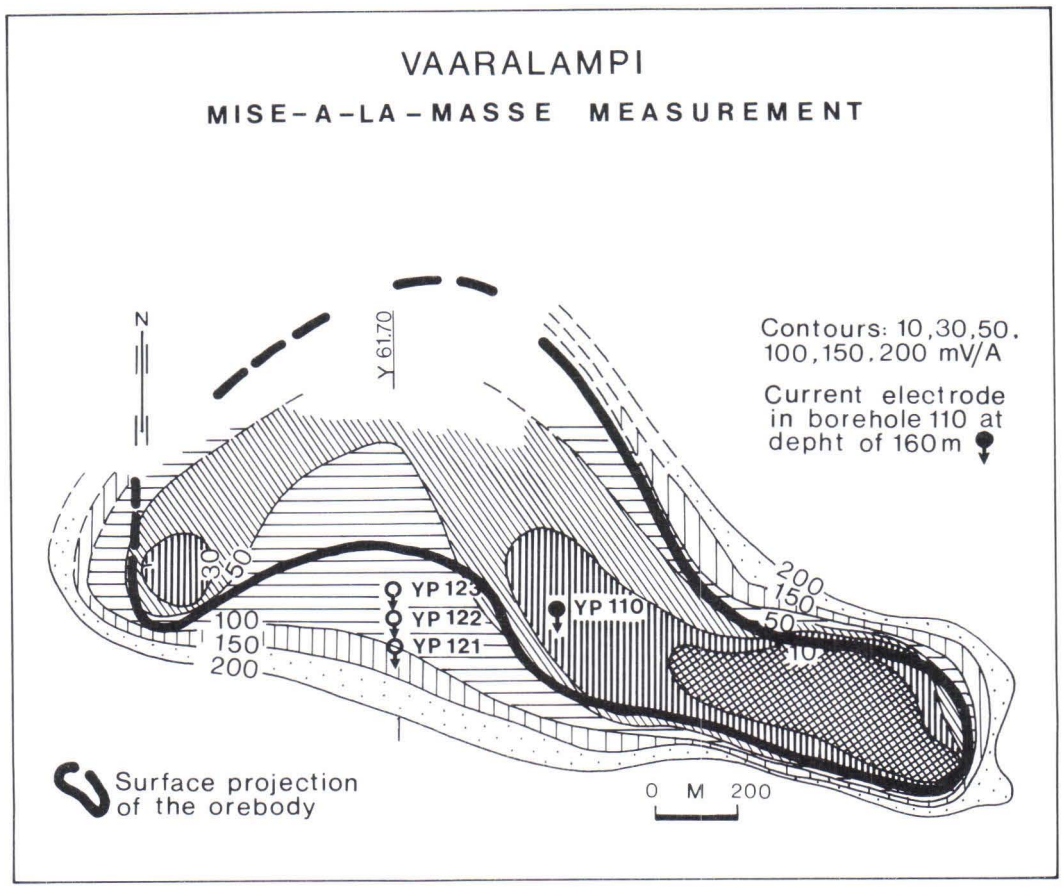

Fig. 5. The results of the mise-à-la-masse measurements.

A current of 1 ampere was fed into drill hole YP-110, which had intercepted the sulphide orebody at a depth of about 160 m, and the distribution of the voltage was measured on the surface and drill holes. Figure 5 illustrates the result of the measurement and shows the inferred sulphide mineralization projected onto the surface.

The distribution of the voltage measured on the ground and in drill holes suggests that the sulphide orebody continues westwards. Resistivity, AMT and VLF-R measurements were done in the western part of the area to verify the continuation.

Recent survey data suggest that the western end of the area is composed of several pyrrhotite orebodies.

Resistivity, AMT and VLF-R measurements

Resistivity, AMT and VLF-R measurements were undertaken on the Suhanko intrusion in 1978—1984. The measurements were done by the Institute of Geophysics of Oulu University and Outokumpu Exploration.

The aim of the measurements was to establish the structure of the whole intrusion and to localize the western extensions of the sulphide orebody at Vaaralampi.

The AMT survey was done with French ECA-541 equipment, and so far 320 stations have been surveyed. The same lines were also surveyed with VLF-R equipment, and some of them have been resistivity surveyed with the Schlumberger electrode array.

Figures 6 and 7 show the survey results and the interpretations from line y = 61.700 in the western part of Vaaralampi, supplemented with the geology verified by drilling.

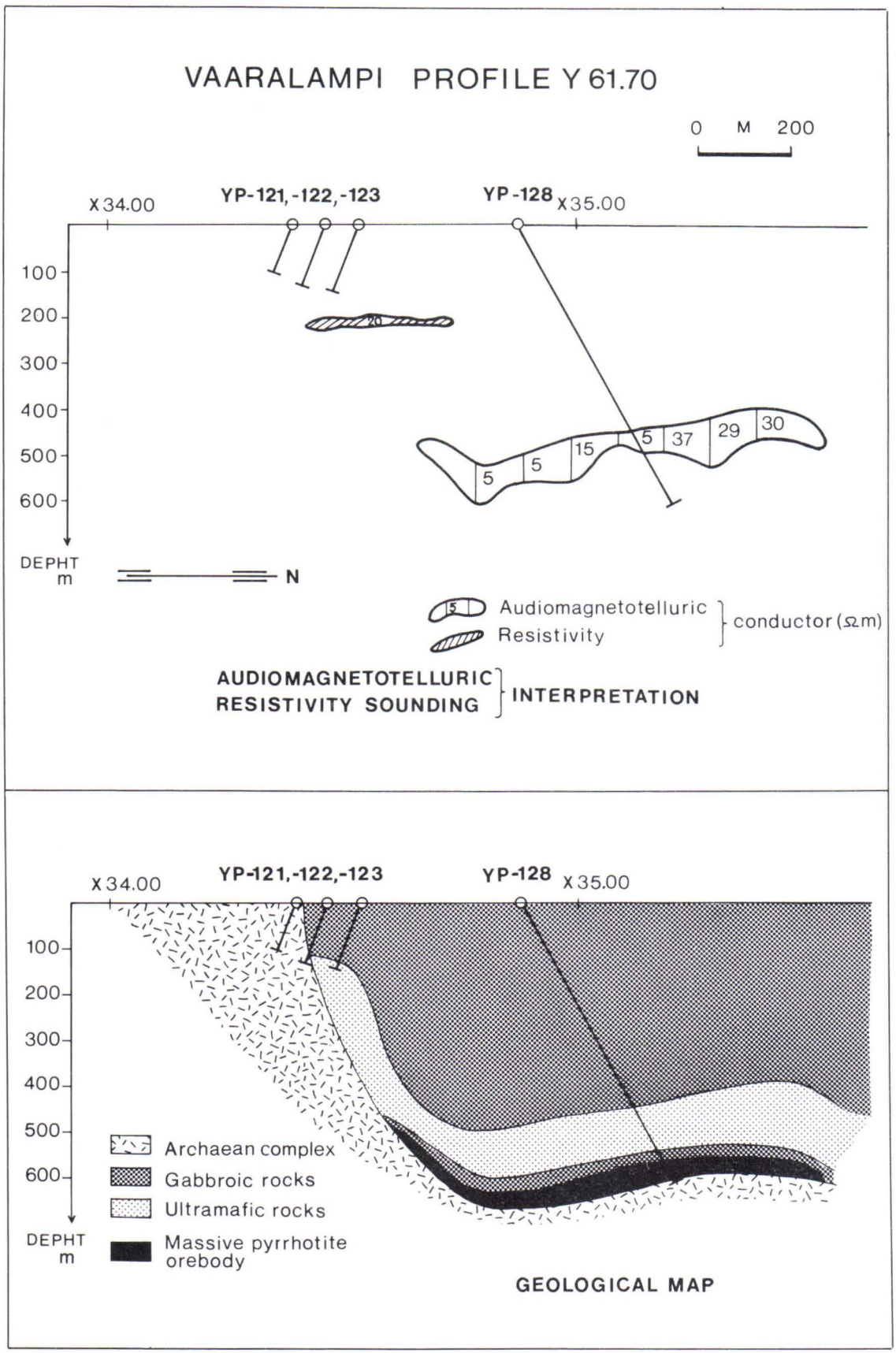

Fig. 6. AMT and resistivity interpretation and the geology of section y = 61.70 at Vaaralampi.

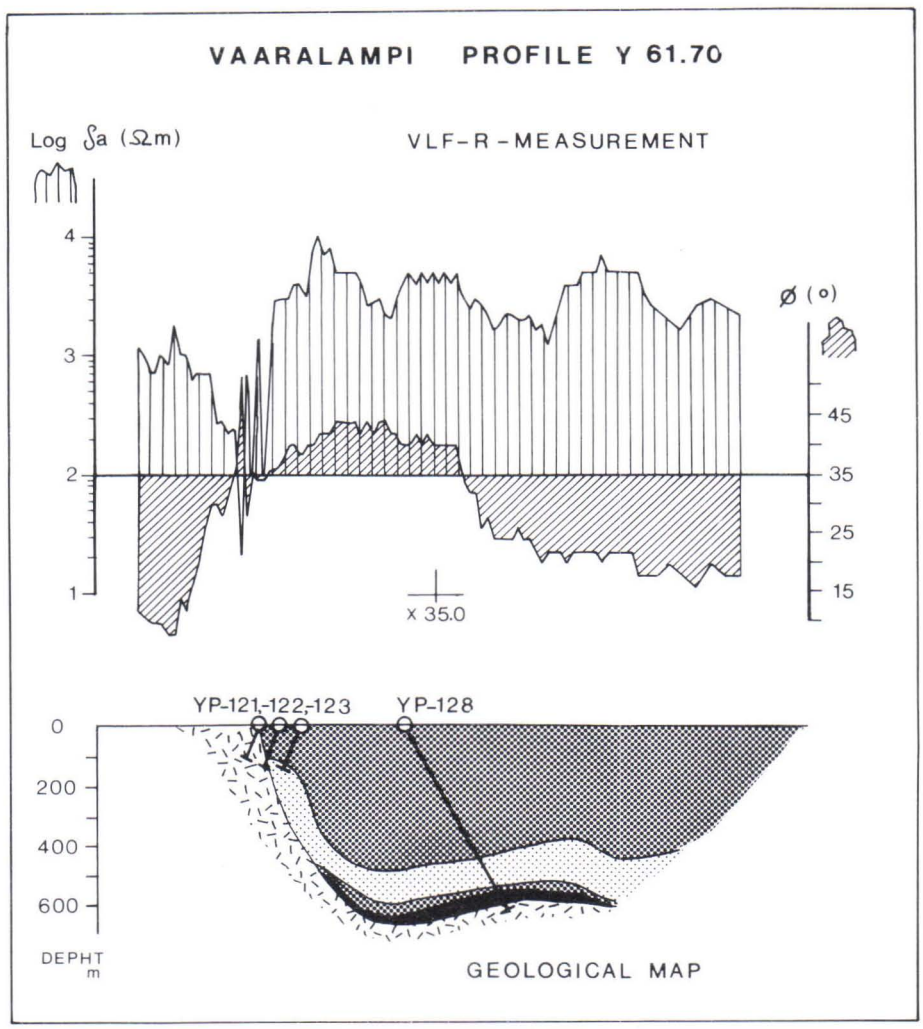

Fig. 7. VLF-R measurement and geology of section y = 61.70 at Vaaralampi.

Interpretation of the AMT data based on the layered earth model (Lakanen 1975) indicated a subhorizontal pyrrhotite orebody in the contact of the layered intrusion with the granite gneiss basement at a depth of about 600 m. After the measurements, the interpretation was verified with drill hole YP-128, but the interpretation was hampered by the finite width of the sulphide plate (c. 1 000 m).

The resistivity survey, whose data were also interpreted with the layered earth model (Lakanen 1975), indicated a good conductor, c. 300 m. wide, at a depth of about 200 m. The finding has not been tested by drilling. Holes YP-121, 122 and 123 were drilled before the survey.

VLR-R soundig with a JXZ (f = 16.4 kHz) transmitter station indicated the contact between the layered intrusion and the gneissose granite basement and the same conductor within the intrusion as did the resistivity survey, Fig. 7.

In conclusion, the resistivity, AMT and VLF-R soundings enabled the layered intrusion to be delineated and provided a reliable concept of its electrical structure from the surface to its base.

Sirotem measurements

In 1980—1982 Suomen Malmi Oy tested electromagnetic transient methods on the pyrrhotite orebody at Vaaralampi using Sirotem, PEM and borehole PEM units.

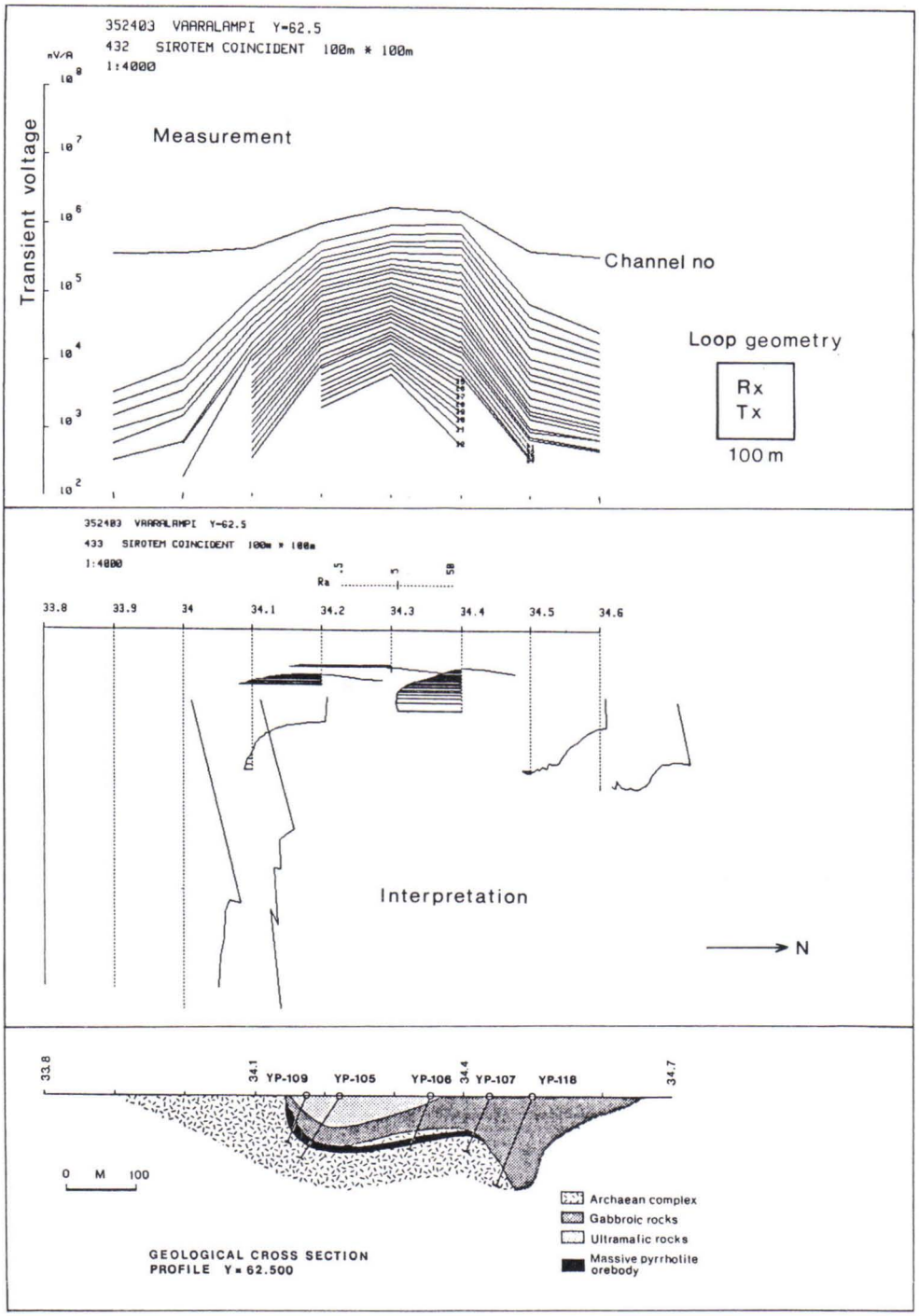

Fig. 8. The Sirotem measurement at Vaaralampi, its interpretation and geology along profile y = 62.500.

The Sirotem measurements were performed along four lines with Australian Sirotem transient EM equipment using 100 x 100 m and 200 x 200 m transmitter-receiver loops.

The survey results of line Y = 62.500 are shown in Fig. 8 as a stack of profiles of 32 channels, with the interpretation and geology verified by five drill holes. The measuring data were interpreted with a layered earth model (Lakanen 1985).

The subhorizontal pyrrhotite orebody at a depth of about 70 m is indicated nicely by the Sirotem survey. The interpretation with the layered earth model is

compatible with the structure verified by drilling, and the apparent resistivity given by the interpretation, $\varrho_a \sim 0.1 — 1\ \Omega m$, is consistent with the petrophysical determinations. The interpretation is somewhat hampered by the finite width of the conductor and the vertical attitude of its southern end. The possible extension of the pyrrhotite slab towards north at greater depth has not been established.

Electromagnetic 3-component borehole soundings

In 1982 Boliden Mineral AB undertook test soundings at Niittylampi with the electromagnetic 3-component borehole equipment they had developed (Piippola 1983). The equipment featured a 500 x 500 m transmitting loop laid on the ground (Fig. 9) and a receiver that measured the amplitude and phase of the three mutually perpendicular components of the magnetic field on the ground and in the drill holes. The transmitting current was I = 3.8 A and its frequency f = 2 000 Hz.

The sounding data were processed and interpreted in Sweden by Boliden Mineral AB.

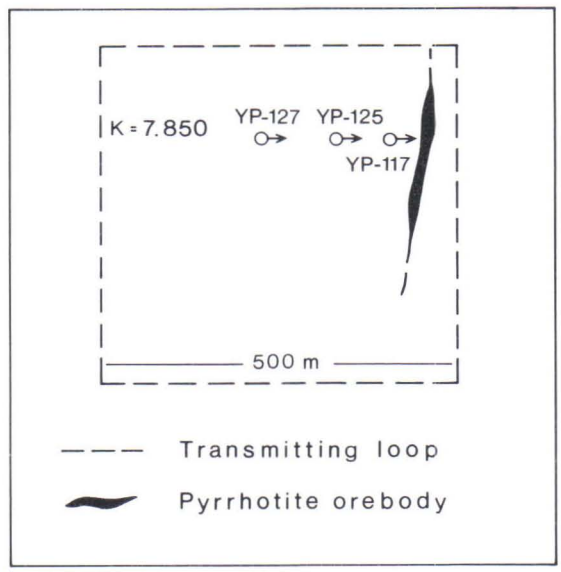

Fig. 9. The sounding arrangement.

Figure 10 depicts the survey data on drilling profile K = 7.850, showing the variation in the secondary field on horizontal and vertical sections. In the calculation of the primary field the resistivity of the environments was assumed to be ϱ = 15 000 Ωm.

The survey data indicate that the orebody dips 25°—40° to southwest and that its upper edge is very near drill hole YP-117. Consequently, the depth to the upper surface is about 40 m, in accordance with the depth interpreted from the ground Slingram measurements (Ketola 1982). The anomaly in the upper part of drill hole YP-127 is due to the ultramafic rocks, whose resistivity is markedly lower than that of the gabbros in the layered intrusion. Unfortunately, the bottom part of the drill hole was blocked and it was not possible to established whether the pyrrhotite orebody extends downwards here.

Summary

This paper describes briefly some of the geophysical electrical methods and the results obtained from them, which Outokumpu Oy, and recently Lapin Malmi (1982—), have applied in the search for an economical ore deposit in the Vaaralampi—Niittylampi area.

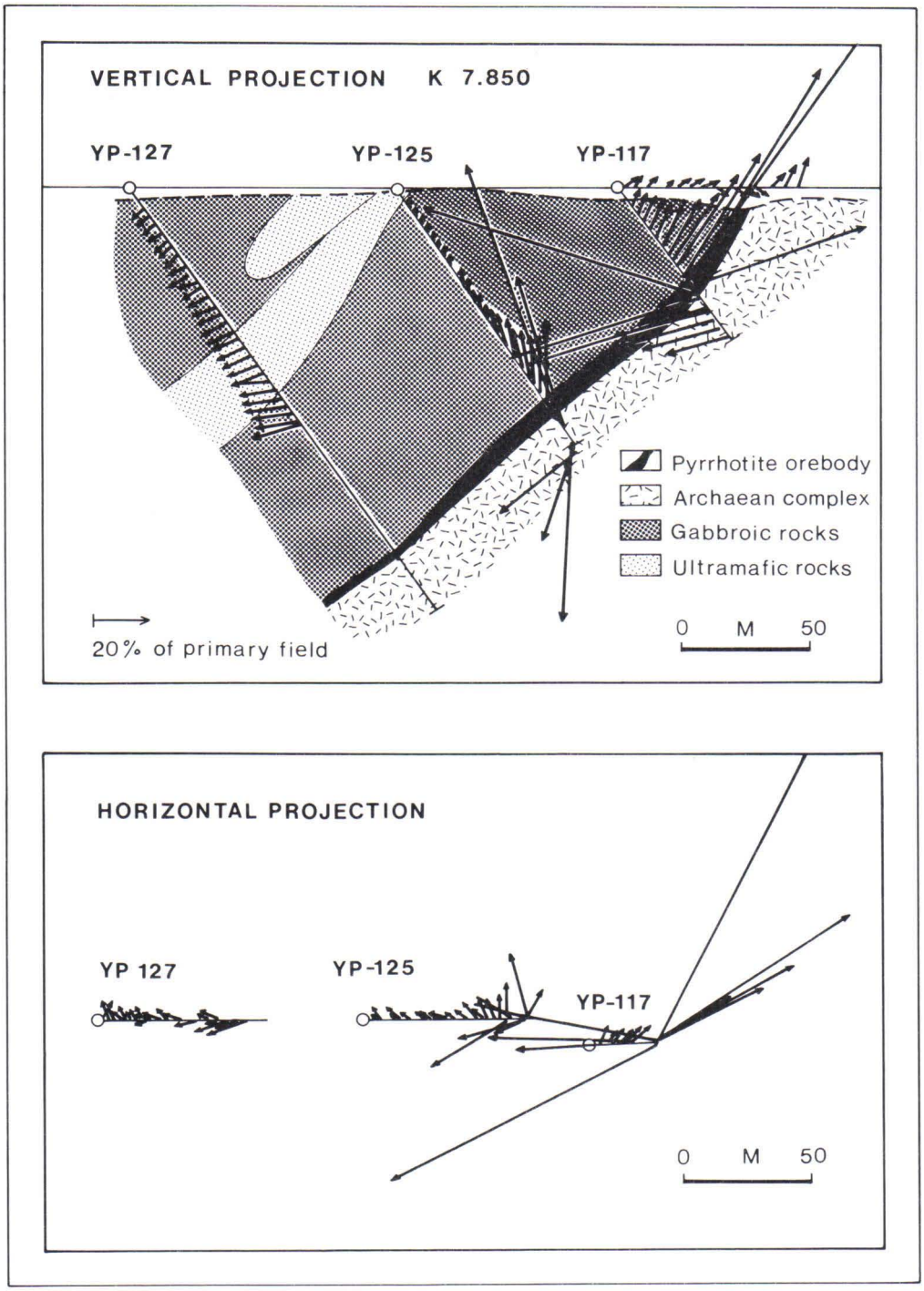

Fig. 10. Variations of the secondary field in drill holes YP-117-125-127 and on the profile K = 7.850. Horizontal and vertical projection.

The surveys have contributed to establishment of the electrical structure of the layered intrusion and allowed the delineation of the pyrrhotite orebodies at Vaaralampi and Niittylampi.

The pyrrhotite orebodies represent as to useage of geophysical electrical methods in one way an ideal case — very good conductors in the resistive surroundings.

Unfortunately, at the current prices of copper and nickel the orebodies are subeconomic; Cu + Ni $\simeq$ 0.5 %.

Acknowledgements

I thank Outokumpu Oy Exploration, Lapin Malmi and Suomen Malmi Oy for permission to publish this paper. Special thanks are due to Mr. J. Lahtinen, a geologist with Lapin Malmi, for having checked the geological part of the paper and for drawing some of the pictures. Mr. H. Silvennoinen, geophysicist, was responsible for the Sirotem survey, Messrs. T. Pernu and T. Keränen, geophysicists, provided me with the VLF-R and AMT data, and Messrs. E. Lakanen and J. Longi undertook the AMT, resistivity and Sirotem interpretations, to all of whom I express my gratitude.

References

Ketola, M., 1982. On the application of geophysics and geology to exploration for nickel-copper ore deposits in Finland. Geol.tutk.keskus, Tutk.rap. 53, 103 p.

Ketola, M., Puranen, M., 1967. Type curves for the interpretation of Slingram (horizontal loop) anomalies over tabular bodies; Geol.tutk.lait., Tutk.rap. 2, 19 p.

Lahtinen, J., 1983. Yhteenveto v. 1982 platinantutkimuksista Tornion—Näränkävaaran kerrosintruusiojaksolla. Lapin Malmin sisäinen raportti. Unpublished report.

Lakanen, E., 1975. Geofysikaalinen tulkinta graafisen tietokonekäsittelyn avulla: Geofysiikan päivät, Oulu.

Lakanen, E., in preparation. A succesful application of the transient method; Electrical prospecting for ore deposits in the Baltic Shield, Part 2: Electromagnetic methods. Ed. by S.E. Hjelt and A.Ph. Fokin. Geol.tutk.keskus, tutk.rap.

Piippola, S., 1983. Raportti koemittauksista Bliden Mineral AB:n monikomponenttilaitteistolla. Unpublished report.

Reino, J., Ilvonen, E., Rekola, T., 1978. Suhanko—Pekkalan -alueen tutkimuksista 1970-luvulla. Outokumpu Oy:n sisäinen raportti. Unpublished report.

Vuorelainen, Y., Häkli, A., Hänninen, E., Papunen, H., Reini, J. & Törnroos, R., 1982. Isomertieite and other Platinum-Group Minerals from the Konttijärvi Layered Mafic Intrusion, Norhtern Finland; Economic Geology, 77 (6), 1511—1518.

PECULIARITIES OF APPLYING THE IP METHOD WHEN SOLVING CERTAIN GEOLOGICAL PROBLEMS INVOLVED IN ORE PROSPECTING IN THE KARELIA-KOLA REGION

by

H.N. Mikhailov, G.P. Vargin and S.N. Shereshevsky

Mikhailov, H.N., Vargin, G.P. & Shereshevsky, S.N., 1986. Peculiarities of applying the IP method when solving certain geological problems involved in ore prospecting in the Karelia-Kola region *Geologian tutkimuskeskus, Tutkimusraportti 73.* 85—90, 3 figs.

The experience acquired during the field application of the IP technique indicates that one of the most effective means of determining the target mineralization in the Karelia-Kola region is a complex analysis of induction and polarization effects in a wide time range.

In a complex geological setting, it is advisable, and from the physical point of view logical, to approximate measured time responses with the sum of the exponential functions with various time constants (τ_i) and to represent the results as spectra where the amplitude values (K_i) characterize the contribution of the exponential signals with the time constants (τ_i).

Key words: electrical methods, induced polarization, metal ores, ultramafics, metasedimentary rocks, Precambrian, USSR, Karelia, Kola Peninsula

Михайлов, Г.Н.,Варгин, Г.П., ШереШевский, С.Н., 1986. Особенности применения метода ВП при решении некоторых геологических задач, связанных с поисками рудных месторождений в Карело-Кольском регионе. Геологический центр Финляндии, Рапорт исследования 73. 85—90. Идд. 3.

Накопленный опыт практического применения ВП свидетельствует, что одним из эффективных средств выявления в Карело-Кольском регионе искомого оруденения является комплексное изучение индукционных и поляризаци онных эффектов в широком временном диапазоне.

В сложно-построенных геологических средаз представляется целесообразным и физически обоснованным аппроксимировать измеряемые временные характеристики суммой экспонент с различными постоянными времени и изображать результаты измерений в виде спектров, в которых амплитудные значения (Kaii) характеризуют весовой вклад в измеряемый эффект экспоненциального сигнала с конкретной постоянной времени.

The peculiarities of applying the IP method in ore prospecting in the Karelia-Kola region are due to the specific geoelectrical structure of the region and, especially, to the indistinct differentiation of the rocks and ores according to their electrical properties. Overlapping of the resistivity range is observed in different lithological formations. The resistivity of the sedimentary-tuffaceous complexes is usually 4,000—6,000 Ωm, and the resistivity of the basic metaeffusive rocks in 6,000—10,000 Ωm. The phyllites and graphite-rich zones or zones containing disseminated impregnations of sulphide (pyrite, pyrrhotite) are characterized by low resistivity (tens and hundreds of Ωm). The resistivity of the gneisses and gneiss-granites is mostly 10,000 Ωm and more. The resistivity of the ores is some tenths of Ωm, while in impregnated ores it amounts to some tens of Ωm. The morainal sediments, together with the weathering crust, are taken separately as a horizon with a resistivity of several hundred Ωm.

The ultrabasic rock chargeability varies in the limits of 0.5—90 %, depending on the quantity of ore minerals (magnetite, sulphies) and their structure and textural peculiarities, which are largely conditioned by the depth of the secondary alterations (serpentinization, chloritization, carbonatization). Most of the sedimentary-volcanogenic formations are characterized by low values of chargeability (up to 2—3 %). Phyllites with a chargeability value of 30—80 % are an exception. The chargeability of the gneisses and gneiss-granites is 1—2 %. It should be pointed out that a high level of chargeability (up to 90 %) is typical of the zones of graphitization and disseminated sulphide mineralization discriminated amidst volcanogenic-sedimentary complexes as well as in gneisses and granite-gneisses.

The observed overlapping of the resistivity and chargeability ranges of the rocks and ores in many cases makes it difficult to carry out electrical prospecting. The peculiarities of applying the IP technique in the Karelia-Kola region are influenced by the high level of industrial noise and interfering geological factors, such as disseminated sulphide (pyrite, pyrrhotite) mineralization and impregnated magnetite in the basites and (especially serpentinized) ultrabasites, the quartz-carbonate veinlets of crush zones, the metadiabases, graphitized rocks, chungite-clay shales, etc. The standard IP technique, as based on a prolonged passage of current through the section and a measurement of the IP secondary field in 0.5 s after the cutoff of current, may be successfully used only in certain regions where the target copper-nickel ores occur amidst plagiogneisses and barren gabbro-norites with high resistivity. Application of the IP technique at the preliminary stage of detailed prospecting must be followed up by a comprehensive analysis of the electrical properties of the rock and ore, by check extration and drilling with subsequent prompt and critical evaluation of the results obtained and necessary correction of the measuring technique.

The experience acquired during the field application of the IP technique indicates that one of the most effective means of locating target mineralizations in the Karelia-Kola region is the comprehensive study of induction and polarization effects in a wide time range. The following parameters are involved here in interpretation: the electromagnetic transient parameter, determined by the early stage of the transient; the rate of IP transient changing in time, determined as the ratio of chargeability measured in the early and late stages; also the more complex parameters involving a correlation between chargeability and rock and ore magnetic properties, and between chargeability and electrical conduction.

Fig. 1 illustrates the results of IP measuring along the profile over pyrite-pyrrhotite massive and densely impregnated ores occurring at depths of 150—200 m and confined to the outlier of volcanogenic-sedimentary rocks amidst ultramafites. In the IP field (apparent chargeability) η_a and apparent resistivity ϱ_a diagrams plotted on the basis

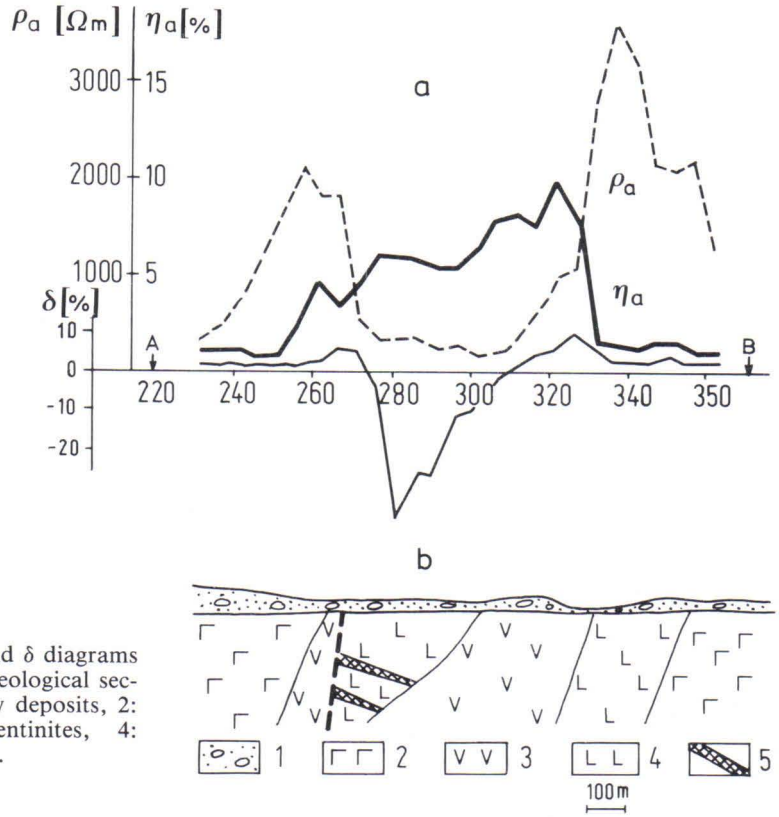

Fig. 1. a) ϱ_a, η_a and δ diagrams and b) schematic geological section. 1: Quaternary deposits, 2: gabbro, 3: serpentinites, 4: tuffs, 5: orebodies.

of gradient array data, one can distinguish broad chargeability anomalies which possess an intensity up to 10 % and reduced resistivity and are confined to the ultrabasic rock massif. Located by sharp η_a and ϱ_a gradients are the contacts of the massif with the effusive-sedimentary rock sequence; representation of the orebody on the plots is, however, ambiguous. The apparatus employed enable the variations of η_a and ϱ_a in time to be traced. As a result, criteria were devised for locating the target mineralization in the conditions of a high chargeability background and low resistivity of country rocks.

Induction, as one of these criteria, enables the orebody epicentre to be spotted by a pronounced negative anomaly in electromagnetic transient parameter δ.

Classifying the anomalies as ''ore'' or ''barren'' in nature is done according to the plots of quantity $\tilde{\eta}$, the derivative of the IP field with respect to the time logarithm (''the differential chargeability'').

The normalized $\tilde{\eta}$ in Fig. 2 either display a clear maximum at 0.5 s, which corresponds to ultrabasic rocks with disseminated sulphide impregnations (diagram 1), or fail to reach this maximum through the measurement range (up to 3 s), which corresponds to the effect over sulphide streaky-impregnated ores (diagram 2). Over effusive-sedimentary rocks (diagram 3), the IP-field derivative represents a curve regularly dropping down throughout the measurement range.

To construct the geoelectrical sections defining the distribution of the interpretation parameters with depth, use was made of a one-electrode sounding array, the effective current electrode being moved over the observation profile with a regular spacing. The construction of the sections is computer-assisted.

In dealing with a complex geological setting, it is advisable, and from the physical point of view logical, to approximate the measured time responses by the sum of exponential functions with various time constants τ_i and to represent the results as spectra, where the amplitude values K_i characterize the contribution of the exponential signals with the specific time constants τ_i to the measured effect. As to the low-contrast media of the Karelia-Kola region, it turned out to be more practical to perform spectral

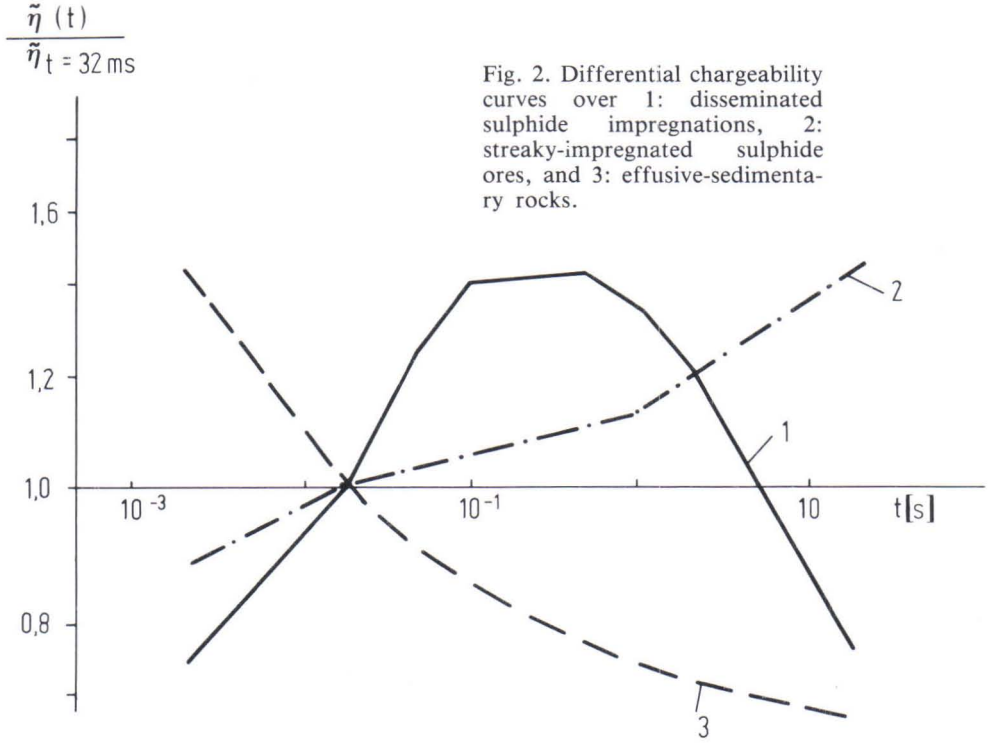

Fig. 2. Differential chargeability curves over 1: disseminated sulphide impregnations, 2: streaky-impregnated sulphide ores, and 3: effusive-sedimentary rocks.

expansion of the second derivative of th IP field with respect to time logarithm U'', the derivative being measured using the apparatus designed by NPO ''Rudgeofizika'' with current pulses following the proper mode.

The expansion approximating U'' is:

$$U''(t) = U_\infty \cdot \eta''(t) = U_\infty \cdot \sum_{i=1}^{\infty} K_i \frac{t}{\tau_i}\left(1 - \frac{t}{\tau_i}\right) \exp\left(-\frac{t}{\tau_i}\right),$$

where U_∞ is the amplitude of IP in steady-state, t the sampling time, and η'' the second rate of chargeability with respect to the logarithm of time. K_i is defined by the ratio of the current charging the equivalent capacitor C_i to the current across the resistance R. The greater the influence of the IP processes, the stronger is the effect of the charging current and the higher the value of K_i.

Let us take one of the field examples indicating that the spectral expansion of η'' (t) may be of use when determining the ore-content degree of mineralized zones. The copper-nickel mineralization in the prospecting area comprises the ore impregnations in the hanging wall of the ultrabasic rock massif occurring in the tuffaceous-sedimentary formations within the pay sequence of the ore field. Along with the ultrabasic rock intrusions, the gabbro-diabase intrusive bodies are also taken into account. Intrusions and tuffaceous-sedimentary formations holding them crop out from under till deposits and plunge at an angle of 30—50°. The ore bodies differ only sligthly in their conductivity from the host rocks and, therefore, they cannot be located by anomalies when applying mise-à-la-masse or resistivity methods. The study of chargeability, when based upon the standard procedure, fails to produce a good result, since ultrabasic and tuffaceous-sedimentary rocks cause the increased chargability background, which is often commensurable with the IP-field anomalous values over the target mineralization zones.

Fig. 3 illustrates the amplitude values K_i of spectra for the curves η'' (t) measured at the site along a profile with the three-electrode (AMN) array

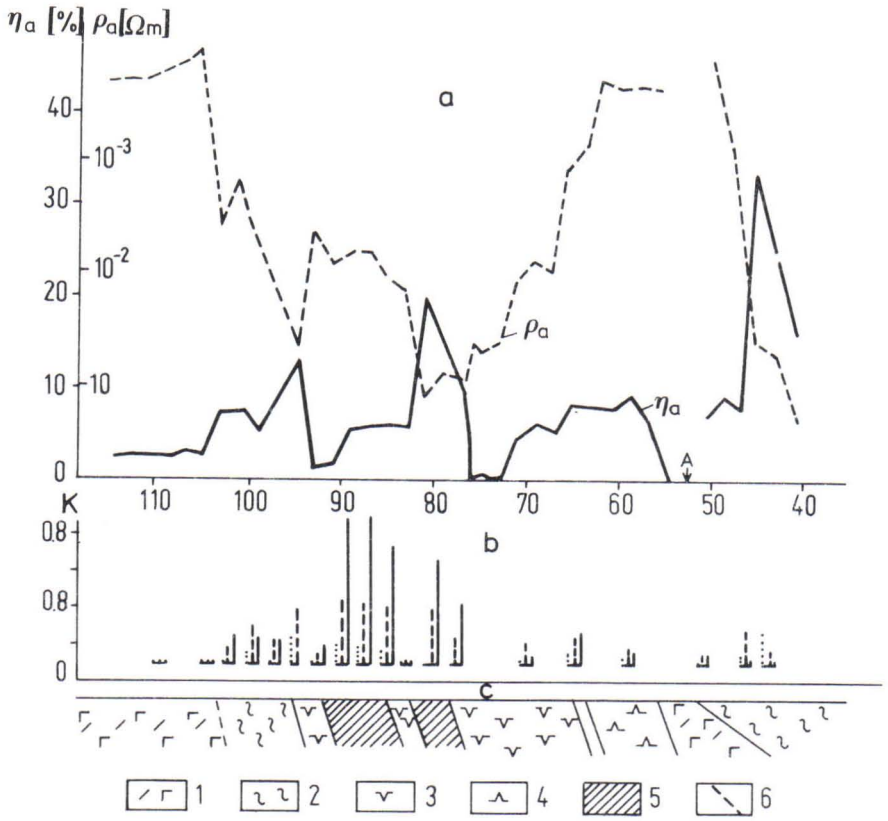

Fig. 3. The results of IP technique operations with the time response measurement. a) η_a (heavy line) and ϱ_a (dotted line) diagrams with the gradient array; b) spectra for time constant values in the regions: $\tau = 1—10$ s (dots), $\tau = 10—100$ s (dotted ine), $\tau = 100—1{,}000$ s (heavy line) of approximation functions for the second derivation of the IP-field with respect to the time logarithm; c) schematic geological section. 1: gabbro-diabases, 2: phyllites, 3: serpentinites, 4: peridotites, 5: ore mineralization, 6: tectonic faults.

($\overline{AM} = \overline{MN} = 20$ m). The time constant values τ vary in the ranges 1—10 s, 10—100 s and 100—1000 s. Given for comparison are ϱ_a and η_a diagrams measured with the gradient array ($\overline{AB} = 700$ m, $\overline{MN} = 30$ m, current I = 0.3 A). Analysis of the data obtained shows that the mineralized zones differ in the range of the spectrum in which time constant values $\tau = 100—1{,}000$ s ($K_i = 0.6—0.8$) prevail. In this range of τ values, no polarization effect over the gabbro-diabases is observed. The ultrabasic rocks are characterized by the spectrum in the range where the contribution of polarization effects with $\tau = 10—100$ s prevails over that of the polarization effects with other τ values, the amplitude K_i not exceeding 0.2. For tuffaceous-sedimentary rocks, $\tau = 10$ s ($K_i = 0.3$) is most typical.

Thus, the measurement of time dependencies of the second logarithmic time derivative of chargeability enable one to sort out the low-contrast IP anomalies caused by the variation in the ore grade. The spectral expansion of the measured responses of the IP-field makes it possible to determine with sufficient accuracy, from the practical point of view, the contribution of the processes with various time constants to the total polarization effect. This approach can be successfully used to solve prospecting and exploration problems in the Karelia-Kola region.

The variety of geological environments in which ore prospects occur demands a skillful approach in choosing the IP procedure to be applied.

References

Komarov V.A. IP electrical prospecting. Leningrad, Nedra, 1981. 391 p. (Электроразведка методом вызванной поляризации).

Chernysh V.J., Shereshevsky S.N., Semenov A.A. EVIP-601 apparatus model for pulse electrical prospecting. — Geophysical instruments (Геофизическая аппаратура), No. 70, 1979, 40—45. (Макет аппаратуры ЭВИП-601 для работ методами импульсианой электроразведки).

Shereshevsky S.N., Litmanovich J.L. The interpretation of IP technique measurements using spectrum expansion of time responses. — In: Methods of exploration geophysics. Ground versions of pulse-field electrical prospecting when searching for ore deposits. Leningrad, NPO ''Rudgeofizika'', 1983, 3—11. (Интерпретация работ методом ВП с использованием спектрального разложения временных характеристик. — В кн.: Методы разведочной геофизики. Наземные варианты электроразведки испульсивными полями при поисках разных месторождений). НПО ''Рудгеофизика'').

Tätä julkaisua myy

VALTION PAINATUSKESKUS

POSTIMYYNTI
PL 516
00101 Helsinki
Puh. (90) 566 0266
Vaihde (90) 56601
Teleksi 123458 vapk sf

KIRJAKAUPAT HELSINGISSÄ

Annankatu 44
(Et. Rautatiekadun kulma)
Vaihde (90) 173 4396

Eteläesplanadi 4
Puh. (90) 662 801

This publication is available from

GOVERNMENT PRINTING CENTRE

MAIL ORDERS
P.O.B. 516
SF-00101 Helsinki Finland
Phone internat.
+ 358 0 56601
Telex 123458 vapk sf

BOOKSHOPS IN HELSINKI

Annankatu 44
Phone (90) 173 4396

Eteläesplanadi 4
Phone (90) 662 801

ISBN 951-690-215-4
ISSN 0781-4240